OPTIMAL DESIGN OF DISTRIBUTED PARAMETER FILTERS

Mohamed El Diwany

A Thesis

in

The faculty

of

Engineering

Presented in Partial Fulfillment of the Requirement

for the degree of Doctor of Engineering at

Concordia University

Montreal, Québec, Canada

September, 1975

TO MY WIFE LEYLA

and

MY PARENTS

ABSTRACT

This thesis is chiefly concerned with the optimal design of transfer functions as active or passive filters using distributed RC lines .

Cascades of $\overline{URC}$'s are used to approximately realize open circuit voltage transfer functions having all the s-plane poles on the negative real axis .

Optimization techniques are used to minimize :

1) The overall substrate area required in the fabrication of distributed RC networks , or ,

2) A weighted sum of substrate area and approximation error in the frequency response for the same class of networks , or ,

3) Substrate area for the lumped RC networks realizing the given class .

It is shown that a considerable saving in substrate area can often be effected by the use of distributed realization .

Next , a new distributed RC active filter is presented . This filter uses two grounded distributed RC networks and three grounded operational amplifiers . It is demonstrated that the filter is capable of realizing an n^{th} order rational transfer function . Realization of the biquadratic function is studied in detail. An optimization program is developed and used to determine the design values for the circuit parameters such that a stable operation , approximating very closely the desired response is obtained

while guaranteeing low sensitivities of Q and ω_o to parameter variations.

A feature of this filter is that Q-sensitivity to the RC-product of the lines is identically zero. The design procedure is shown to result in practical values of circuit elements with low Q and ω_o sensitivities when used to design LP, BP, HP, notch and all-pass filters.

The effect of amplifier finite gain-band-width product on the response is studied and in this respect the proposed circuit is found to compare favourably with other circuits using distributed elements.

Experimental tests on several prototypes are carried out to support theoretical calculations.

A simple scheme is also introduced to extend the useful frequency of operation which is limited by the finite gain-band-width product of the operational amplifiers.

A study of the effect of line taper on the performance of the filter leads to the conclusion that tapered lines should be used when when low frequency operation is desired.

ACKNOWLEDGEMENT

The author is deeply indepted to Dr. J.C. Giguere for his supervision of this thesis, and for his constant encouragement during the course of the research.

The author also wishes to thank Dr. B.B. Bhattacharyya for many useful discussions and suggestions during this work.

Appreciation is extended to Dr. M.S. Abougabal for many useful discussions during the preparation of this thesis.

Thanks are due to my wife Leyla and Miss Hoda Mohsen for typing the manuscript.

This work was supported by the National Research Council of Canada, Grant number A7244 awarded to Dr. J.C. Giguere.

TABLE OF CONTENTS

NOMENCLATURE

a	constant
b	constant
c	constant
e	error in the frequency response
e_o	amplifier output
e_i	amplifier input
f_1 , f_2	functions
f_{zi} , f_{pi}	p-plane zeros and poles
g_i	constraint equation
p	transformation variable
p_i	v-plane pole
q	transformation variable
r_i	amplifier feedback ratio
r_{ij}	ratio of resistances R_i/R_j
r	maximum ratio of line resistances
s	complex frequency
s_1 , s_z , s_p	s-plane roots
u_i	u-plane pole
r^*	optimal r

u	transformation variable
v	transformation variable
z_i	v-plane zero
z_{11}	driving point function
A_n	chain matrix of cascade of n uniform $\overline{RC}$ lines
A	chain matrix parameter
D	denominator of transfer function
F_1 , F_2	circuit impedances of transmission lines
GB	gain-band-width product
H	scaling factor
J	objective function
K_i	amplifier gain
N	numerator of transfer function
N1 , N2	networks
Q	quality factor
Q_d	desired value of Q
Q_a	actual value of Q
Q_z	numerator Q
R_i	resistance
S	sensitivity matrix
S_y^x	sensitivity of x with respect to y
S_e , S_n	regions in the s-plane
T_d	desired open circuit voltage transfer function

T_a	actual open circuit voltage transfer function
U_o, U_n	regions in the s-plane
W_i	weighting constant
$\underline{Y}$	parameter vector
$\underline{Y}'$	transpose of $\underline{Y}$
α	u-plane zero
β	taper factor, in Chapter 3 only
γ	u-plane pole
σ	real part of s
ω	radian frequency
ω_o	pole center frequency
ω_z	zero center frequency
ω_n	notch frequency
ϵ and Δ	small variations
μ, μ_o	amplifier open circuit gains
λ	line RC product
ψ	slack variable

LIST OF FIGURES

LIST OF TABLES

CHAPTER 1

INTRODUCTION

1.1 GENERAL

With the increasing complexity of electrical equipment, and the resultant emphasis on reduction in size, weight and power dissipation, efforts have been concentrated on the design and fabrication of micro-miniature circuits.

One method currently used by industry for the realization of linear system functions is to interconnect passive components fabricated using thin film technology and active semiconductor devices. One popular semiconductor device is the operational amplifier (OA). Low cost OA's with excellent characteristics are now widely available and have been extensively used in the production of filters for a wide variety of applications. Thin film components available are the resistor, the capacitor and a hybrid unit known as the distributed RC ($\overline{RC}$) line. Good quality thin film inductors are not yet available and do not seem likely to be available in the near future [1].

Although the $\overline{RC}$ line has received considerable attention in the last few years [2], it has not as yet been widely adopted by industry. It is our purpose in this thesis to show that it is possible to design $\overline{RC}$ filters which have good performance characteristics and to indicate that in some cases significant savings in substrate area may be achieved through the use of $\overline{RC}$ lines.

1.2 THE BUILDING BLOCKS

1.2.1 The $\overline{RC}$ Line

The $\overline{RC}$ line consists of resistive, dielectric and conductive layers superimposed as shown in figure 1.1. The electrical properties of the line are described through its series impedance and shunt admittance per unit length [3], that is,

$$z(s,x) = z_o(s)\ f(x) \qquad 0 < x < \ell \qquad (1.1)$$

$$y(s,x) = y_o(s)\ g(x) \qquad (1.2)$$

The uniform $\overline{RC}$ line ($\overline{URC}$) is a special case where $z_o = R$, $y_o = sC$, $f = g = 1/\ell$ and R and C now represent the total series resistance and shunt capacitance of the line, respectivaly.

Different materials and methods can be used for the fabrication of $\overline{RC}$ lines [4]. While it is easy to fabricate a tapered $\overline{RC}$ line by varying the line geometry [5], $\overline{URC}$'s are the simplest to design. Practical values of R's and C's lie in the ranges 10Ω - 100 KΩ and 6 μF - 0.03 μF. For future reference, the chain matrix of the $\overline{URC}$ is given below:

$$[a] = \begin{bmatrix} \cosh\sqrt{sRC} & \dfrac{R \sinh\sqrt{sRC}}{\sqrt{sRC}} \\ \sqrt{sRC}\ \sinh\sqrt{sRC}\ /R & \cosh\sqrt{sRC} \end{bmatrix} \qquad (1.3)$$

1.2.2 The Operational Amplifier

Since operational amplifiers (OA) are used in this thesis, it is worthwhile to discuss their properties. Inexpensive and reliable commercial OA's are now available in monolithic integrated form.

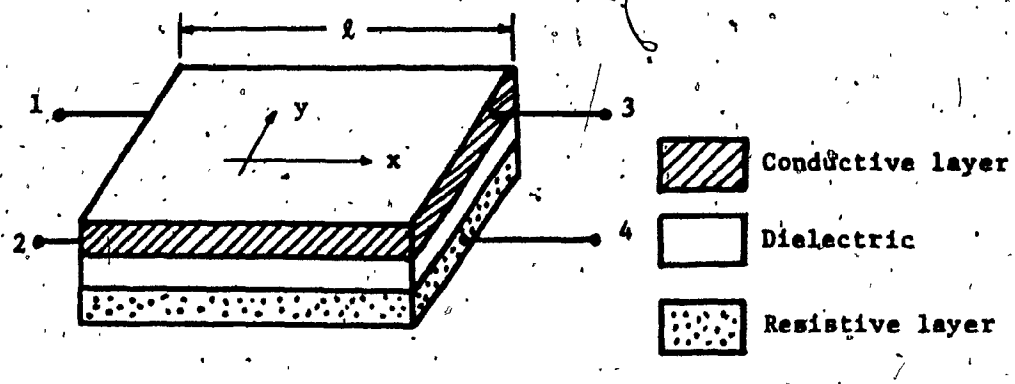

Figure 1.1.a: Thin Film Realization of $\overline{URC}$

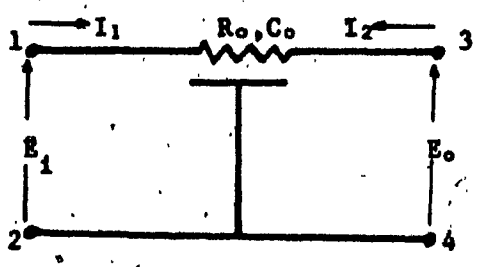

Figure 1.1.b: Symbol of $\overline{URC}$

An example is the Fairchild μA 741 which is internally compensated, and is input over voltage and output short circuit protected. It has an input resistance of 2MΩ, an output resistance of 75Ω and a gain bandwidth product of 1MHz (15MHz for LM 318). This unit is available for about one dollar.

The most commonly used OA is a d.c. voltage amplifier with differential input and single output. The network symbol for the idealized unit is shown in figure 1.2

Differential output OA's are also available but are not widely used at present [6] - [7].

The OA is a nonreciprocal two-port, ideally of infinite gain, infinite input impedance and zero output impedance. However, as indicated above the OA has a frequency dependent finite gain, μ, a finite differential input impedance and a finite output impedance. For a frequency compensated OA, the differential open loop gain is given by:

$$\mu = \mu_o \, \omega_c / (s + \omega_c) \qquad (1.4)$$

where, μ_o, ω_c and $GB = \mu_o \, \omega_c$ are respectively the d.c. gain, cut-off frequency and the gain-band-width product.

1.3 SYNTHESIS USING DISTRIBUTED ELEMENTS

Previous work in the design of $\overline{RC}$ networks has proceeded along two general lines. In one case, it was assumed that the given specification had already been approximated or stated in terms of rational functions of s. Efforts were then directed towards the exact

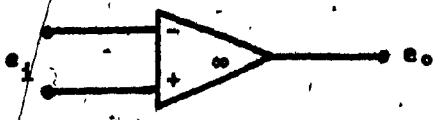

Figure 1.2: Symbol of OA

Figure 1.3: Examples of Distributed Lumped Symmetric Structures

realization of these network functions using a suitably shaped $\overline{RC}$ network [8] - [14]. However, all these methods seem to suffer from some drawbacks. It is necessary to introduce cuts in the conducting layer, the shape of these cuts depending on the transfer function being realized. These cuts, once made, are not easily altered giving rise to difficulties in tuning. Further, it is often necessary to use lumped passive or active terminations. In particular, designs carried out using negative impedance converters to realize difference decompositions of the denominator polynomial may be subject to high Q - sensitivity with respect to variations in component values.

The second approach [15] - [21] assumes that it has been possible to approximate the given specification by a rational function of some frequency dependent variable f(s).

The variable f(s) is chosen so that the approximating function can be realized as an interconnection of ficticious lumped elements which can be directly related to distributed elements. The main advantage of the technique lies in its generality. Once suitable approximations have been found, the synthesis techniques are applicable to a wide range of problems [15], for example, realizations using $\overline{RC}$ structures containing leaky dielectrics ($\overline{RCG}$ lines), $\overline{RC}$ structures containing lumped elements, figure 1.3, or lossless distributed structures [22]. The disadvantage of the approach is the necessity of using unorthodox approximation procedures. For example, Wyndrum [15] has proposed a procedure to approximate frequency response specifications in terms of the exponential function:

$$f = e^{a\sqrt{s}}$$

which approximation leads to synthesis using $\overline{URC}$'s. Such approximations are difficult to obtain in practice and seem to offer a limited scope of application.

Another approach used to approximately realize a second order rational transfer function of the frequency variables is the dominant pole technique [23] - [27]. A higher order function may then be realized as a cascade of second order sections.

The sensitivity of Q to the amplifier gains for all these methods is of the order of Q. Further, the ωRC product of the lines is very high (for example some designs give ωRC values of 18 and more). Therefore, assuming thin film technology, where the maximum RC product available now is about 3×10^{-3} seconds it is evident that these designs will only cover adequately frequencies above several KHz. [38]

Recently, a new transformation has been found to realize exactly rational transfer functions in s [28]. This transformation, however requires the use of gyrators.

1.4 ACTIVE FILTERS

As indicated in section 1.1, it has not yet been possible to fabricate inductors with reasonable values and quality factors which would be compatible with thin film elements designed to operate in the 0 - 100 KHz frequency range. This drawback has been offset by the development of cheap reliable integrated active elements such as the operational amplifier. These, when used in conjunction with passive

linear elements provide the filter designer with a wide range of options. In particular, active filters may be designed so that [7] :

(1) the filter output impedance is very low, thereby making the response independent of the load impedance. Filters may therefore be cascaded without significant interaction.

(2) the filter input impedance is high; hence little power is drawn from the source.

(3) the filter often provides insertion gain hence eliminating the need for additional amplifiers.

It should be noted, however, that the use of active elements may result in high sensitivity of the transfer or associated functions to deviation in component values. Such deviations may also result in instability, particularly in the case of high Q filters. Particular care must therefore be exercised when designing active filters.

A great deal of emphasis has been placed on the design of filters which realise second order transfer functions, more complex filters being realized as a cascade of second order sections. It is often simple to design a second order section than a more complex section. Further, second order sections useful for a wide range of applications can generally be manufactured and sold in large numbers (batch processing). This results in lower cost per filter than can be realized from the manufacture of a smaller number of special purpose units [29] - [37]

Often, factors pertinent to the design of hybrid active filters are:

(1) Tunability, that is the ease with which a particular unit can be adjusted to realise a desired function.

(2) Overall substrate area required for the realization. This depends primarily on the area of the passive subnetwork. It is generally possible to reduce the substrate area by minimizing the spread between the values of the largest and smallest elements [49].

(3) The desirability of using grounded capacitors or $\overline{RC}$ lines which results in a reduced number of contacts and in the elimination of an etching process thereby leading to a greater circuit reliability [38] - [42].

(4) The useful frequency range which can often be expanded through designs requiring low amplifier voltage gains.

1.5 DISTRIBUTED REALIZATIONS OF NETWORK FUNCTIONS

1.5.1 Realization

Let $F_1(s)$ and $F_2(s)$ be the short and open circuit impedances $1/y_{11}$ and z_{11} of an $\overline{RC}$ line. It has been shown [43] that a necessary and sufficient condition on the realizability of a driving point impedance as a finite interconnection of one-port impedances of the types H_1F_1 and H_1F_2 is that it be expressible in the form:

$$z(s) = F_1 \text{ [rational RC impedance function in } u = F_1/F_2] \quad (1.5)$$

If, in addition the given line is symmetric ($z_{11} = z_{22}$) then $z(s)$ may always be realized as a cascade of symmetric sections [44].

The $\overline{URC}$ is a symmetric structure having short and open circuit impedances given by: [45]

$$F_1(s) = \frac{\tanh\sqrt{\lambda s}}{\sqrt{\lambda s}} \quad (1.6)$$

and

$$F_2(s) = 1/\sqrt{\lambda s}\ \tanh\sqrt{\lambda s} \tag{1.7}$$

where λ is the total RC product of the line

hence:

$$u = F_1/F_2 = \tanh^2\sqrt{\lambda s} \tag{1.8}$$

In the u-plane, the chain matrix of a $\overline{\text{URC}}$ is given by

$$[a]_1 = (1-u)^{-\frac{1}{2}} \begin{bmatrix} 1 & RF_1 u \\ \dfrac{u}{RF_1} & 1 \end{bmatrix} \tag{1.9}$$

and that a cascade of n commensurate $\overline{\text{URC}}$'s is given by:

$$[a]_n = \frac{1}{(1-u)^{n/2}} \begin{bmatrix} H_\alpha \prod_1^k (u+\alpha_i) & H_\beta F_1 \prod_1^\ell (u+\beta_i) \\ H_\gamma \frac{u}{F_1} \prod_1^\ell (u+\gamma_i) & H_\delta \prod_1^k (u+\delta_i) \end{bmatrix} \tag{1.10}$$

$$= \begin{bmatrix} A_n & B_n \\ C_n & D_n \end{bmatrix}$$

where k and ℓ equal the largest integers of $\frac{n}{2}$ and $\frac{n-1}{2}$ respectively and $\alpha_1 > \gamma_1 > \alpha_2 > \gamma_2$ .... etc. [46]

Therefore, a cascade of $\overline{\text{URC}}$'s can always realize functions of the form:

$$T[u(s)] = \frac{1}{A_n} = \frac{(1-u)^{n/2}}{\prod_{i=1}^k (1 - u/\alpha_i)} \tag{1.11}$$

and

$$z_{11}[u(s)] = \frac{A_n}{C_n} = H_1 F_1 \frac{\prod_{1}^{k} (1 + u/\alpha_i)}{\prod_{1}^{\ell} (1 + u/\gamma_i)} \qquad (1.12)$$

The realization of (1.12) as a cascade of $\overline{URC}$'s can be performed using a modified form of Richard's theorem [47] by extracting 2-port sections in a recurrence relation. Another method which will be used in Chapter 2 is to rewrite (1.12) as follows

$$z(s) = \frac{H_2}{q} \left[\frac{(p - \alpha_1)(p - \alpha_2)(p - \alpha_{n+1})}{(p - \beta_1)(p - \beta_2)(p - \beta_n)} \right] \qquad (1.13)$$

$$-1 \leq \alpha_{n+1} < \beta_n \ldots < \beta_1 < \alpha_1 \leq 1$$

and $H_2 > 0$.

where

$$p = \cosh \sqrt{\lambda} s \qquad (1.14)$$

$$q = \sqrt{\lambda} s \sinh \sqrt{\lambda} s \qquad (1.15)$$

With the transformation $p = v + 1$, (1.13) is converted to an RL driving point function in the v-plane. This can be synthesized as a lumped ladder network consisting of series inductances and shunt resistances which represent sections of the $\overline{URC}$ cascade [48].

1.5.2. The s → u Mapping

The mapping s → u indicated in (1.8) exists and in particular the mapping of the imaginary axis segment $|\omega| < \frac{\pi^2}{2\lambda}$ is shown in figure 1.4.a. The inverse mapping u → s is not one to one. However, one can establish regions in the s-plane (figure 1.4.b.) for which a one to one inverse mapping exists [50].

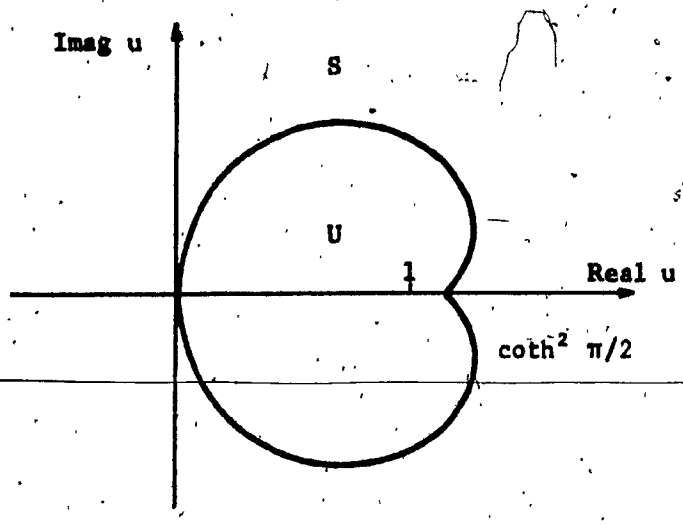

Figure 1.4.a:The s → u Mapping , u-plane

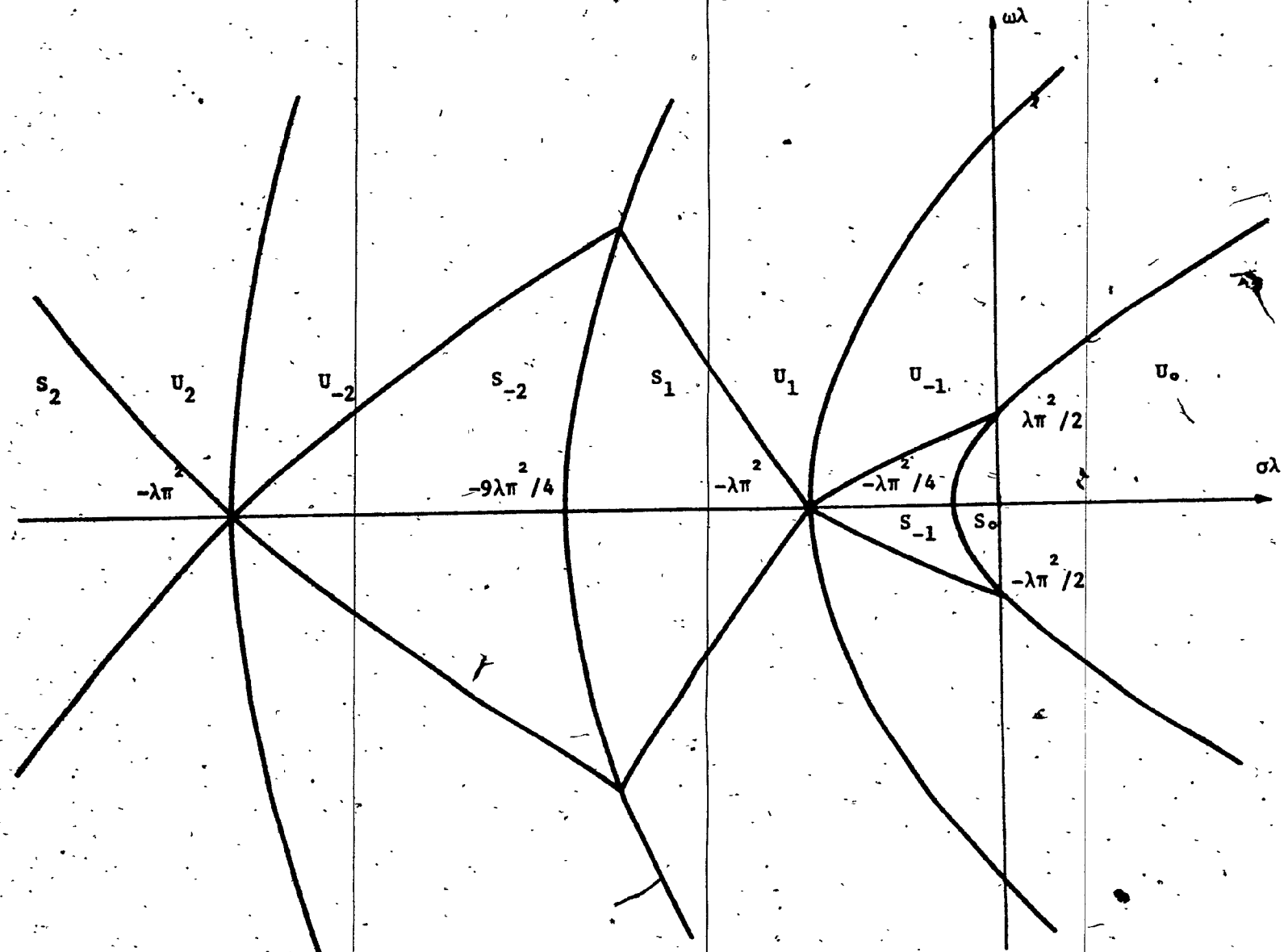

Figure 1.4.b: The s → u Mapping , s-plane

Let $z = \sqrt{s} = (x+jy)^2$ (1.16)

The s and u planes will be represented by C' and C'' respectively. We now define a region $D_o \subset C'$ such that:

$$\left.\begin{array}{ll} x \geq 0 & \text{or} \quad x < 0 \\ 0 \leq y \leq \pi/2 & \quad 0 < y \leq \pi/2 \end{array}\right\} \qquad (1.17)$$

It is elementary to show that $u: D_o \rightarrow C''$ is one to one onto and hence that $u^{-1}: C'' \rightarrow D_o$ exists. We now partition D_o into two disjoint subregions U_o and S_o where $z \in S_o$ implies that $3\pi/4 < \arg \sqrt{z} < \pi/4$. S_o lies entirely in the left half s-plane.

It may be shown that $u(S_o) = S$ and $u(U_o) = U$. The Union of S and U constitute C'. The set of all other regions $\{D_n : n \neq -2, -1, 0, 1, 2, \ldots\}$ which give rise to the one to one onto map $u(D_o) = C''$ is defined as follows:

$$s_n = s_o - \frac{n^2\pi^2}{\lambda} + 2jn\pi\sqrt{s_o/\lambda} \qquad (1.18)$$

where $s_n \in D_n$ and $s_o \in D_o$.

Plots of $|u(j\omega)|$ and $\arg u(j\omega)$ are given in figure 1.5. The low and high frequency portions of these curves illustrate the facts that

$$\lim_{s \to 0} u(s) = \lambda s, \qquad \lim_{\omega \to \infty} |u(j\omega)| = 1$$

The curves suggest that a factor of the form $(1 - s/s_o)$ might be approximated by a factor of the form $(1 - u/u_o)$.

According to (1.18) the above functions will give rise to s-plane zeros s_o, s_{-1}, s_1, s_{-2} etc. We now consider the effect of non-principal zeros. In particular we note that the smaller the value of the RC-product λ,

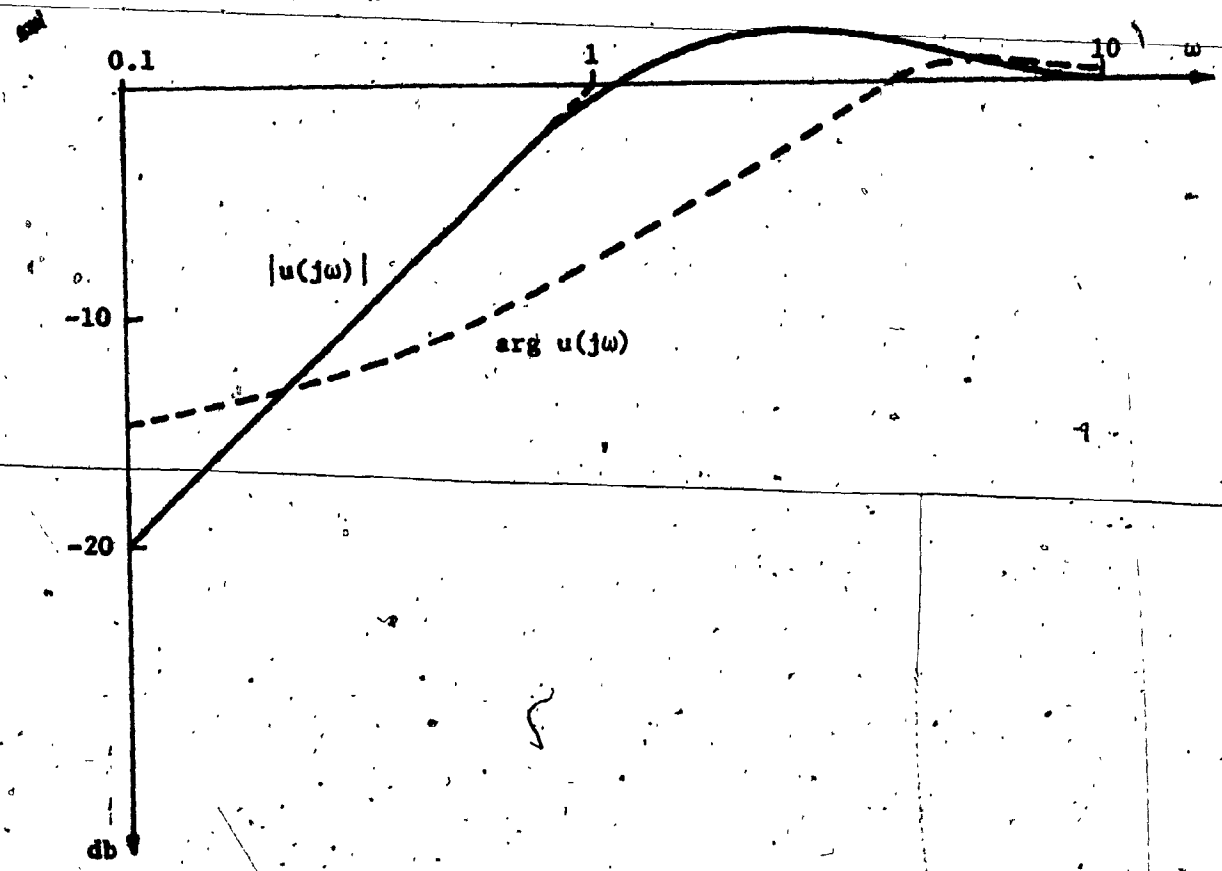

Figure 1.5: Frequency Response of u(jω)

the farther removed are the non-principal zeros and hence the better the approximation. Conversely, increasing the value of λ results in a poorer approximation.

In order to assess the usefulness of the approximation, the functions $e_1 = \frac{1-u/u_o}{1-s/s_o}$ for s_o real, and $e_2 = \frac{1-u/u_o}{1-s/s_o}\frac{1-u/\bar{u}_o}{1-s/\bar{s}_o}$ for s_o complex were considered for a normalized value of $\lambda = 1$, and for values of s_o which correspond to typical λs_o products used throughout this thesis. From the results given in figure 1.6, we note the following:

a- Both magnitude and phase errors increase monotonically with frequency.

b- Errors for high Q factors ($Q > 10$) are approximately those for the case of imaginary factor.

c- In the case where a good phase approximation is desired, it will be necessary to use a smaller value of λ than in the case of a magnitude approximation.

It is noted that increasing λ may result in stability problems. It is easily seen from (1.18) that the distance between s_{-1} and s_o decreases by increasing λ until s_{-1} coincides with s_o at the value of λ given by the positive root of the equation,

$$\lambda^2 - \lambda \frac{\pi^2 \sigma_o}{\omega_o^2} - \frac{\pi^4}{4\omega_o^2} = 0 \qquad (1.19)$$

where

$$s_o = \sigma_o + j\,\omega_o, \qquad (1.20)$$

If λ is increased yet further such that $\beta_o \in U_{-1}$, then the inverse mapping $u \to s$ will give rise to a zero $s_o \in U_o$, which lies in the right half s-plane. We will throughout this thesis ensure that λ is

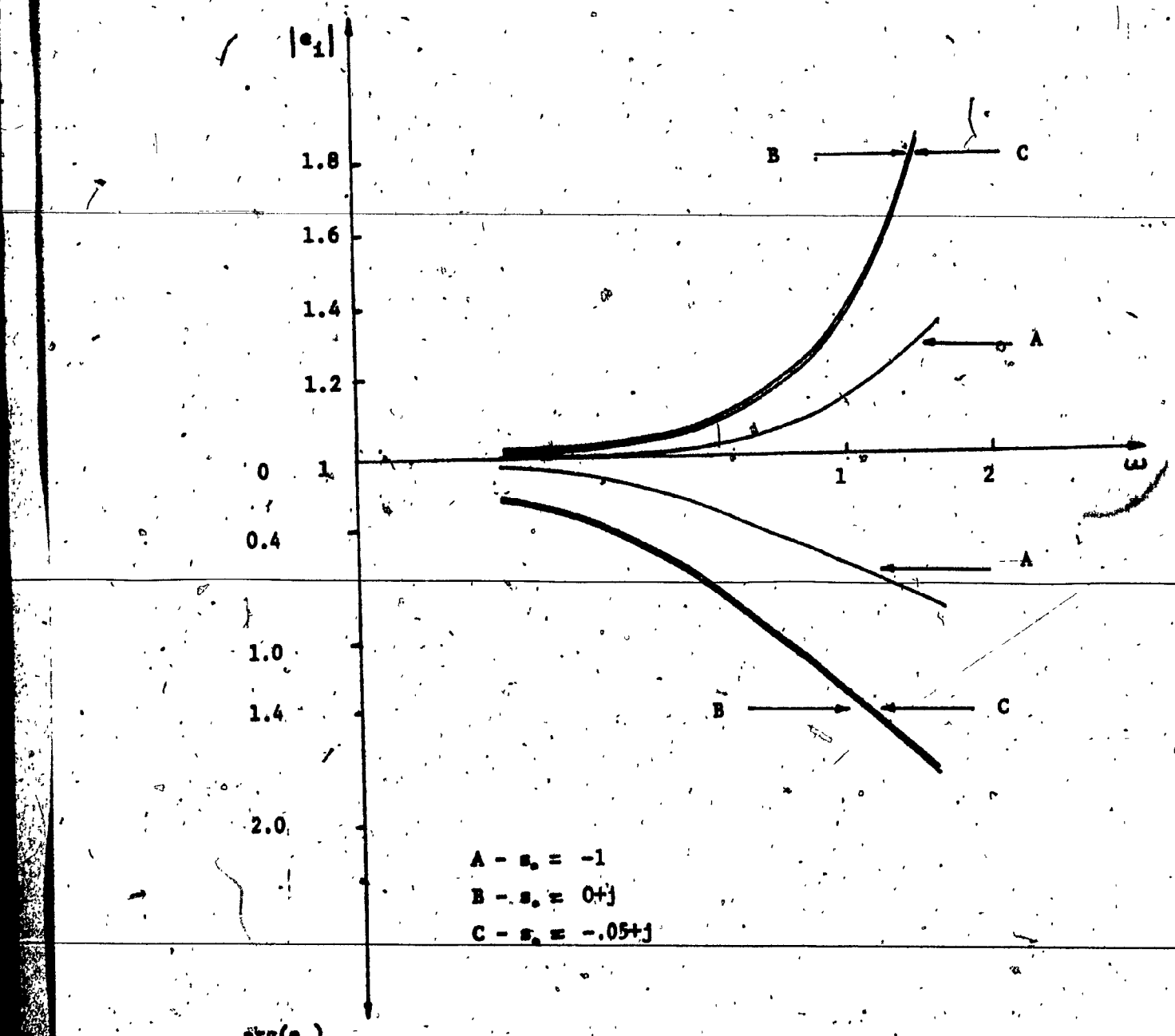

Figure 1.6: Approximation Error

chosen such that $\beta_o \in s_o$, which will be guaranteed if

$$\lambda < \lambda \text{ max} \qquad (1.21)$$

where λ max is the positive root of the equation (1.19).

1.6 SCOPE OF THE THESIS

In this work we are concerned with optimal design of distributed parameter networks. Throughout the thesis, specifications will be given for frequency responses of filters having low-pass, band-pass, high-pass, all-pass or notch characteristics. After an approximation to these specifications is found a design procedure is carried out to obtain an optimum performance criterion associated with the filter requirements.

In Chapter 2 the approximate realization of all-pole open circuit voltage transfer functions is considered. We start by the synthesis of a cascade of uniform $\overline{RC}$ lines which is assumed to approximate the given function. The synthesis is carried out through an optimization procedure which seeks to minimize substrate area. As a next step, frequency fit is incorporated into the performance criterion. Finally, substrate areas of distributed realizations are compared with those for lumped realizations for a series of specific examples. It will be concluded that a significant reduction in substrate area can often be obtained through the use of $\overline{RC}$ networks.

In Chapter 3 the realization of filters with complex poles and zeros of transmission are considered. The networks of Chapter 2 are incorporated here in a grounded active filter structure. The case of second order filter is discussed in detail and several designs are carried out for low-pass, band-pass and high-pass filters using an optimization procedure to minimize an objective function such as to guarantee a best approximation

and lowest sensitivities of the response to parameter variations while ensuring a stable operation. The possible advantages and disadvantages of the use of smoothly tapered $\overline{RC}$ lines in the design is investigated and the special case of an exponential line is considered.

Chapter 4 is a natural extension of Chapter 3 where the design of general biquadratic functions using $\overline{URC}$'s is studied in detail. Optimal designs are obtained as in Chapter 3 for the five different kinds of filters mentioned above. The effect of the amplifiers finite gain-bandwidth product on the circuit performance is investigated and a compensation scheme is introduced to increase the useful frequency range of the circuit. Experimental results are also obtained where some filters were built and compared with theoretical calculations.

The performance of the circuit is also compared to some other existing filters from the point of view of the effect of finite GB and its variation on the response.

Chapter 5 contains conclusions and suggestions for further work.

CHAPTER 2

OPTIMUM TRANSFER FUNCTION REALIZATION USING GROUNDED UNIFORM RC LINES

2.1 INTRODUCTION

In this chapter we consider the approximate realization of voltage transfer functions of the form:

$$T_d(s) = \frac{1}{\prod_i (1-s/\sigma_i)} \qquad (2.1)$$

as a cascade of commensurate $\overline{URC}$'s where σ_i's are distinct real axis poles.

Two specific problems are considered. First, we assume that an approximation for the required response is given and a realization is to be found such that the total area of the network is minimized. Next we assume that we are given the specification in the form of the equation (2.1) and are required to find a realization while minimizing an objective function which contains a measure of both the area of the minimized network and the deviation of its frequency response from the specification. Given that the frequency response of an approximate realization of equation (2.1) as a distributed network is acceptable, a criterion for deciding whether to use a lumped or a distributed realization is a comparison of the areas required. We will illustrate through examples that the minimum area required to realize approximately a $T_d(s)$ of the form (2.1) using $\overline{URC}$'s is comparable to, and often less than that of a design using lumped elements, the same technology being used in both cases.

2.2 THE SYNTHESIS

It will be shown in a later section of this chapter that $T_d(s)$ given by equation (2.1) can be approximately realized by a cascade of URC's having the open circuit voltage transfer function of the form (1.11) and associated impedance function of the form of (1.12). While the cascade synthesis of equation (1.12) can be carried out using Richard's theorem, it is rather difficult to relate the parameters of the realizing network to the coefficients of (1.12). It is also desirable from the point of view of computational accuracy to find a transformation for equation (1.12) by which the parameters of the network can be obtained using the least number of computations.

A transformation of (1.12) to the v-plane is adopted here where the transformation variables are given by:

$$u = \frac{p^2-1}{p^2} \qquad (2.2)$$

$$p = \cosh \sqrt{\lambda s} \qquad (2.3)$$

$$v = p-1 \qquad (2.4)$$

As a result of this transformation the negative real axis u-plane poles and zeros of $z_{11}(u)$ are mapped onto the line segment [0, -2] of the v-plane as shown in figure 2.1.

Another advantage of the u-v transformation will be the ease of adding constraints to the optimization problem to be formulated in section 2.3.2. The inclusion of these constraints will result in a rapid convergence to the optimal solution.

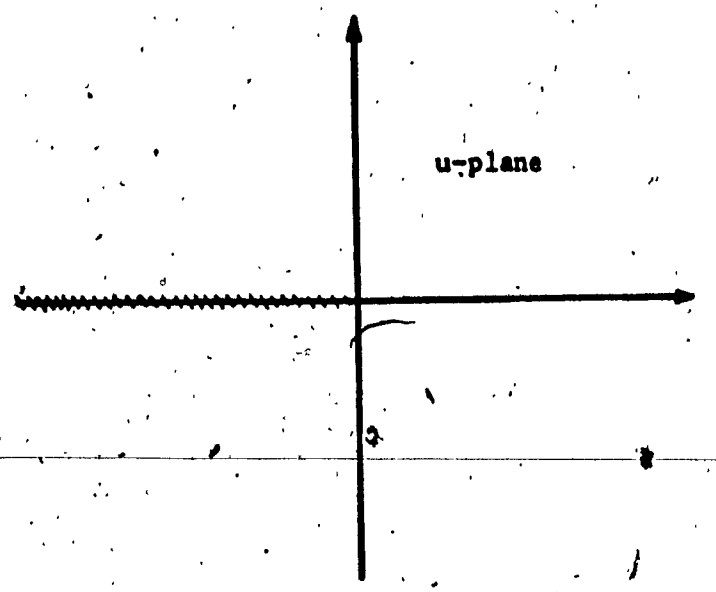
u-plane

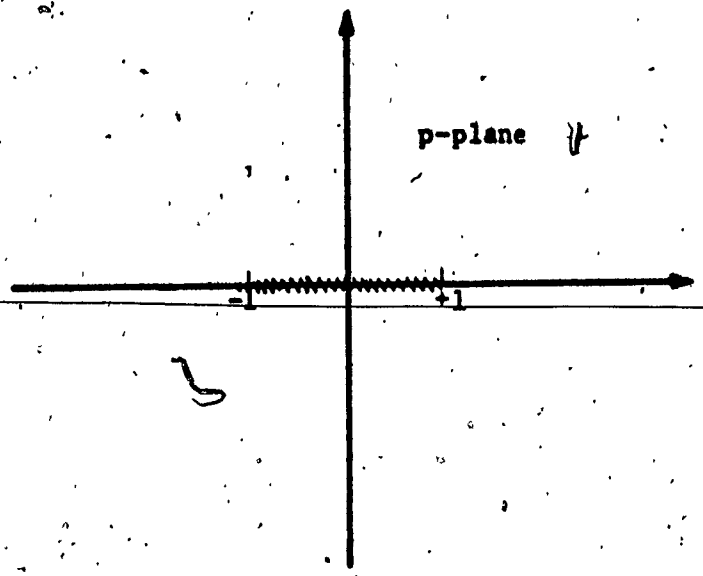
p-plane
-1
+1

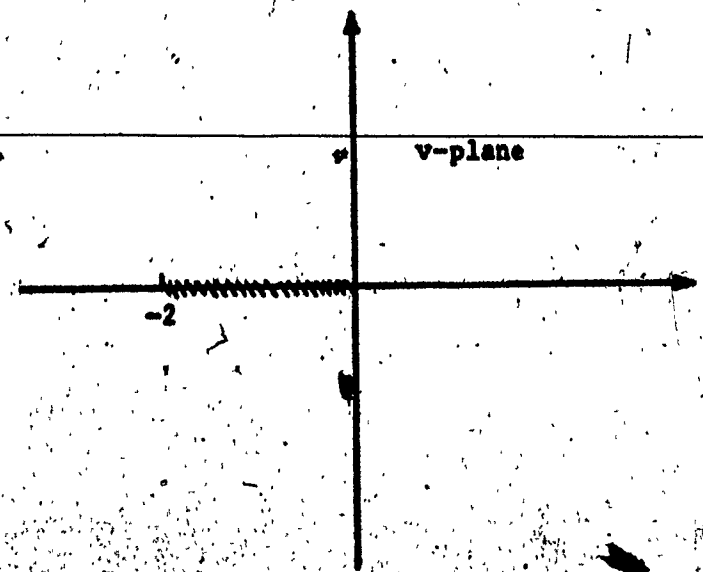
v-plane
-2

Using the above transformation, we can rewrite (1.12) as [48]

$$z_{11}[p(s)] = \frac{Hp}{q} \frac{(p^2 - f_{z1}^2) \quad (p^2 - f_{zk})^2}{(p^2 - f_{p1}^2) \ldots (p^2 - f_{pk}^2)} \tag{2.5}$$

where z_{11} has a p-plane zero or pole at the origin, or,

$$z_{11}(v) = \frac{v^{m+1} + a_m v^m + a_{m-1} v^{m-1} + \quad + a_0}{v^m + b_{m-1} v^{m-1} + \quad + b_0} \tag{2.6}$$

Where $H_1 > 0$, $0 \leq f_{pn}^2 < f_{zn}^2 \ldots < f_{p1}^2 < f_{z1}^2 \leq 1$ and $m = 2k$.

The number of $\overline{URC}$'s required to cascade synthesize this impedance function is one less than or equal to the degree of the numerator polynomial of qz_{11} [48]. Equation (2.6) can be expanded by continued fraction to yield an RL ladder network where the values of the resistances in the v-plane are directly related to the line sections resistances [48] of a cascade of n $\overline{URC}$'s.

2.3 AREA MINIMIZATION

In this section we consider the cascade realization of the open circuit voltage transfer function of the form:

$$T_d[u(s)] = \frac{1}{A_n} = \frac{(1-u)^{n/2}}{\prod_{i=1}^{k} (1 + u/\alpha_i)} \tag{2.7}$$

which have been obtained through an approximation of equation (2.1).

2.3.1 Preliminary Considerations

As a minimal area is the objective of the design, it is important to be able to relate the area of the network to the different parameters. For this we consider the configuration shown in figure 2.2 and note that:

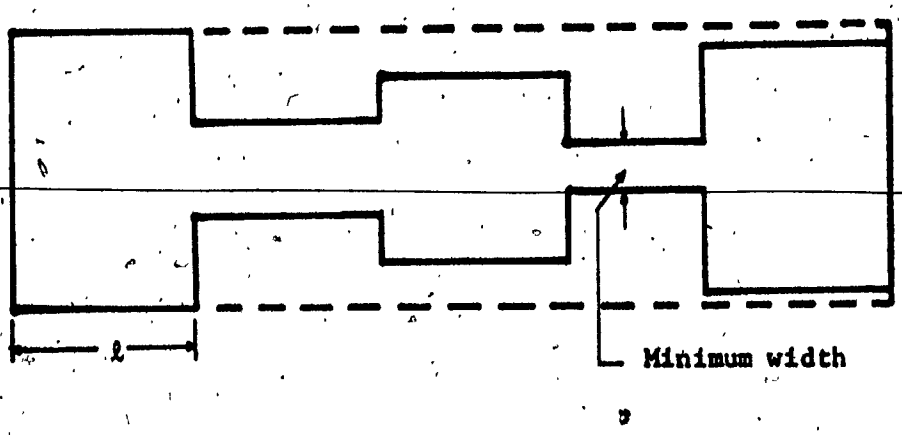

Figure 2.2: Layout of Cascade of $\overline{\text{URC}}$'s

(1) the length of the $\overline{URC}$ is proportional to $\sqrt{\lambda}$ which is fixed in our case.

(2) the minimum width of the line and consequently the maximum resistance is determined by the technology to be used in the fabrication.

(3) the width of the $\overline{URC}$ is proportional to $\frac{1}{R}$ where R is the line resistance.

Considering these points it can be seen that for a fixed technology and a fixed number of lines the area is proportional to the maximum ratio of the line resistances R_i.

2.3.2 Formulation of the Minimization Problem

In forming the impedance function (1.12) the choice of the poles γ_i was arbitrary. This suggests that a control of the ratios r of the different line resistances can be achieved through proper choice of the poles γ_i.

Denoting the ratio between R_i and R_j of lines i and j respectively by r_{ij}, we can formulate a minimax problem as follows:

Minimize the maximum of r_{ij} given that the v-plane pole and zeros p_i and z_i are interlaced on the negative real axis between 0 and -2.

In mathematical terms we can write, as problem A:

minimize $J(\underline{Y}) = \psi$

subject to the constraints:

$$g_\ell = \psi - r_{ij} > 0 \quad ; \quad i, j = 1,2 \ldots n \qquad (2.8)$$

$$\ell = 1, 2 \ldots n(n-1)$$

and

$$g_k = p_k - z_{k+1} > 0 \quad ; \quad i = 1,2 \ldots\ldots n-1 \qquad (2.9)$$

Where ψ is an upper bound on $\hat{r}$ as indicated in (2.8) and the minimization of ψ will result in $\hat{r}$ equal to the optimal value $\overset{*}{r}$.

$\underline{Y}$ is the parameter vector given by

$$\underline{Y} = \{p_i\} \; ; \; i = 1,\ldots\ldots n$$

The interlacing property indicated earlier is guaranteed through the inclusion of constraints (2.9).

Problem A is similar to the nonlinear programming problem † described by Fiacco and McCormick [51] - [52] and stated in appendix A. The fact that problem A satisfies the conditions for the existance of a solution, is proved in appendix B.

It immediately follows from the proof in appendix B that we can write the following theorem:

Theorem 2.1

Let $z_{11}(v)$ be an RL impedance function of v having fixed zeroes and arbitrary poles which is realized as a cascade of $\overline{\text{URC}}$'s. Then there exists some pole distribution such that the ratio, $\hat{r}$, of the maximum to the minimum line width of the $\overline{\text{URC}}$'s has a global minimum $\overset{*}{r}$.

The objective function:

$$J_1 = \psi \qquad (2.10)$$

was incorporated into a digital computer program based on the Sequential Unconstrained Minimization Technique (SUMT) [53] - [54] and solved on a CDC 6400 computer. A flow chart is given in Appendix D.

---

† See footnote on page 41.

Initial values of γ_i are chosen, the u-plane impedance function (1.12) is transformed into the v-plane (equation (2.6)), and then the values R_i are calculated. The values of p_i's are then varied as indicated in Appendix D to obtain an optimum solution.

In order to obtain a more uniform distribution of the line widths an objective function of the form:

$$J_1 = \sum_{i=1}^{n} \frac{R_{max}}{R_i} (R_{max} - R_i) \qquad (2.11)$$

was also used for problem A instead of ψ where:

$$R_{max} = \max \{R_i\} \quad ; \quad i = 1, \ldots, n$$

2.4 EXAMPLES

Transfer functions with different pole distributions were realized by minimizing (2.10) and 2.11). Results for 4,5 and 6 section lines are shown in table (2.1). An indication of the improvement obtained through optimization can be seen by comparing columns 3 and 5 of table 2.1. The results using objective function J_1 are shown in column 4 of table 2.1 and in figures 2.3.a and 2.3.b where a more uniform distribution is obtained. This is of course at the expense of a larger value for r^*. Different controls on the shape of the distributed structure can be achieved through the use of other forms of objective functions.

2.5 THE OPTIMIZATION

As a first step towards incorporating frequency fit into the optimization procedure, we now include λ as a part of the vector $\underline{Y}$.

TABLE 2.1

MINIMIZED $\hat{r}$ FOR A CASCADE OF $\overline{\text{URC}}$'s

u-plane poles of $T_d(u)$	Number of line-sections	$\hat{r}^*$ using (2.10)	$\hat{r}^*$ using (2.11)	$\hat{r}^*$ for arbitrary design
-.333, -.61	4	53.1328	53.6351	353.7215
-.333, -.61, $-\infty$	5	45.9805	46.0434	437.946
-.15, -1.29, -12.3	6	5.7651	6.1767	251.185
-.268, -1.79, -21.9	6	30.9028	31.718	7165.49
-.35, -1.45, -18.7	6	44.4842	45.2896	505.107
-.01, -1.31, -14.9	6	41.6776	43.6054	102.467
-.03, -1.59, -10.36	6	3.6828	5.4532	260.456
-.07, -1.115, -25.65	6	1.4383	1.452	296.665
-.01, -1.07, -13.9	6	17.9182	24.25	61.1613

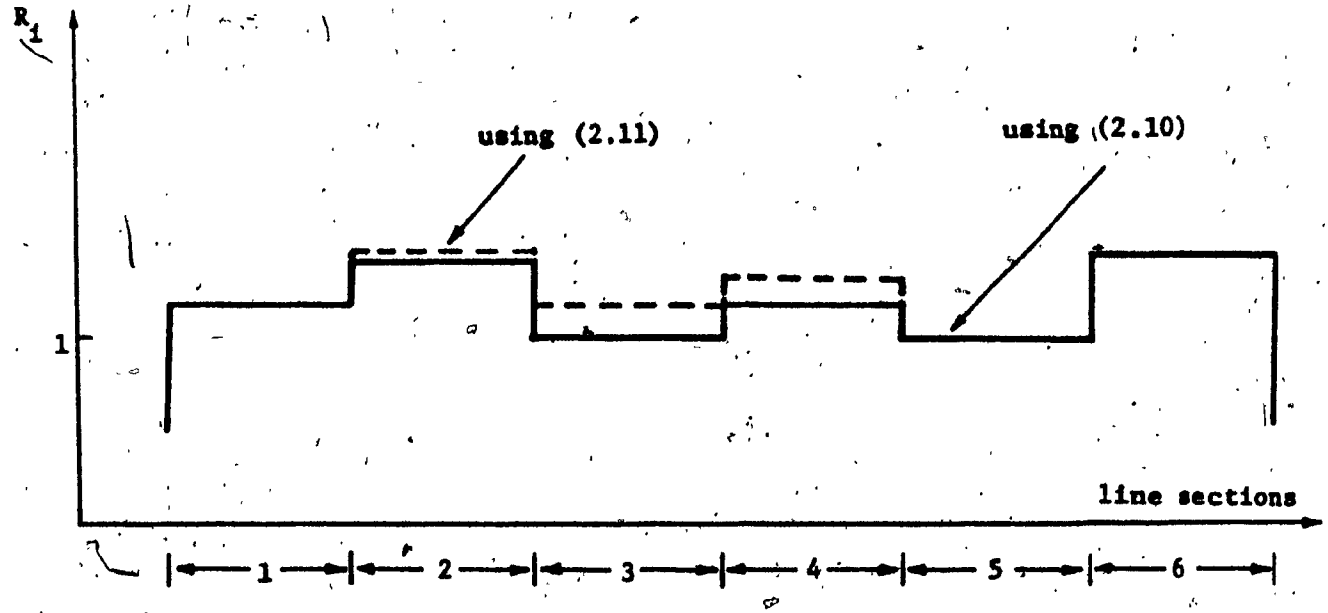

Figure 2.3.a: Optimized Profile of Cascade of $\overline{URC}$'s

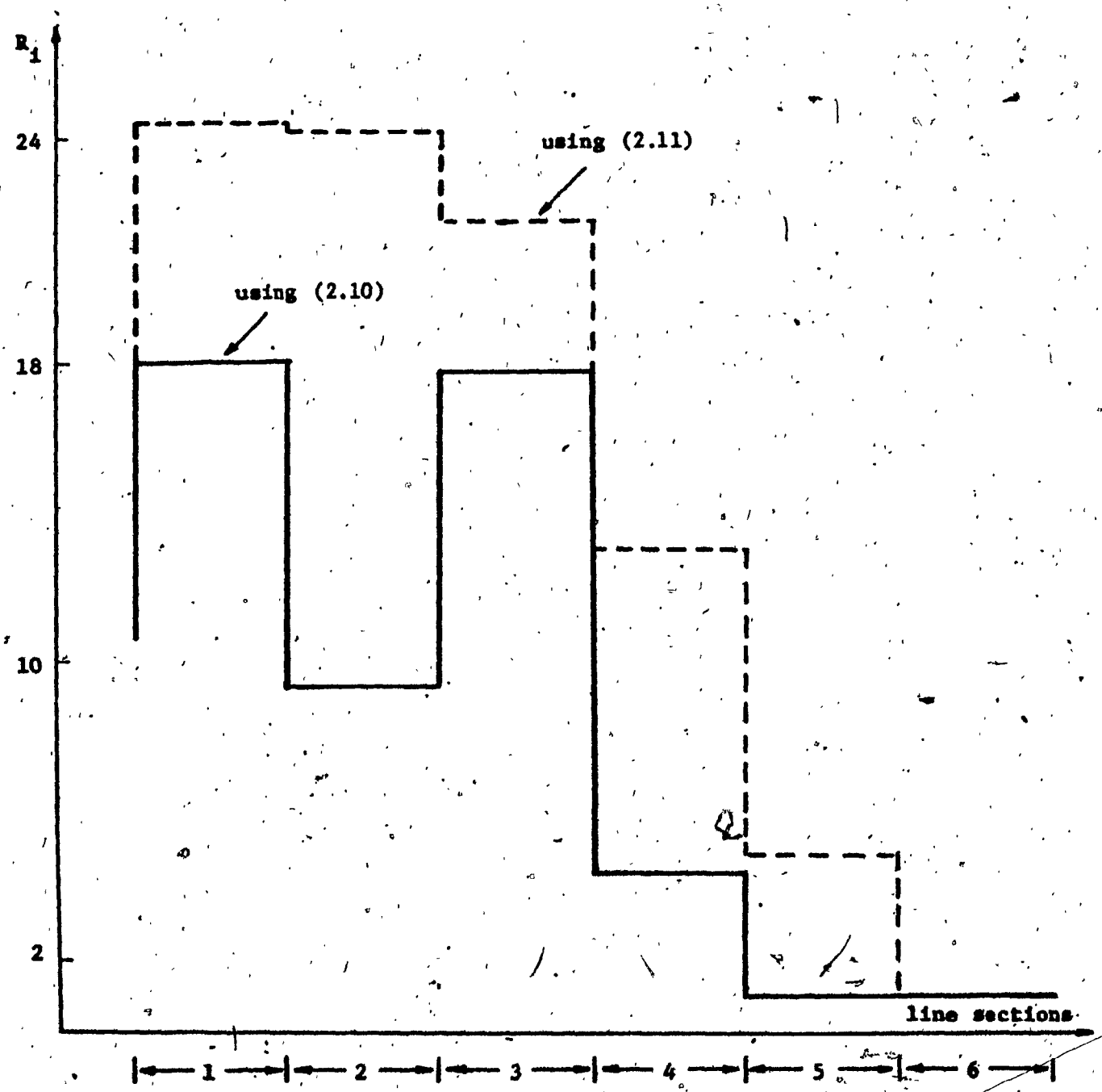

Figure 2.3.b: Optimized Profile of Cascade of URC's

More specifically, we formulate the problem as follows:

$$\text{minimize } J_2 = \psi$$

subject to:

$$\left.\begin{aligned} g_\ell &= \psi - r_{ij}(\bar{Y}) > 0 \quad ; \quad i,j = 1,2 \ldots n \\ g_k &= p_k - z_{k+1} > 0 \quad ; \quad k = 1,2 \ldots (n-1) \\ g_n &= \lambda_{max} - \lambda > 0 \end{aligned}\right\} \text{B}$$

where $\bar{Y} = \{p_1, p_2 \ldots p_{m-1}, \lambda\}$

where ψ and g_i are the same as introduced in problem A. This problem is similar to problem A in that it can be solved using the SUMT. This similarity is a result of the following corollary to theorem 1.

Corollary 1

Let $z_{11}(v)$ of theorem 2.1 be used to approximate equation (2.1) where the RC product of the lines (λ) is arbitrary. Then there exists some value of λ together with some pole distribution such that the ratio f possesses a global minimum, f^*.

Proof: From the proof of Theorem 2.1 it is seen that the relation between f and the pole positions, P_i's, define a convex hull. Next we note that the relation between λ and all p_i's is monotonic and single valued as proved in Appendix C. Combining the two results we see that the relation between f and λ is convex. Hence we have the proof.

Although the choice of $\underline{Y}$ has thus far been influenced only by requiring the ratio f to be minimum, it was found, in all examples tried, that the resulting frequency response approximates specification (2.1)

fairly well. We can improve the goodness of fit, still further, by including in the objective functions a term characterizing the error in the frequency response. The objective function now takes the form:

$$J_3 = W_1 \psi + W_2 f_2 [e(\omega)] \tag{2.12}$$

It is of course to be expected that there will be a trade-off between ψ and $f_2 [e(\omega)]$. The function f_2 is chosen to be:

$$f_2 [e(\omega)] = \Sigma_i a_i e(\omega_i) \tag{2.13}$$

where

$$e(\omega) = \text{Abs}\left(\log \frac{|T_d (\omega)|}{|T_a (\omega)|} \right) \tag{2.14}$$

T_d is the desired response, T_a the actual response, ω_i's are selected frequencies in the range of interest, W_1, W_2 and a_i's are suitably chosen weighting constants.

2.6 CHOICE OF NUMBER OF SECTIONS

As seen from equation (2.5), the cascade structure may be designed to contain either m or m+1 sections. The effect of this choice on the minimized value r^* and on the resulting frequency response was investigated by considering a number of specific cases.

Typical results are shown in table 2.2 and Figure 2.4. It can be seen that although there is a slight improvement in the frequency response through using m+1 instead of m sections, there is no clear indication as to which choice will result in a smaller area. We will restrict ourselves to realizations using the smaller number of sections.

TABLE 2.2

COMPARISION BETWEEN AREAS FOR DIFFERENT NUMBER OF LINES

Transfer function	Result with n = m		Result with n = m + 1		Ratio $\frac{A_1}{A_2}$ *
	λ	r^*	λ	r^*	
1/ (s + 1) (s/2 + 1)	0.8467	13.106	0.4630	19.3097	0.993
1/ (s/10 + 1) (s + 1)	0.1424	1.1312	0.0909	1.1585	1.221
1/ (s/99 + 1) (s/10 + 1)	0.01481	1.2594	0.00867	1.607	0.757

* A_1 = total area when n = m

A_2 = total area when n = m + 1

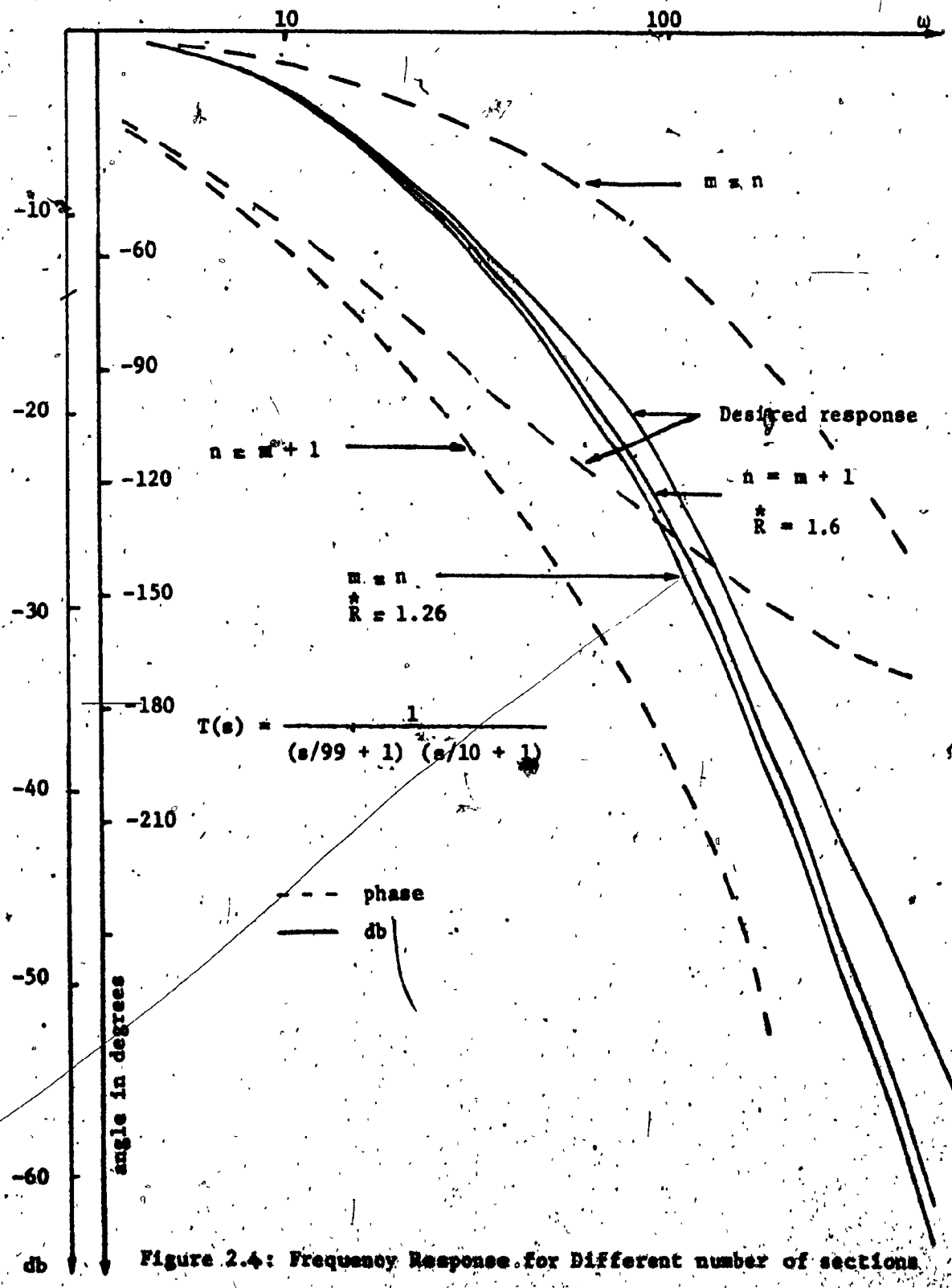

Figure 2.4: Frequency Response for Different number of sections

2.7 EFFECT OF WEIGHTING CONSTANTS

In this section we examine the effect of varying the weighting constants W_2 and a_i specified in equation (2.13). To study the effect of W_2 on the design we specify the a_i's and vary W_2. One of the transfer functions used for the study was:

$$\frac{1}{(s/10 + 1)\ (s + 1)}$$

Typical results are shown in figure 2.5 for the case $a_i = 1$ and in figure 2.6 for the case $a_i = i$. Both figures indicate that the improvement in the frequency response fit is obtained at the expense of increased values of r^*. Finally, in figure 2.7 it is seen that the use of increasing weighting coefficients results in a better frequency response but again in higher values of r^*.

2.8 COMPARISON BETWEEN LUMPED AND DISTRIBUTED REALIZATIONS

The purpose of this section is to demonstrate through examples that, in many cases distributed realizations result in a considerable saving of substrate area when compared with lumped ladder realization of transfer functions of the form (2.1).

In order to have a valid basis for comparison, (2.1) is realized in such a way that the total area required for all capacitors and resistors is minimized.[3] The objective function used for this purpose is:

$$J_4 = R_t + KC_t \qquad (2.15)$$

where

$$R_t = \Sigma R_i, \quad C_t = \Sigma C_i$$

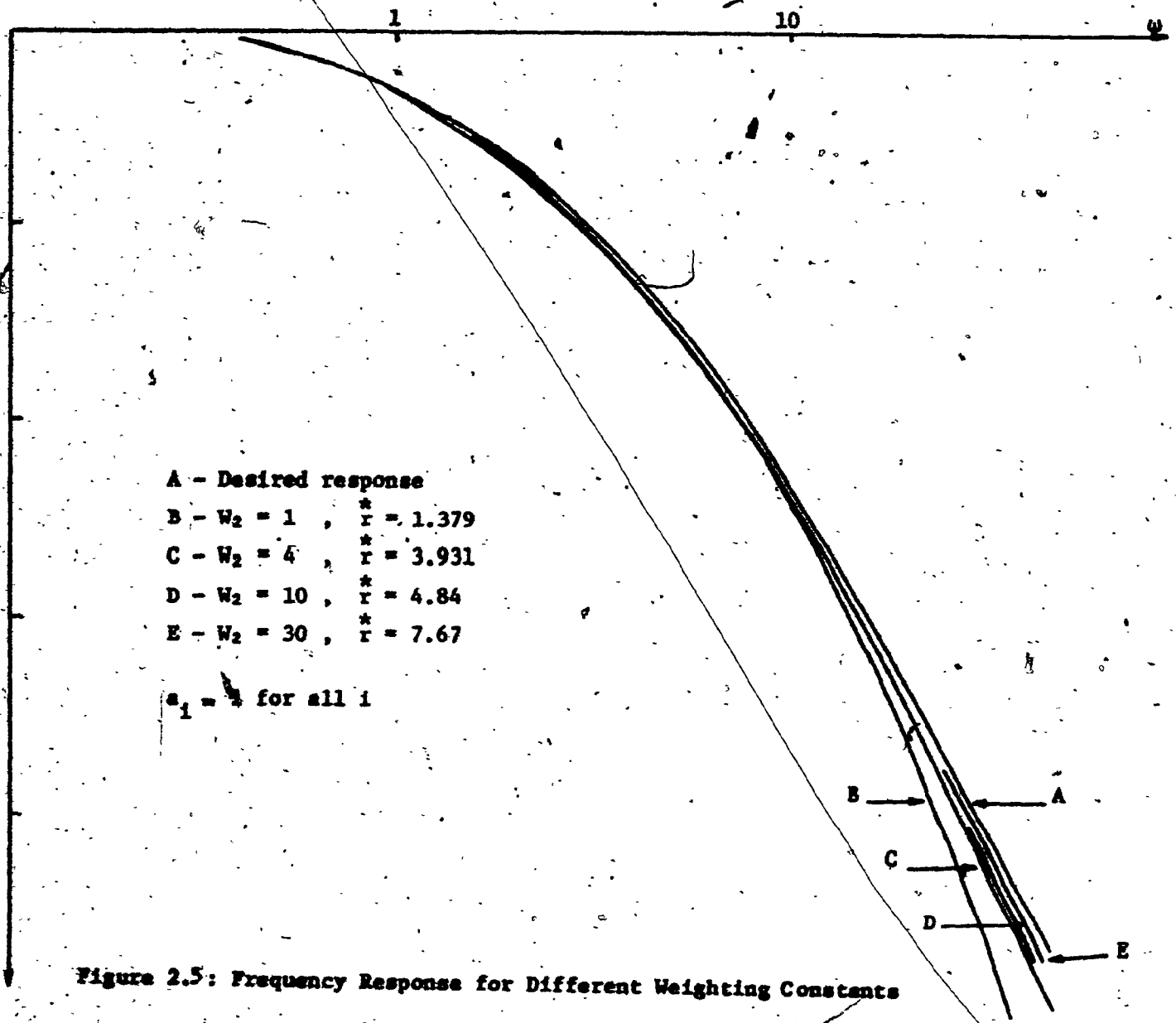

Figure 2.5: Frequency Response for Different Weighting Constants

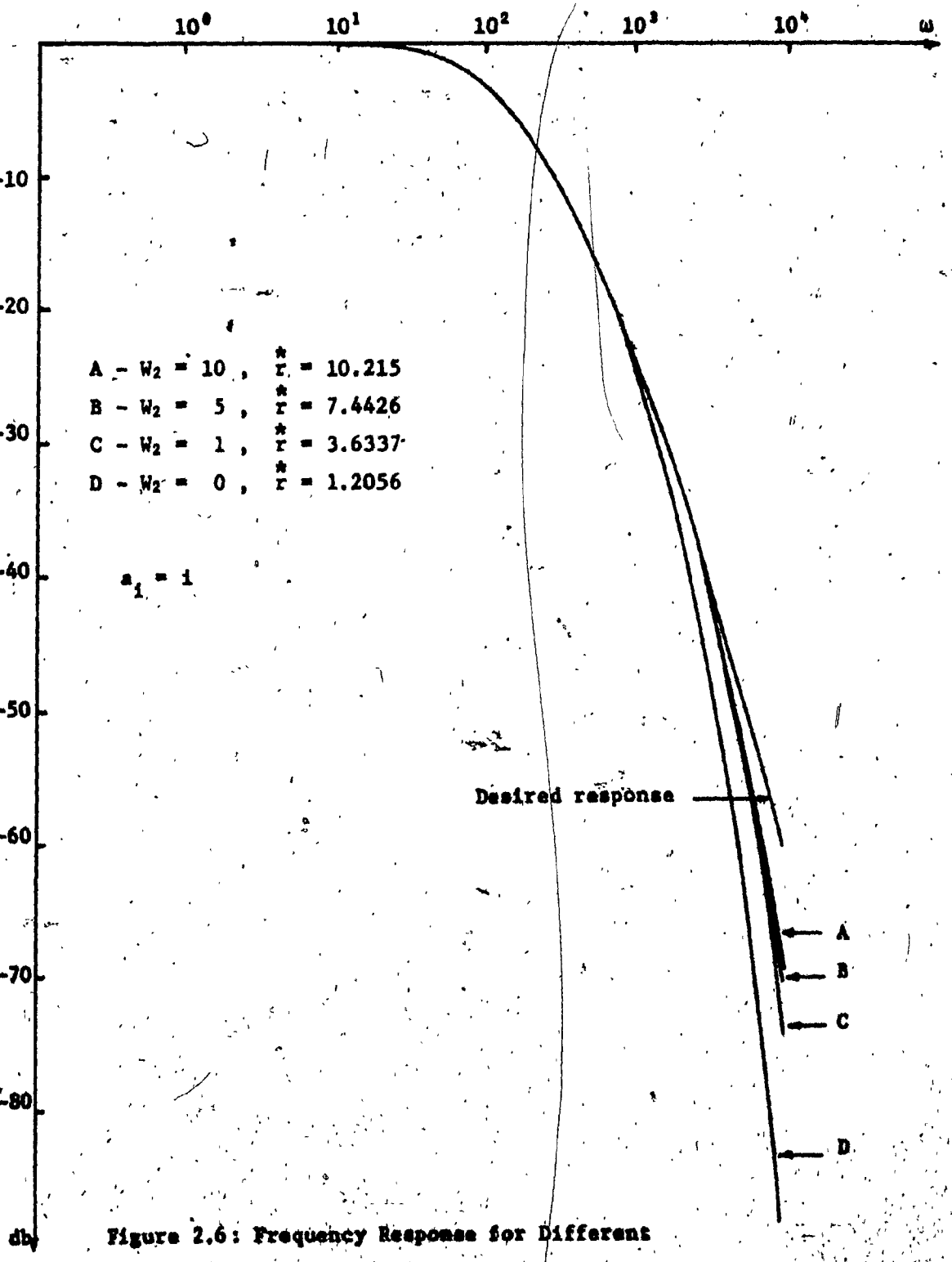

Figure 2.6: Frequency Response for Different Weighting constants With Increasing a_1

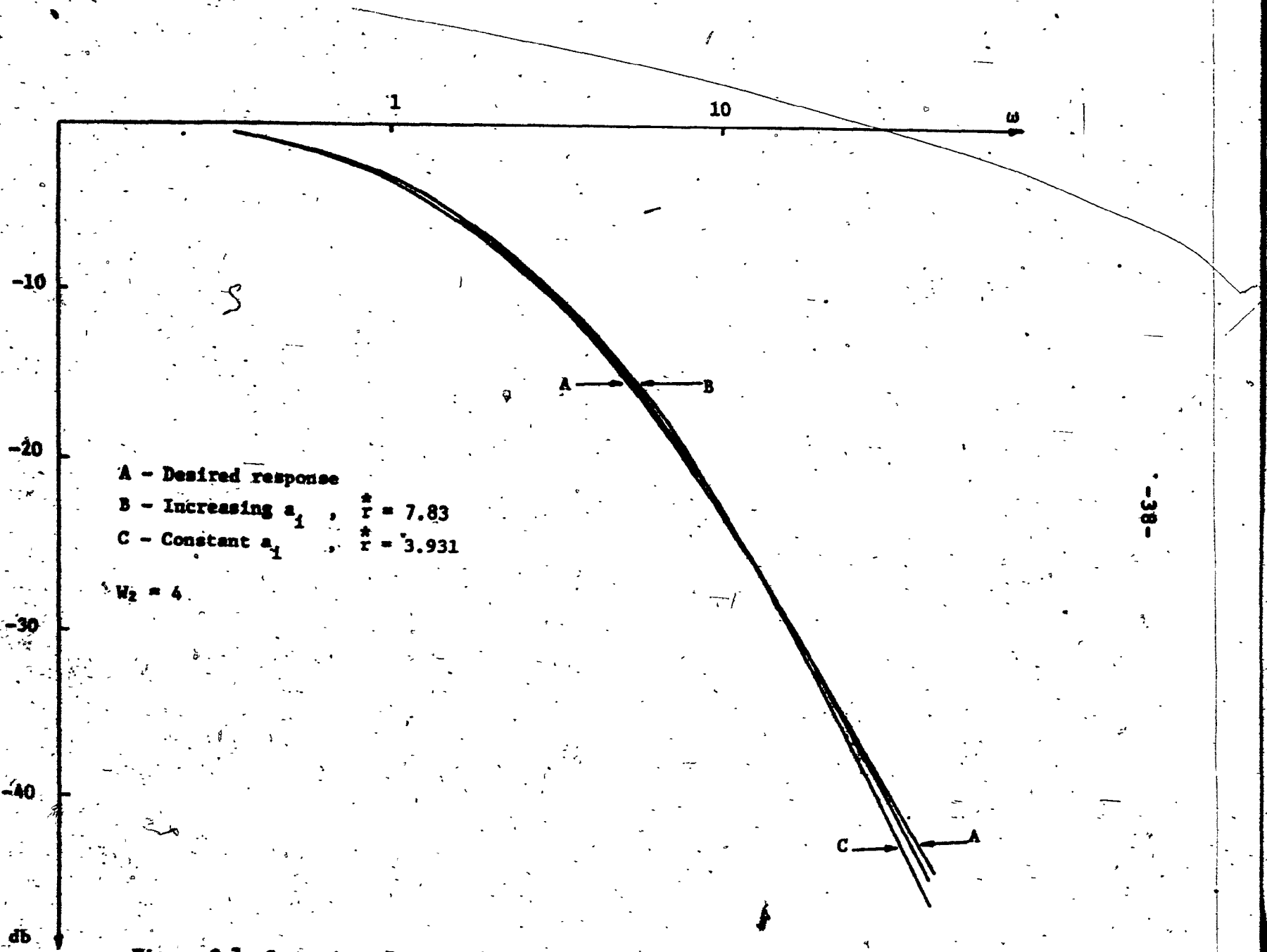

Figure 2.7: Comparison Between Using Increasing Weights And Constant Weights

R_1 and C_1 are element values and K is a constant depending on the technology used in the fabrication. For a thin film tantalum and tantalum dioxide fabrication process, the value of K was found to be equal to 9.04×10^{12} Ω/F [55].

The optimization procedure was similar to that described in section 2.6 above.

We assume that the distributed elements are fabricated by the same technology, i.e. values of capacitance per square and resistivity are the same as those used for the lumped realization. The maximum line width used was determined to be that which could be easily fabricated with good tolerences. This was taken to be 5 mils [55].

Total areas for the distributed realizations were calculated in two ways. In the first method, the area A_1, is the product of the line length, the number of line sections and the maximum line width. In the second method, A_2 is the sum of the line section areas. The actual area will lie somewhere between these two limits.

A large number of examples were solved, with $W_2 = 1$, and a representative sample of them appear in table 2.3. It can be seen that areas required for lumped and distributed realizations are at worst close, and that in many cases considerable savings can be effected through the use of cascaded $\overline{URC}$'s

2.9 CONCLUSION

In this chapter the frequency response of equation (2.1) was realized with a very good accuracy using a cascade of commensurate

TABLE 2.3

COMPARISON BETWEEN AREAS OF DISTRIBUTED AND LUMPED REALIZATIONS

Transfer function	Distributed Realization				Lumped ladder realization		
s-plane poles	λ	r^*	area in cm^2		elements		Area of components cm^2
			A_1	A_2	KΩ	μF	
-400, -1k	0.11×10^{-2}	13.5711	1.71	0.72	15.35,138.2	0.087,0.011	1.039
-2000, -7K	0.145×10^{-3}	7.1728	0.329	0.169	11.92,38.64	0.019,0.008	0.295
-1000, -10K	0.883×10^{-4}	3.6337	0.1298	0.0704	15.04,22.47	0.012,0.024	0.363
-5000, -20K	0.486×10^{-4}	5.8175	0.153	0.0878	5.99,16.65	0.013,0.008	0.213
-10K, -20K	0.545×10^{-4}	33.49	0.938	0.288	3.14,28.27	0.021,0.003	0.248
-50K, -1M	0.708×10^{-6}	10.067	0.032	0.0114	2.27,2.77	0.0008,0.004	0.0484
-500, -1000, -10K	0.131×10^{-3}	49.94	3.24	0.672	6.76 8.69 131.72	0.028 0.083 0.011	0.83
-1000, -3K, -8K, -10K	0.104×10^{-3}	24.86	1.93	0.835	5.1 10.8 27.2 57.7	0.036 0.032 0.008 0.005	1.247

$\overline{\text{URC}}$'s. The parameters of the different line sections were chosen so as to minimize the overall area required for the network. For this, an optimization procudure was adopted where the design problem was formulated as a convex programming problem and shown to have a unique solution. This problem was solved on the digital computer where the convergence of the solutions was very fast, the average time being five seconds for a six section cascade.

When it was assumed that the approximation of (2.1) has been fixed, the saving in area using the optimization procedure as opposed to random design was very considerable, the optimum solution requiring 0.5% of the area needed for a design where the choice of the poles of $qz_{11}(u)$ was arbitrary.

The problem of achieving a desired frequency response while minimizing substrate area was studied next. Good fits were achieved with little increase in substrate area. Finally, optimally designed distributed networks were compared to minimial area lumped networks realizing the same transfer functions. Although no definitive conclusion could be drawn, it was found that the substrate area required for a distributed realization was at worst close to that needed for a lumped design and that very often considerable savings could be effected through the use of a distributed structure.

---

† Although the inequalities (2.8) - (2.9) differ from the conventional nonlinear programming formulation, problem A could still be solved using an interior penalty function due to the fact that the objective function tends to infinity at the boundary of the feasible region.

CHAPTER 3

ACTIVE SYNTHESIS OF TRANSFER FUNCTIONS USING $\overline{RC}$ LINES

3.1 INTRODUCTION

In Chapter 2 optimization techniques were used to design passive filters with negative real axis poles. In this chapter, optimization techniques were again used to study a new active filter with grounded $\overline{URC}$'s and operational amplifiers, proposed for the realization of the general biquadratic open circuit voltage transfer function. The filter is constructed using grounded $\overline{URC}$'s and operational amplifiers. Element values for this circuit are chosen in order to optimize certain characteristics related to the overall performance of the filter. The possible advantages of using tapered $\overline{RC}$ lines ($\overline{TRC}$) is also investigated through consideration of the exponential line ($\overline{ERC}$) and the cascade of two commensurate $\overline{URC}$'s as special cases.

3.2 THE ACTIVE STRUCTURE

The network shown in figure 3.1 will be used in this chapter to approximately realize rational voltage transfer functions of the form:

$$T(s) = \frac{a_1 s^2 + b_1 s + c_1}{d_1 s^2 + e_1 s + f_1} = H \frac{(s - s_z)(s - \overline{s}_z)}{(s - s_p)(s - \overline{s}_p)} \qquad (3.1)$$

Assuming ideal amplifiers, the open circuit voltage transfer function of the structure in figure 3.1 can be written as

$$T = \frac{K_5 K_3 A_1 A_2 + (K_5 + K_8 K_1 K_6) A_1 + K_1 K_3 A_2 + K_1}{A_1 A_2 - K_2 A_1 - K_2 A_2 - K_4} \qquad (3.2)$$

Where N1 and N2 are made up of interconnections of $\overline{RC}$ lines and are assumed to have open circuit voltage transfer functions

$$T_1 = 1/A_1, \qquad T_2 = 1/A_2 \qquad (3.3)$$

Assuming N1 and N2 to be cascades of $\overline{URC}$'s, we have

$$A_1(u) = \frac{1}{T_1(u)} = \frac{\prod_{i=1}^{k_1} (1 + u/\alpha_i)}{(1-u)^{n_1/2}} \qquad (3.4)$$

where n_1 is the number of lines in the cascade (N1) and $k_1 = n_1/2$ for n_1 even and $(n_1 - 1)/2$ for n_1 odd. A similar relation holds for N2.

Equations (3.2) and 3.4) indicate that the structure can be used to realize filters of arbitrary degree in u through a suitable choice of the number of sections in each cascade. However, it is well established [30] - [34] that sensitivity consideration often makes it preferable to realize higher order filters by cascading second order sections. We shall therefore restrict our study to second order functions.

3.3 THE SECOND ORDER FILTER

To obtain a second order function we let N1 and N2 consist of two sections each. Equation (3.4) can now be written as:

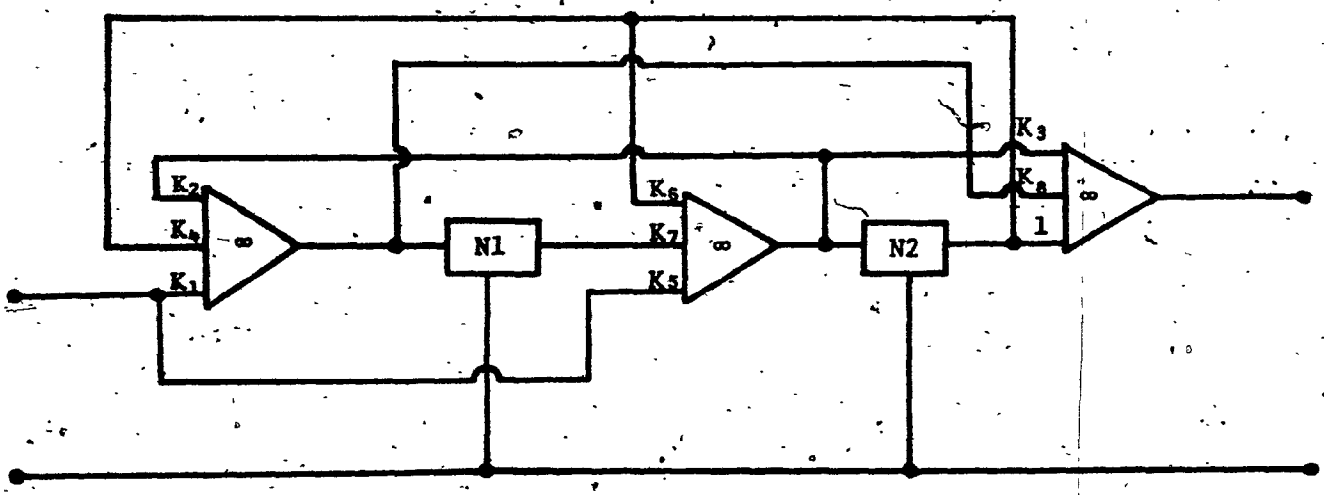

$K_6 = K_2$, $K_7 = 1$, $K_8 = 0$

Figure 3.1: Active Filter Structure

$$A_1(u) = \frac{1}{T_1(u)} = \frac{1 + r_1 u}{1 - u} \tag{3.5}$$

where

$$r_1 = \frac{R_{11}}{R_{21}} \tag{3.6}$$

is the ratio between the resistances of the lines in N1. A similar statement holds for N2.

Using (3.2) and (3.5) the overall transfer function can be written as:

$$T(u) = \frac{\begin{array}{l}(K_5K_3r_1r_2 - K_5r_1 - K_1K_3r_2 + K_1 - K_1K_8K_6r_1)\,u^2 \\ + (K_5K_3(r_1+r_2) + K_5(r_1-1) + K_1K_3(r_2-1) - 2K_1 + K_1K_8K_6(r_1-1))u \\ + (K_5K_3 + K_5 + K_1K_3 + K_1 + K_1K_8K_6\end{array}}{\begin{array}{l}(r_1r_2 + K_2(r_1+r_2) - K_4)\,u^2 + (r_1 + r_2 - K_2(r_2-1) - K_2(r_1-1) + 2K_4)u \\ + 1 - 2K_2 - K_4\end{array}} \tag{3.7}$$

Using the approximation procedure of Chapter 2, the parameters (λ_1 r_1, r_2 and all K's) in equation (3.7) can be chosen such that the principal s-plane poles and zeros of (3.7) coincide with those of (3.1).

It can be seen from the above discussion that there is a large number of parameters which could be used as variables in an optimization program. There is also a possibility of adding two more parameters if we consider the case when the lines in N1 have a different RC product than those in N2. Letting $\lambda_1 = a_1\lambda$ and $\lambda_2 = a_2\lambda$ be the RC product of lines in N1 and N2 respectively and rewriting (3.7) as a function of $u_1 = \tanh^2 \sqrt{a_1\lambda s}$ and $u_2 = \tanh^2 \sqrt{a_2\lambda s}$, we may add a_1 and a_2 to the list of parameters.

3.4 PRELIMINARY CONSIDERATIONS

It is our purpose in this section to carry out a preliminary investigation of the effect of some of the variables listed above in order to determine if they could be preset and thus eliminated from the optimization problem.

We will, as a first step, restrict ourselves to a study of the denominator of equation (3.7). There will be no loss of generality in doing this since the conclusions reached will also be applicable to the numerator.

Considering the denominator of equation (3.1), we may define the quantities:

$$\omega_{od} \simeq |s_p|$$

and

$$Q_d \simeq \frac{|s_p|}{2R_e\, s_p}$$

where it is assumed that $|s_p| >> 2Re\ s_p$

These two quantities are sufficient to characterize equation (3.1). We will use ω_o and Q to describe the associated characteristics of equation (3.7).

We can now list the parameters needed for our study as

$$\underline{Y} = \{K_2,\ K_4,\ \lambda,\ r_1,\ r_2,\ a_1,\ a_2\}$$

where a_1 and a_2 are set equal to unity for the rest of the chapter there being no apparent reason for using noncommensurate lines. One or more of these parameters was preset and the remainder allowed to vary in order to achieve a minimum value of the performance criterion.

$$J = [Q-Q_d]^2 + [\omega_o + \omega_{od}]^2 \qquad (3.8)$$

Sensitivities† S_y^Q and $S_y^{\omega_o}$ where $y \in \underline{Y}$ were then calculated for several designs with preset values of the different parameters. It was found in all cases that $S_y^{\omega_o} < 0.5$ and we therefore limit our presentation here to results of S_y^Q. Two sets of results relating to Q sensitivity are of particular interest. The first set (figure 3.2) show the effect of λ on the various sensitivities and indicates that a value of λ can be found to give minimal sensitivities.

The second set (figure 3.3) show the variation of the various sensitivities due to change in r_1 and r_2. In particular, figures 3.3 a. and 3.3 b. show that the variation of $S_{K_2}^Q$ and $S_{K_4}^Q$ as r_1 changes, is a mirror image to the variation of $S_{K_2}^Q$ and $S_{K_4}^Q$ when r_2 changes. Figures 3.3 c. and 3.3 d. show that an increase in r_2 results in an increase in $|S_{a_2}^Q|$ and $|S_{r_2}^Q|$ and a decrease in $|S_{a_1}^Q|$ and $|S_{r_1}^Q|$. The same effect will also result from a decrease in r_1. Finally, we note that $|S_{a_1}^Q| = |S_{a_2}^Q|$ and $|S_{r_1}^Q| = |S_{r_2}^Q|$ when $r_1 = r_2$. It would therefore seem reasonable to preset $r_1 = r_2 = r$.

---

† Expressions for sensitivities of Q and ω_o are derived in Appendix E.

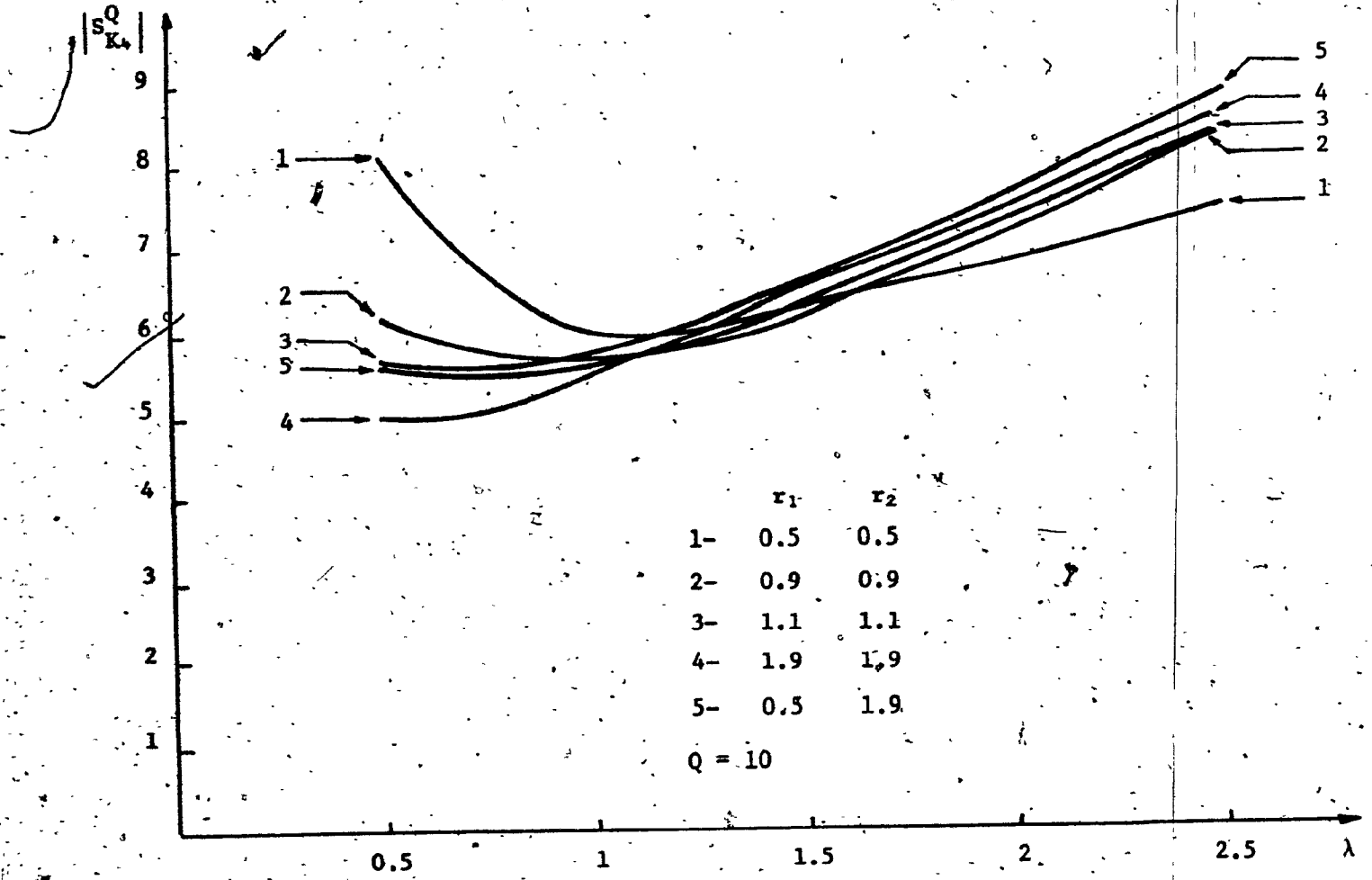

Figure 3.2.a: $S^Q_{K_4}$ - λ Relation

Using Cascades of Two $\overline{URC}$'s

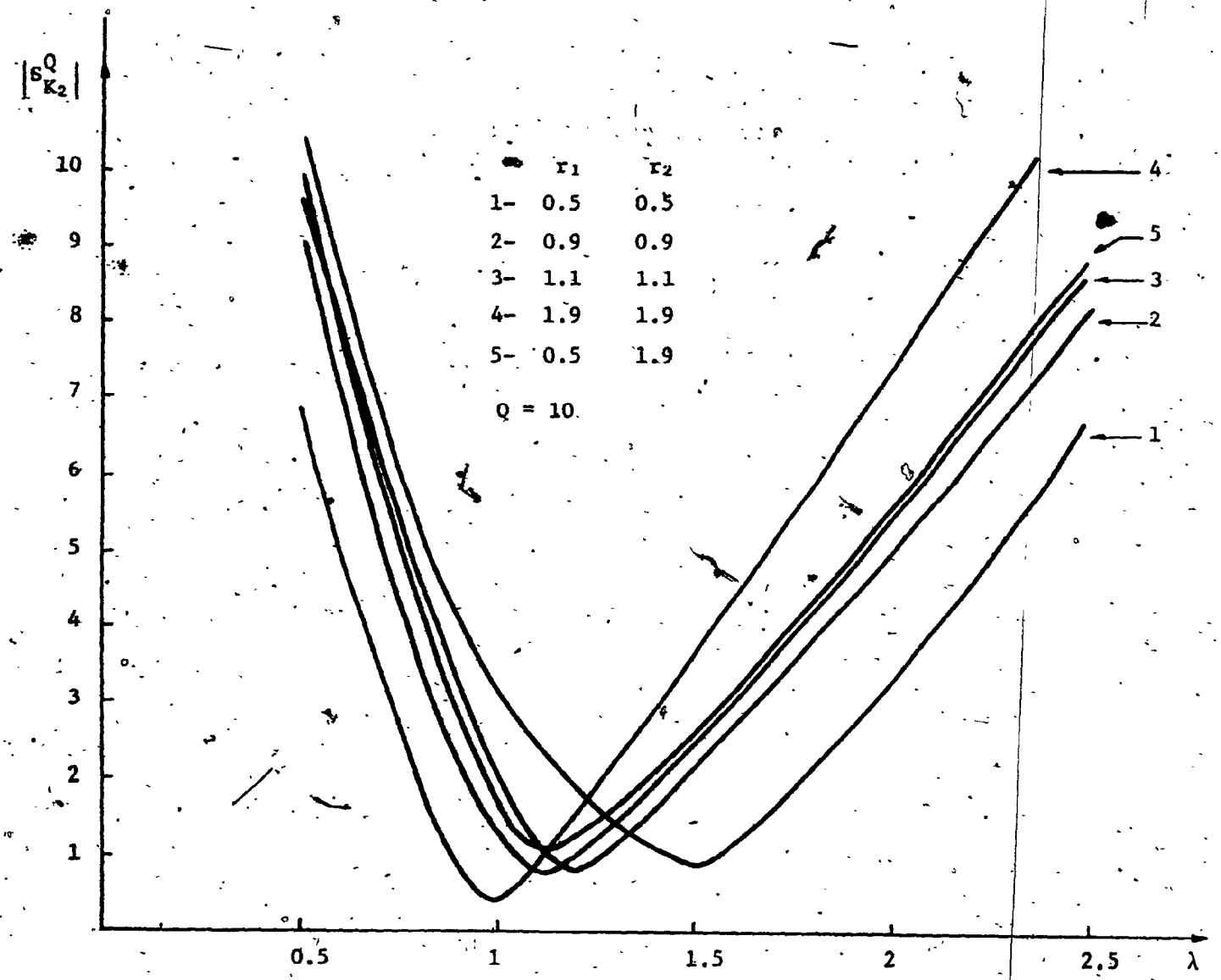

Figure 3.2.b: $S^Q_{K_2}$ - λ Relation

Using Cascades of Two $\overline{URC}$'s

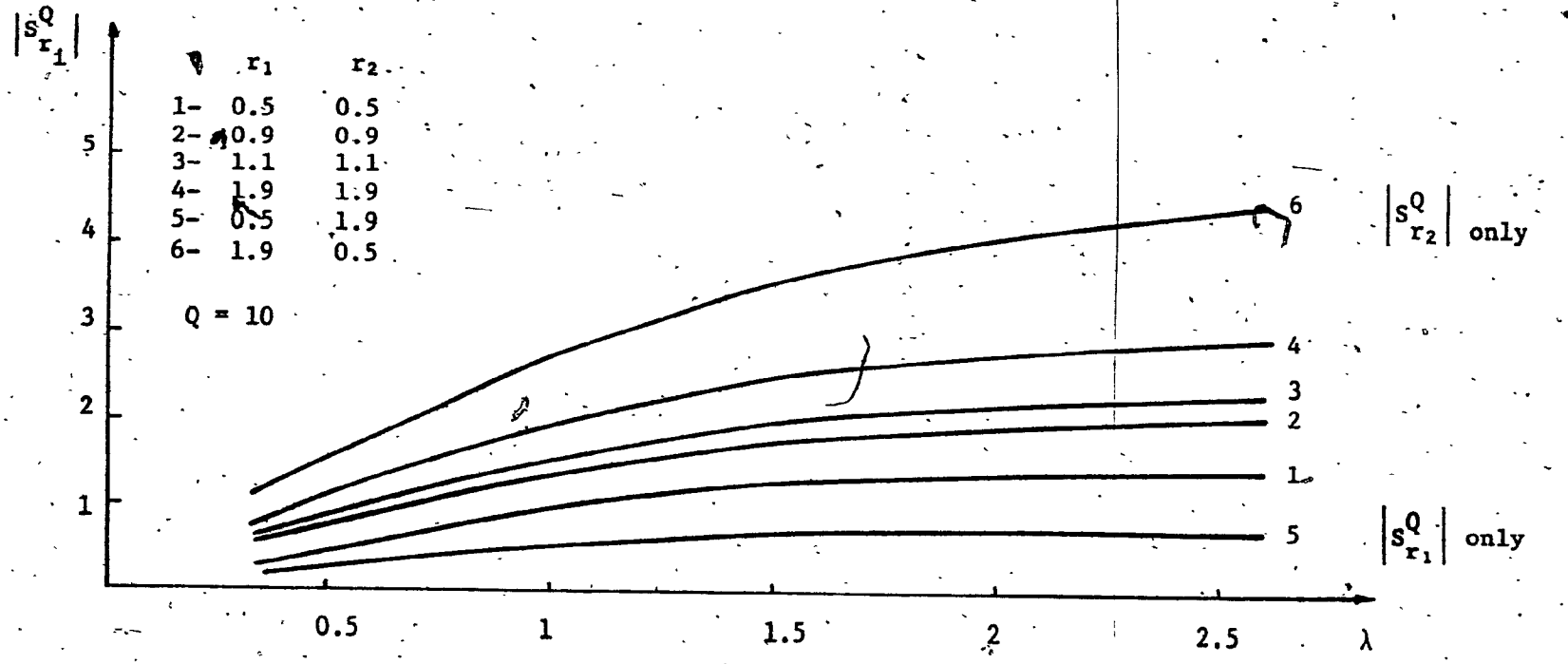

Figure 3.2.c: $S^Q_{r_i}$ - λ Relation

Using Cascades of Two $\overline{\text{URC}}$'s

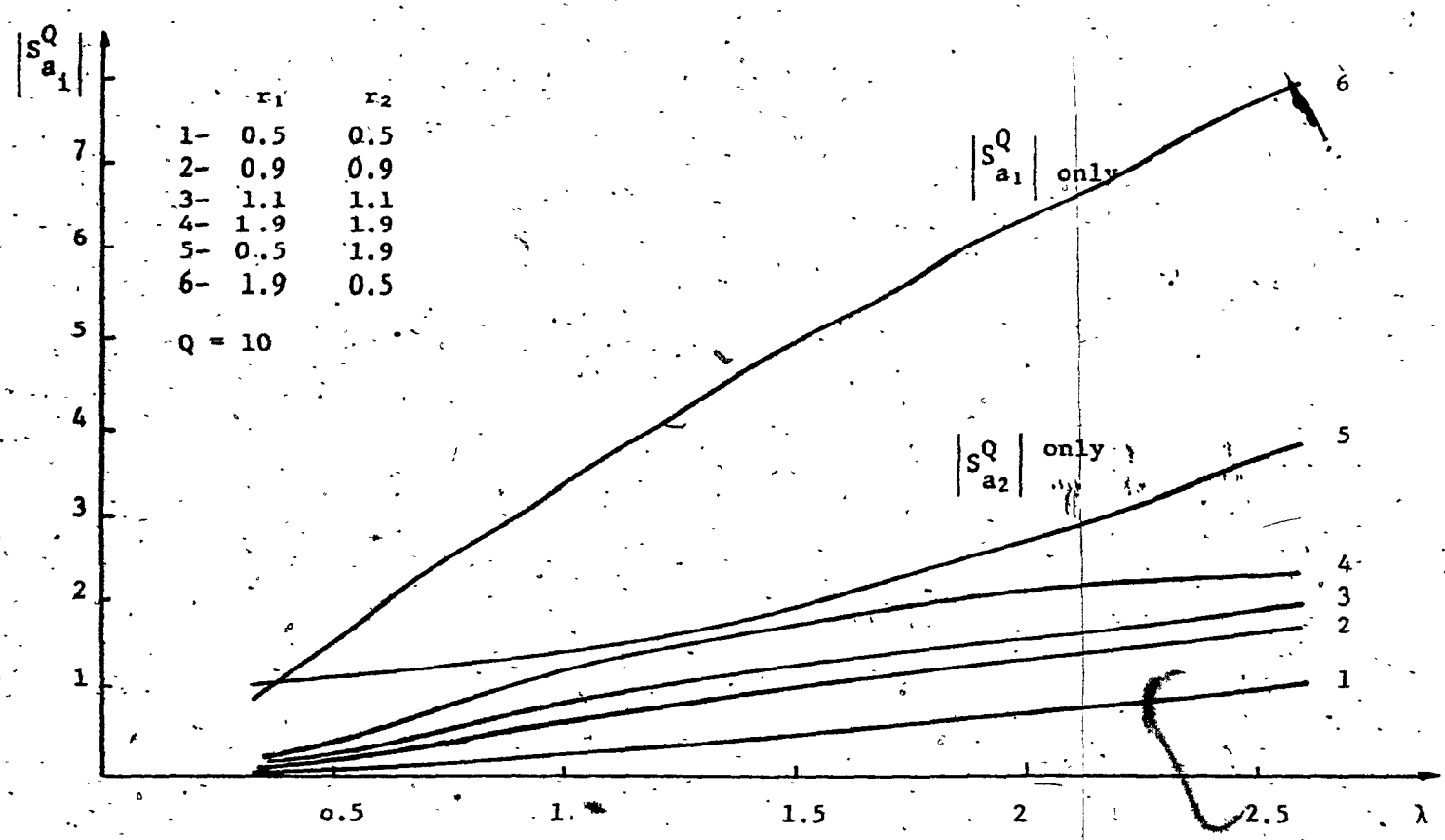

Figure 3.2.d: $S^Q_{a_i}$ - λ Relation

Using Cascades of Two $\overline{URC}$'s

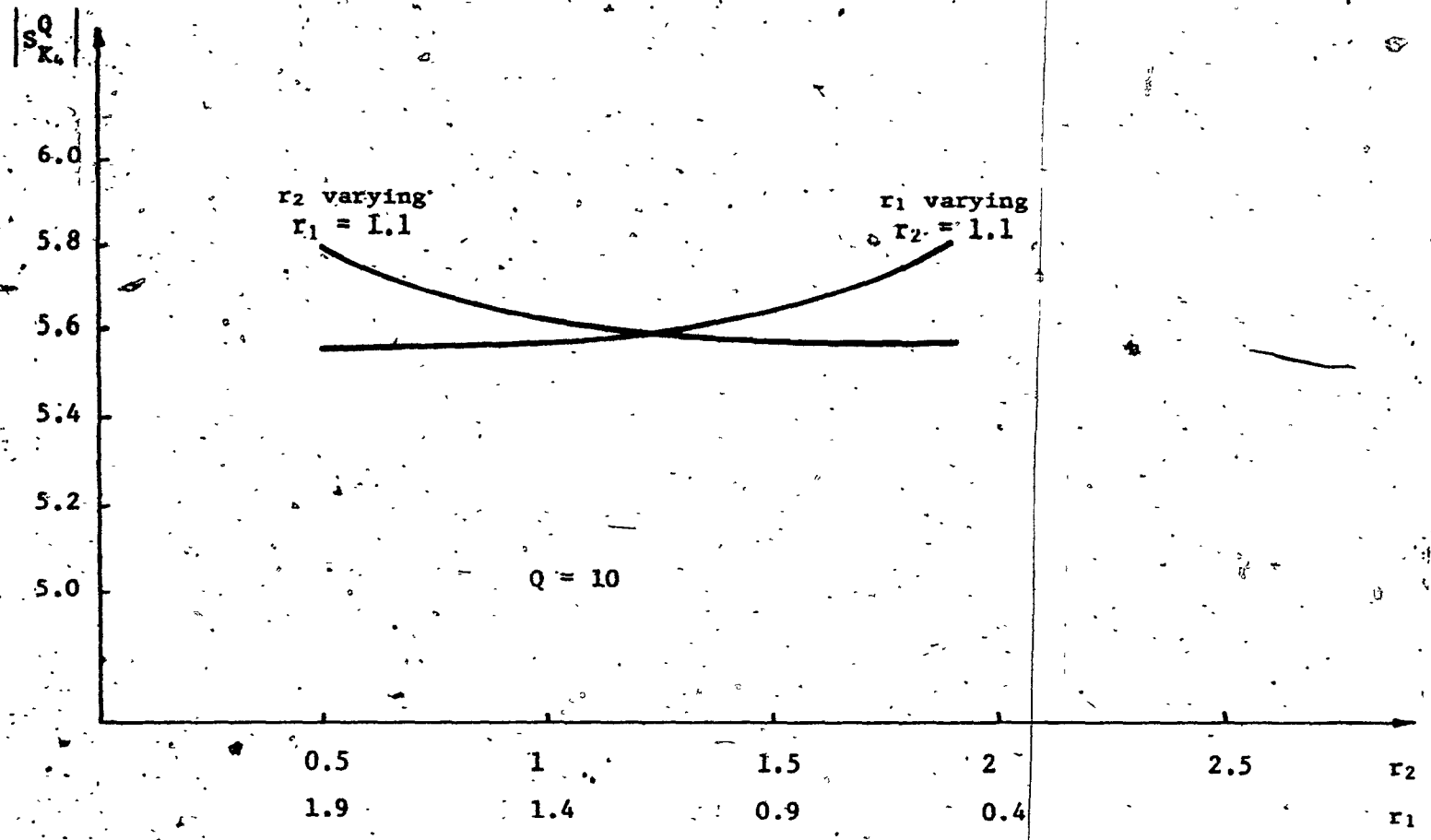

Figure 3.3.a: $S^Q_{K_4} - r_i$ Relation

Using Cascades of Two $\overline{\text{URC}}$'s

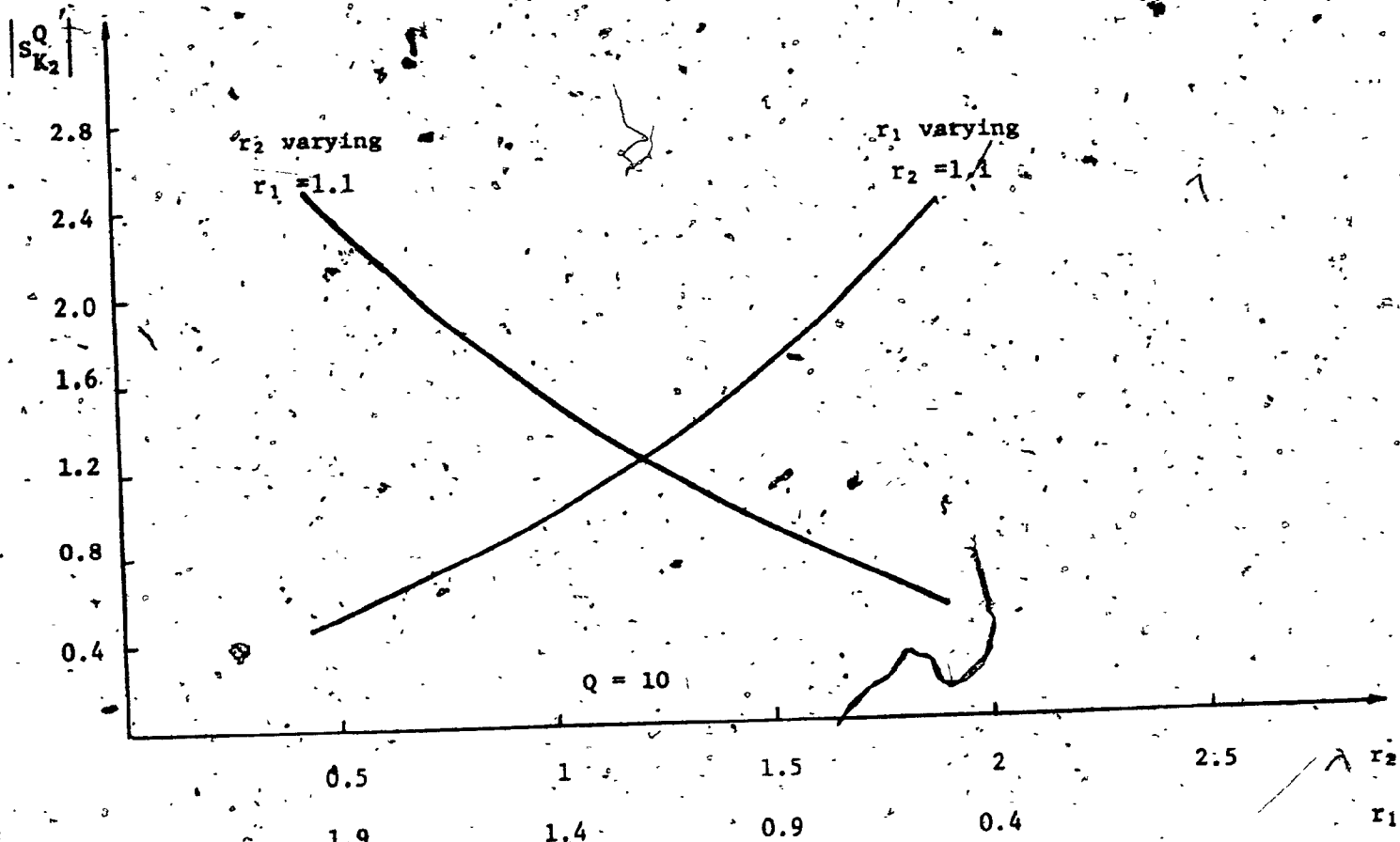

Figure 3.3.b: $S^{Q}_{K_2}$ - r_i Relation

Using Cascades of Two $\overline{URC}$'s

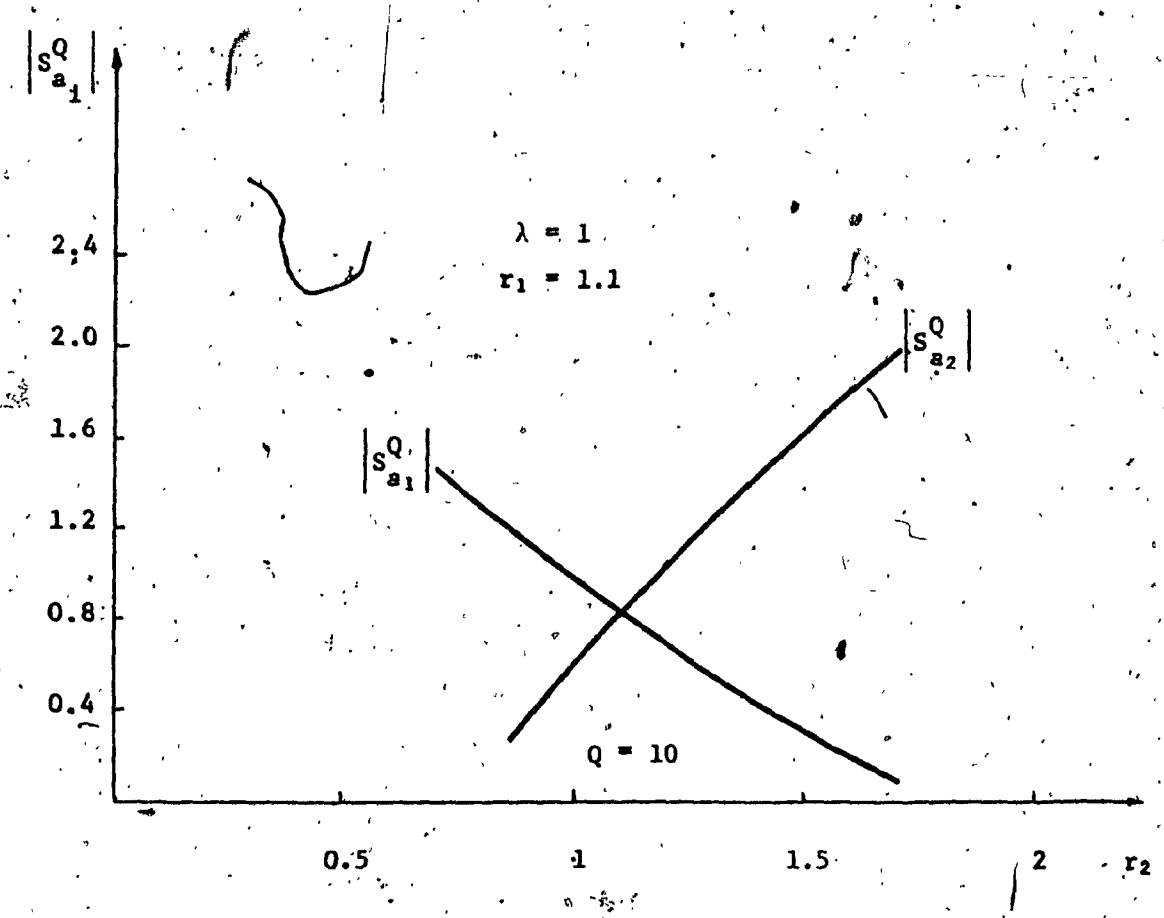

Figure 3.3.c: $S^Q_{a_i}$ - r_i Relation

Using Cascades of Two $\overline{\text{URC}}$'s

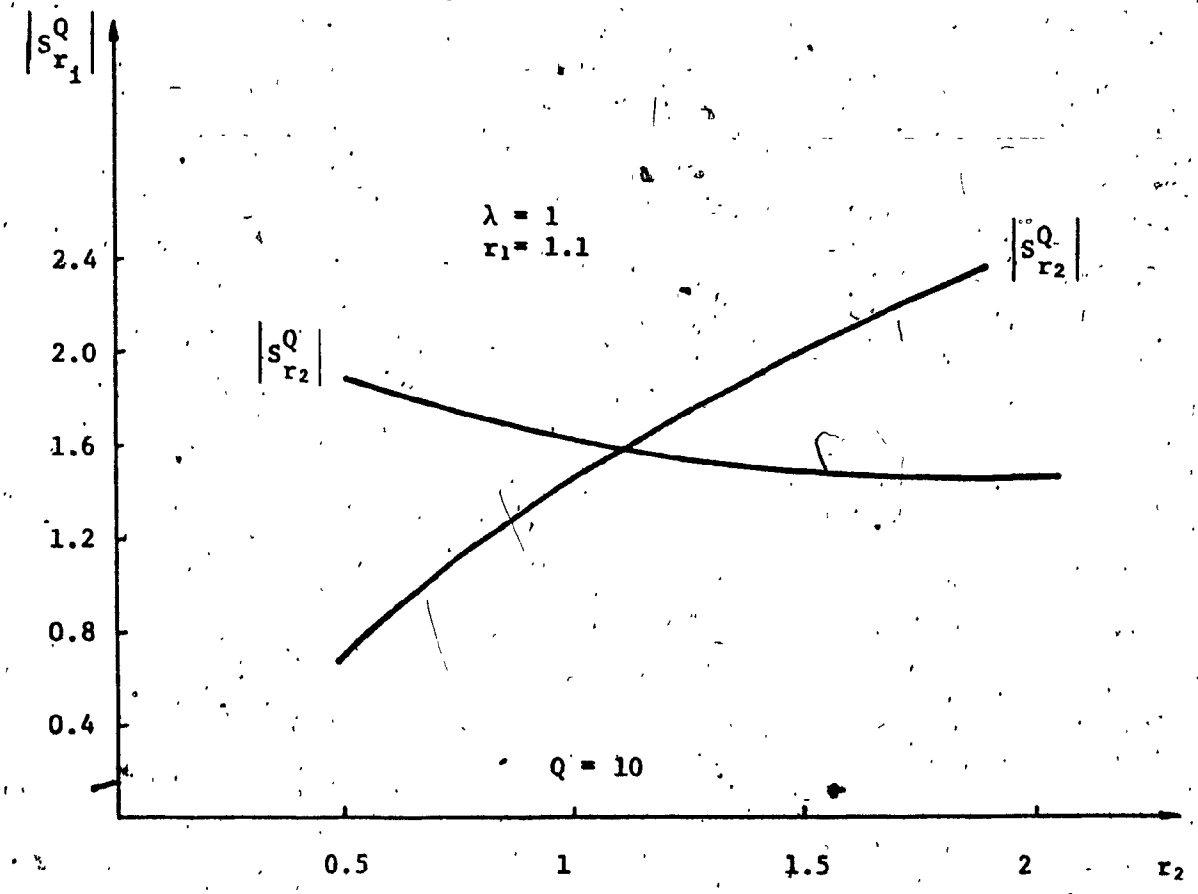

Figure 3.3.d: $S^Q_{r_i} - r_i$ Relation
Using Cascades of Two $\overline{\text{URC}}$'s

3.5 OPTIMIZATION PROCEDURE AND EXAMPLES

The performance criterion chosen for the design should contain not only a measure of deviation from the desired values of Q and ω_o but also a measure of the sensitivities S_Y^Q and $S_y^{\omega_o}$ where $y \in \underline{Y} = \{K_2, K_4, \lambda, r\}$. Stability must also be ensured in this design. As can be seen from the discussion in Chapter 1, the stability of the active $\overline{URC}$ network approximately realizing (3.1) will depend exclusively the value of λ. In fact we must have $\lambda < \lambda_{max}$ where λ_{max} is calculated from equation (1.18). This restricion can be included in the performance criterion through the addition of a term inversely proportional to $(\lambda_{max} - \lambda)$.

The overall performance criterion chosen was

$$J = W_1 (Q - Q_d)^2 + W_2 (\omega_o - \omega_d)^2 + W_3/(\lambda_{max} - \lambda) + \sum_i b_i |S_{y_i}^Q| + \sum_i c_i |S_{y_i}^{\omega_o}| \qquad (3.9)$$

where W's , b's and c's are weighting coefficients.

The Fletcher-Powell method was used for the optimization. Because analytical expressions for the gradients were not readily obtainable, derivatives were evaluated numerically. The effectiveness of the Fletcher-Powell method was reduced near the minimum becuase of using numerical derivatives. Therefore the more simple method of steepest descent was used at the final stages of optimization. The accuracy of the search was taken to be 10^{-4} and convergence was concluded when both the variation in the objective function and the values of the derivatives were less than 10^{-4}.

A flowchart of the optimization procedure followed is shown in Appendix F. Representative results are listed here for the following transfer functions

$$1\text{-}\quad T_d(s) = H \frac{1}{s^2 + 0.125\, s + 1}$$

$$2\text{-}\quad T_d(s) = H \frac{s}{s^2 + 0.125\, s + 1}$$

$$3\text{-}\quad T_d(s) = H \frac{s^2}{s^2 + 0.1\, s + 1}$$

with $W_1 = W_2 = 2$, $W_3 = 0.25$, b_i's and c_i's = 1 parameter values were obtained for the optimum designs and are listed in table 3.1. It is seen that the values of the amplifier gains are low and that the largest Q sensitivity is of the order of Q/2. We also notice that the sensitivity of ω_o to all parameters (except λ) is less than 0.5 , Frequency responses for these designs are also shown in figure 3.4 .

3.6 EFFECT OF LINE TAPER ON THE RESPONSE

The fabrication of the filter could be slightly simplified if the cascade of two lines used for N1 and N2 could be replaced by a single uniform line. It would also be of interest to investigate whether the cascade could be replaced by a single line having a smooth taper, say, by an exponential line. Such a possibility has already been investigated to some extent [56] where it has been shown that a cascade of five commensurate $\overline{\text{URC}}$'s resulted in a good approximation of a smooth taper.

TABLE 3.1

RESULTS FOR DESIGNS OF LP, BP AND HP FILTERS USING CASCADES OF LINES

	LP Q = 8	BP Q = 8	HP Q = 10
K_1	1.0	1.0	1.0
K_2	0.13	0.103	0.244
K_3	0.0	-1.0	-2.0
K_4	-5.48	-5.98	-6.17
K_5	0.0	0.0	0.084
r	1.55	2.03	2.52
λ	1.006	0.866	0.738
$s_{K_2}^{Q}$	-0.058	0.478	1.48
$s_{K_4}^{Q}$	4.63	4.3	4.81
s_{λ}^{Q}	0.0	0.0	0.0
s_{r}^{Q}	-1.48	-1.44	-1.67
$s_{K_2}^{\omega_o}$	-0.003	-0.02	-0.0512
$s_{K_4}^{\omega_o}$	-0.345	0.381	0.4145
$s_{\lambda}^{\omega_o}$	-1.0	-1.0	-1.0
$s_{r}^{\omega_o}$	-0.277	-0.314	-0.34

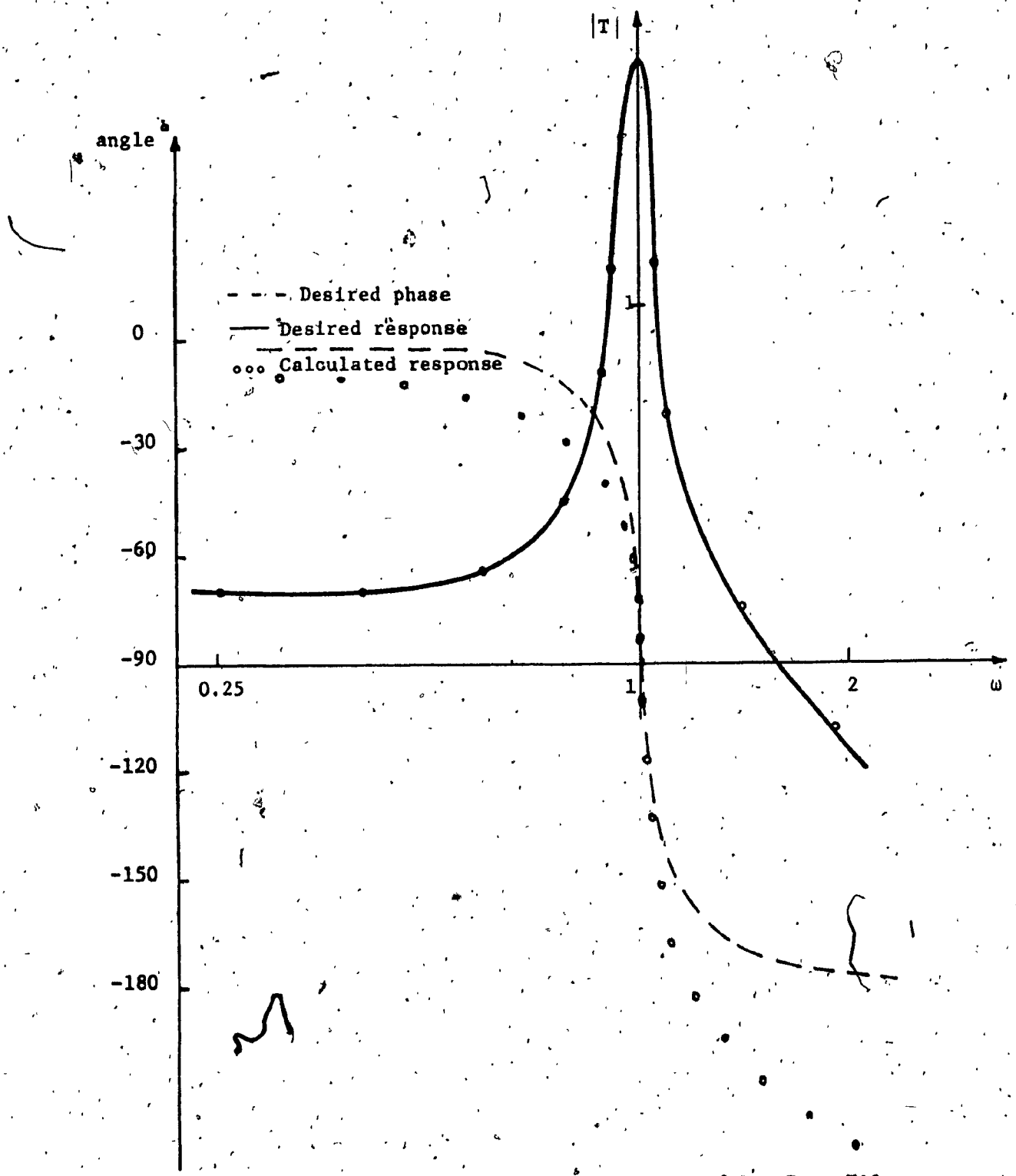

Figure 3.4.a: Frequency Response of Low Pass Filter

Q = 8

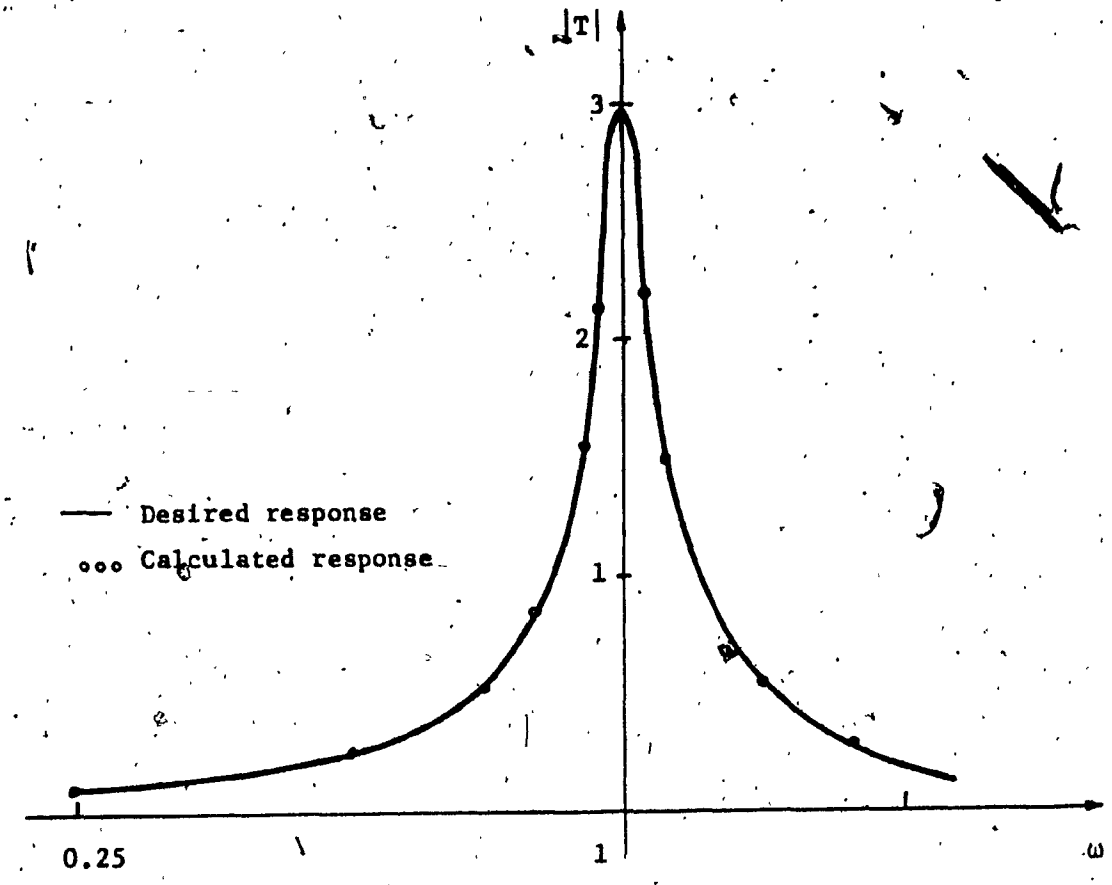

Figure 3.4.b: Frequency Response of Band Pass Filter

Q = 8

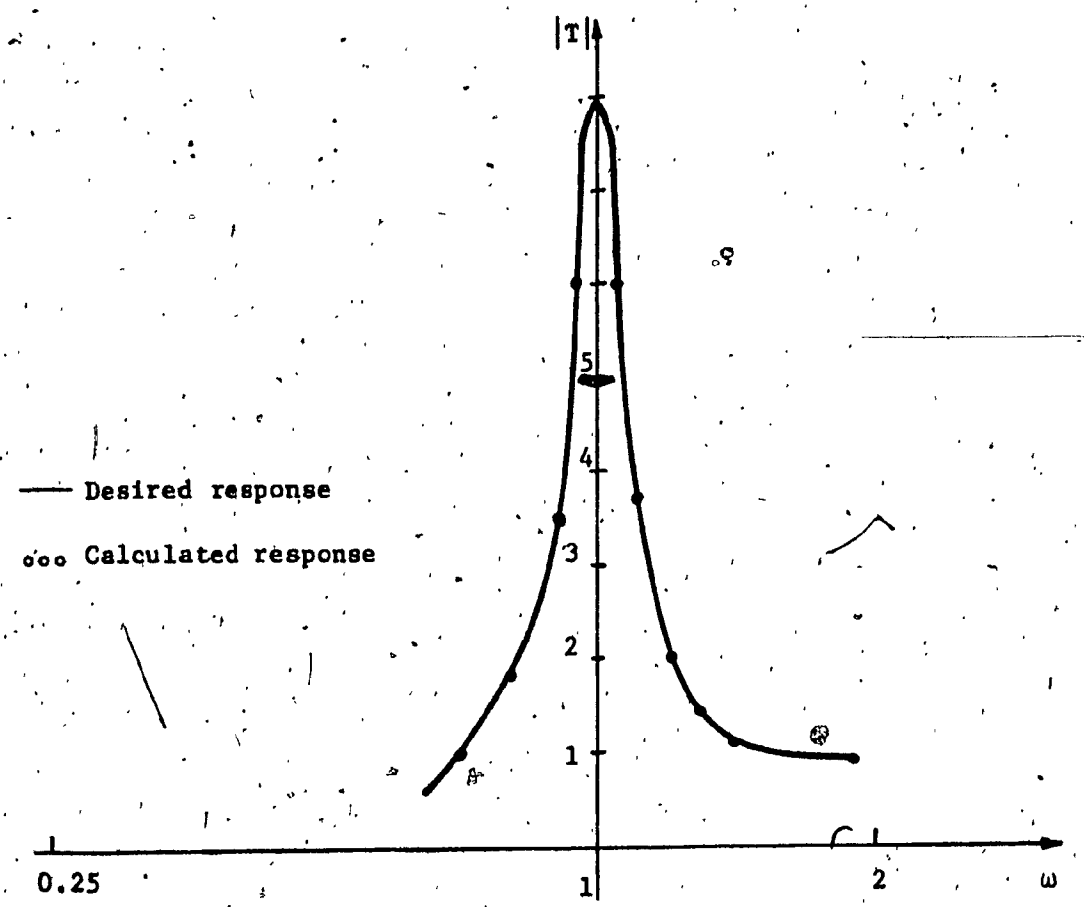

Figure 3.4.c: Frequency Response of High Pass Filter

Q = 10

We will in this section carry out the design using a uniform line, simply by letting $r = 1$, and compare the results obtained to those of designs using cascade of lines .

Table 3.2 show the results for the designs of the previous three examples using uniform lines . The main differences between the results presented in tables 3.1 and 3.2 are in the values of λ and the amplifier gains . It is seen that the amplifier gains needed with cascades of lines have larger values . This means that the useful frequency range of the filter will be limited on the high end by the operational amplifier cut-off frequency . This cut-off frequency varies inversely with the amplifier gain . On the other hand we notice that the value of the RC product λ is smaller when using cascades of lines . The value of λ has a special bearing on the response of the filter . If we consider λ as a means of frequency scaling , and recalling that there is an upper practical value on λ dictated by the technology (see Chapter 1) , then we can see that the design value of λ sets a lower limit on the useful operating frequency .

The above discussion indicates that when $r = 1$, that is the case of a $\overline{\text{URC}}$, the filter is advantageous for use at high frequencies . As the value of r increases the values obtained for λ and the amplifier gains make the filter more suitable for operation at lower frequencies .

TABLE 3.2

RESULTS FOR DESIGNS OF LP, BP AND HP FILTERS USING $\overline{URC}$'s

	LP Q = .8	BP Q = 8	HP Q = 10
K_1	1.0	1.0	1.0
K_2	0.507	0.418	0.561
K_3	0.0	-1.0	-1.0
K_4	-2.49	-2.733	-2.335
K_5	0.0	0.0	-1.0
λ	3.17	3.43	2.99
$S_{K_2}^{Q}$	-3.536	-2.664	-5.072
$S_{K_4}^{Q}$	5.56	4.562	5.56
S_{λ}^{Q}	0.0	0.0	0.0
$S_{K_2}^{\omega_o}$	0.241	-0.1795	0.3012
$S_{K_4}^{\omega_o}$	-0.44	-0.4087	-0.472
$S_{\lambda}^{\omega_o}$	-1.0	-1.0	-1.0

3.7 DESIGN USING EXPONENTIAL LINES

A logical extension of the work carried out in the previous section is to investigate the possible merits of using $\overline{ERC}$ for low frequency designs rather than cascades of $\overline{URC}$'s.

The transfer function of the $\overline{ERC}$ is given by [57]

$$T(s) = \frac{e^{-\beta\ell}}{\cosh \Gamma\ell + \frac{\beta\ell}{\Gamma\ell} \sinh \Gamma\ell} \qquad (3.13)$$

where $\beta\ell$ is the taper factor , and

$$\Gamma = \sqrt{\beta^2 + R_o C_o s} \qquad (3.14a)$$

$$R(x) = R_o e^{-2\beta x} \quad , \quad C(x) = C_o e^{2\beta x} \qquad (3.14b)$$

The above transfer function is used to replace (3.4) in deriving the overall transfer function of the filter. Using this new function, designs can be obtained for the $\overline{ERC}$ case using the same design procedure where, now, β replaces r as a design parameter .

A comparison is made between the designs using cascade and exponential lines . During the course of comparison, the parameter λ is set at different values and the remaining parameters are used in each case to find an optimum value of the objective function (3.9) .

The important result of this comparison for the case of a low pass filter of $Q = 20$ and $\omega_o = 1$, are shown in figures 3.5.a-b-c-d, where, for all these designs, the values of the amplifier gains lie between 0.11 and -22.0 for the design using cascades of $\overline{URC}$'s, between 2.69 and - 11.8 for the design using $\overline{ERC}$'s.

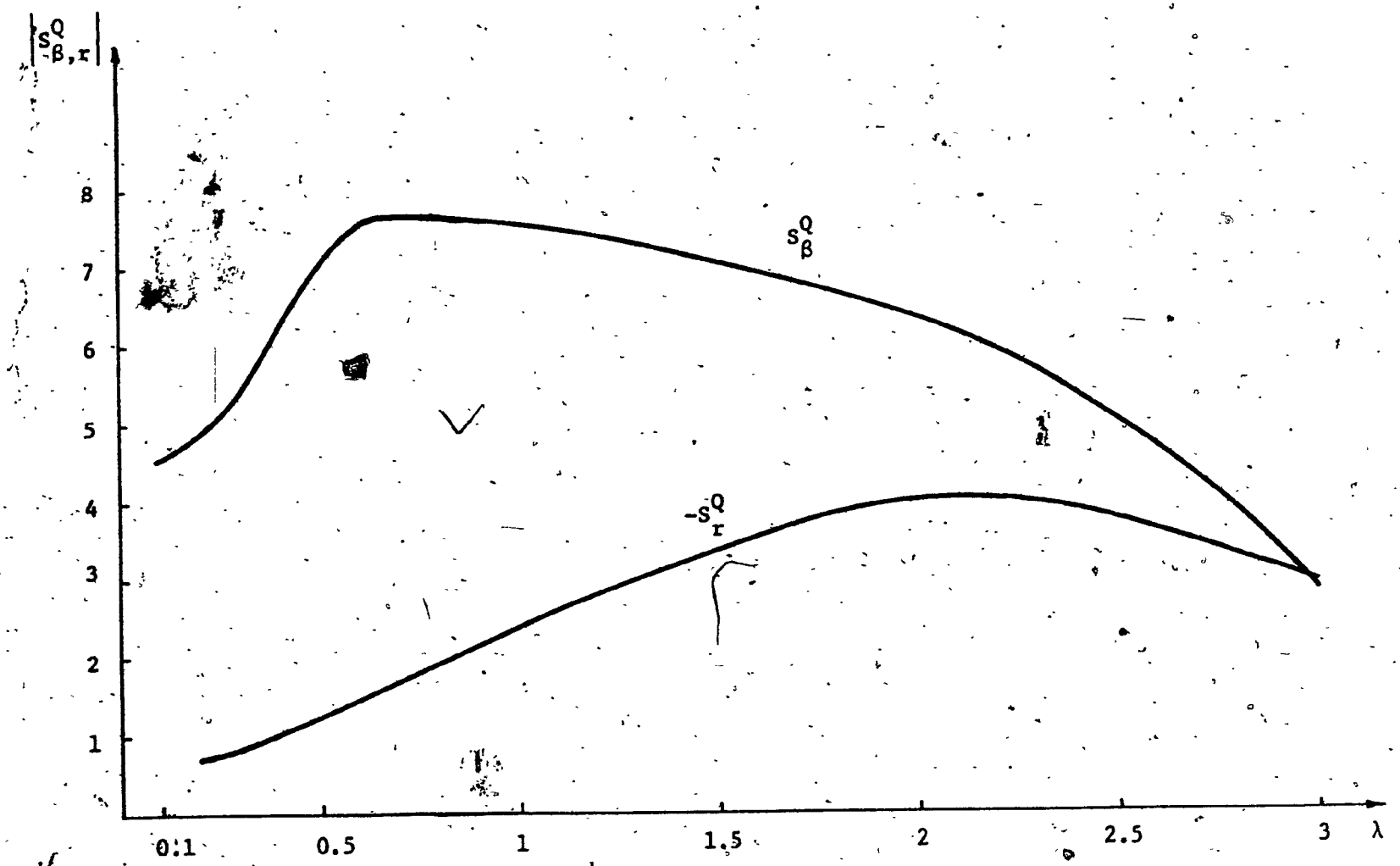

Figure 3.5.a: $S^Q_{\beta,r}$ - λ Relation

For Cascade And Exponential Designs

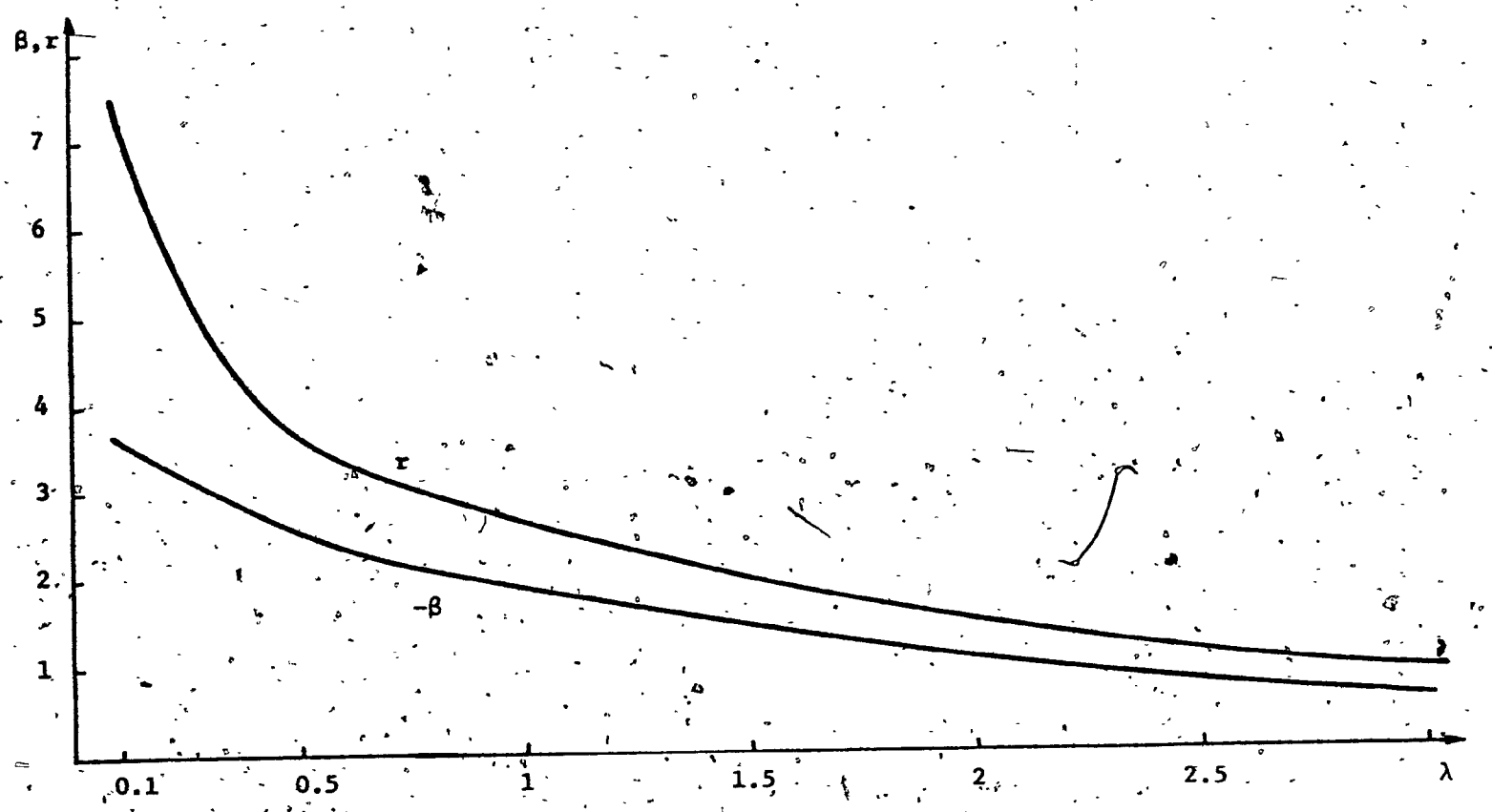

Figure 3.5.b: $\beta, r - \lambda$ Relation

For Cascade And Exponential Designs

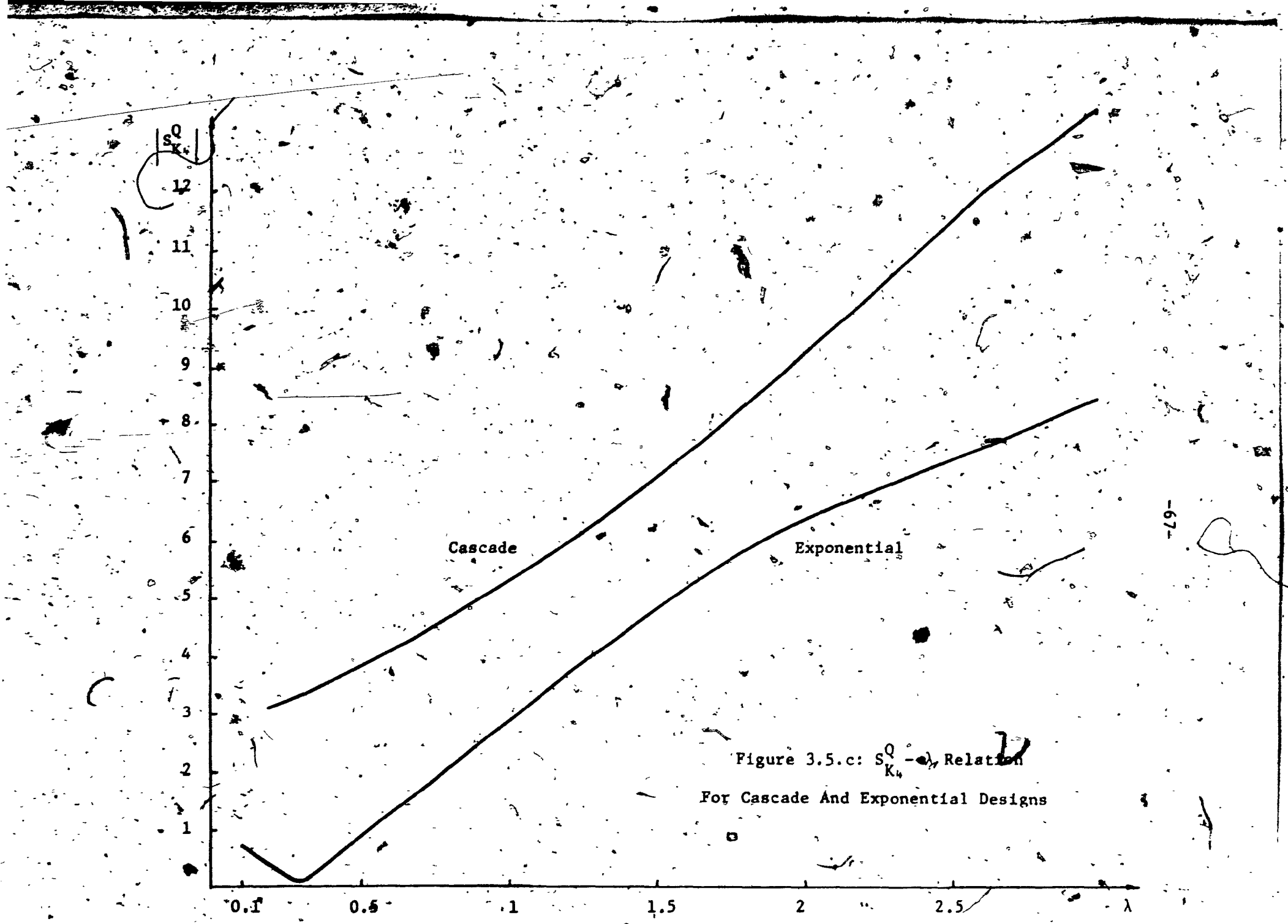

Figure 3.5.c: $S^{Q}_{K_4}$ - λ Relation For Cascade And Exponential Designs

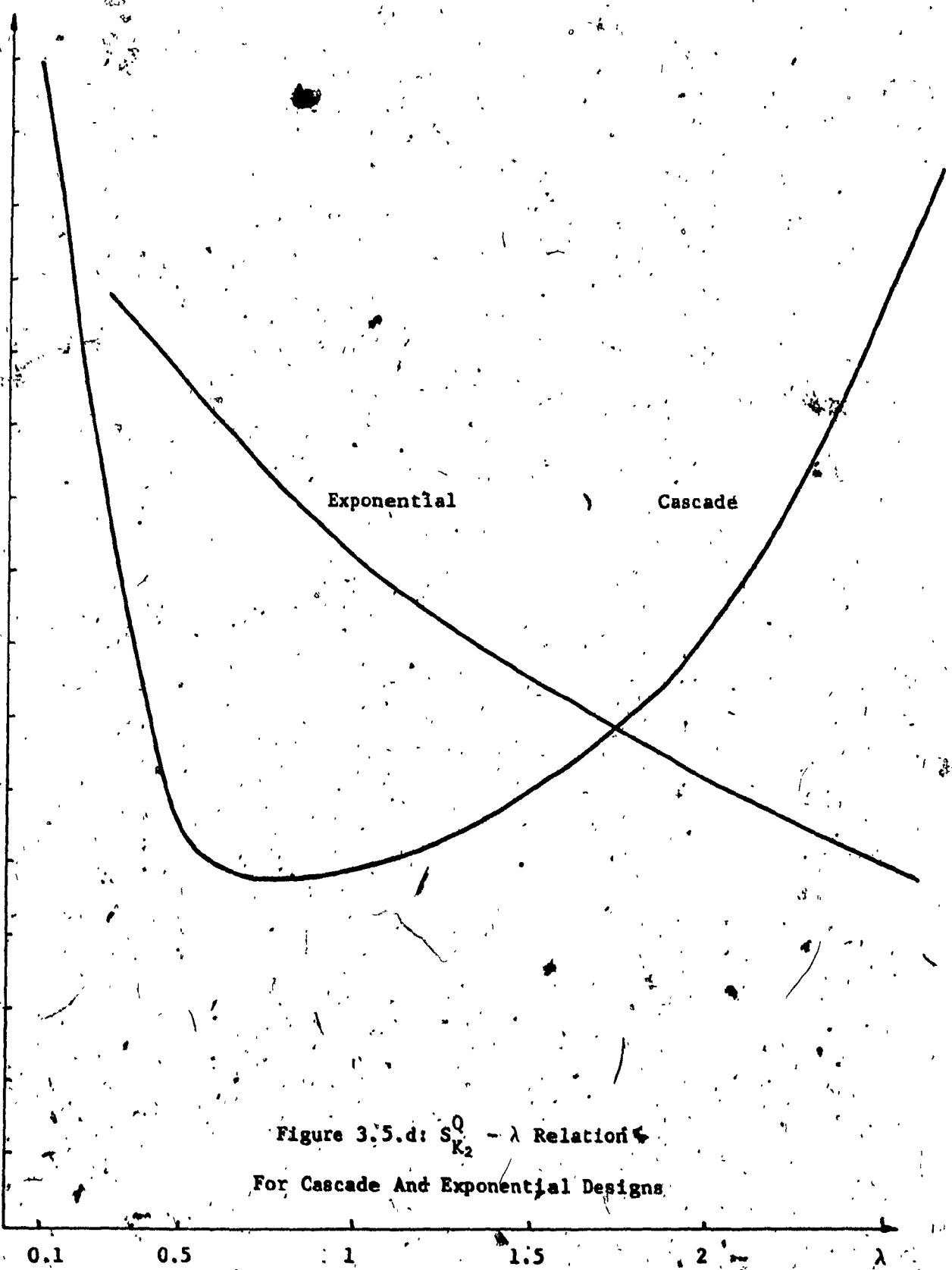

Figure 3.5.d: $S^Q_{K_2}$ - λ Relation

For Cascade And Exponential Designs

These results suggests that the use of the $\overline{ERC}$ is advantageous for low frequency application, which is consistent with the findings in the previous section.

In order to show the effect of taper on the design value, calculations were carried out for both designs using $\overline{URC}$'s and $\overline{ERC}$'s. Several values of $R_o C_o \ell^2$ were selected and optimal designs obtained for each value, once using $\overline{URC}$'s and again using $\overline{ERC}$'s. Typical results are shown in table 3.3 where it is seen that for low values of $R_o C_o \ell^2$ the sensitivities are very high when using $\overline{URC}$'s but low for the $\overline{ERC}$ designs.

Several designs were carried out using $\overline{ERC}$'s. The values of the sensitivities of Q to the amplifier gains were less than Q/2 and those of Q to β were of the order of Q/4 while the $\omega_o R_o C_o \ell^2$ product was as small as 0.02. As mentioned in Chapter 1, the upper practical limit for $R_o C_o \ell^2$ is 3×10^{-3} seconds, thus a design value of $\omega_o R_o C_o \ell^2 = 0.02$ will make it possible to design a filter with a centre frequency in the vicinity of 1 Hz. It is thus preferable to use $\overline{ERC}$'s (or tapered lines in general) for low frequency applications. However, the high amplifier gains limit the use of $\overline{ERC}$'s at high frequencies and it is preferable to use $\overline{URC}$'s for such applications. It should be noted that studies using lines having values of $\beta > 0$ showed no advantage and were thus not pursued.

TABLE 3.3

COMPARISON BETWEEN $\overline{URC}$ AND $\overline{ERC}$

LP Q = 20

$R_oC_o\ell^2 = \lambda_1$	*	$\beta\ell$	K_2	K_4	S^Q_β	$S^Q_{K_2}$	$S^Q_{K_4}$	$S^{\omega_o}_\beta$	$S^{\omega_o}_{K_2}$	$S^{\omega_o}_{K_4}$
0.1	U	—	.998	-.999	—	-1330	267	—	-399	200
	E	-3.71	.901	-9.64	4.65	-12.3	.737	.16	-.09	.54
0.2	U	—	.995	-1.	—	-464	33.4	—	-99.5	50.1
	E	-3.32	.859	-11.8	4.83	-12.3	.344	.17	-.07	.53
0.3	U	—	.992	-1.	—	-264	.0315	—	-44.1	22.4
	E	-3.03	.831	-11.6	5.37	-12.2	-.047	.17	-.076	.53
0.4	U	—	.988	-1.01	—	-181	-8.4	—	-24.7	127
	E	-2.71	.821	-9.33	6.51	-12.1	-.46	.163	-.097	.536

TABLE 3.3 continued

0.5	U	——	.983	-1.03	——	-136	-10.9	——	-15.8	8.22
	E	-2.49	.8	-8.7	7	-11.6	-.867	.154	-.1	.535
0.6	U	——	.977	-1.04	——	-109	-11.2	——	-10.9	5.79
	E	-2.32	.787	-7.65	7.71	-11.0	-1.29	.142	-.119	.537
0.7	U	——	.97	-1.06	——	-89.7	-11.5	——	-7.98	4.32
	E	-2.21	.754	-8.05	7.59	-10.6	-1.67	.135	-.11	.529
0.8	U	——	.963	-1.08	——	-76.2	-11.3	——	-6.08	3.37
	E	-2.19	.69	-10.2	7.56	-10.1	-2.	.135	-.08	.513
0.9	U	——	.955	-1.11	——	-65.9	-11.9	——	-4.78	2.72
	E	-2.04	.69	-8.16	7.58	-9.56	-2.43	.118	-.103	.518

* U = URC , E = ERC

$K_1 = 1$, $S_{\lambda_1}^{\omega_q} = -1$, $S_{\lambda_1}^{Q} = K_3 = K_5 = 0$

3.8 conclusion

In this chapter a new grounded active distributed RC-filter is introduced. The circuit is intended to approximately realize any open circuit voltage transfer functions having real or complex roots. The important case of second order functions is considered in detail, where a preliminary study has led to the use of commensurate $\overline{RC}$ lines.

Several filters were designed using an optimization procedure to minimize an objective function which contains a measure of parameter sensitivities and goodness of approximation while ensuring a stable operation of the resulting network. All designs resulted in a very good approximation of the desired response as well as low amplifier gains and low sensitivities. The maximum Q-sensitivity to amplifier gains was of the order of Q/2. The sensitivity of ω_o to all parameters was never more than 0.5.

The design procedure was then used to explore the changes in the performance of the filter when different types of lines are used. This study indicated that if the filter is to be used for high frequencies (in the Vicinity of 1-10 KHz without compensation) then it becomes advantageous to use single $\overline{URC}$'s. If the filter is to be used for low frequencies (as low as 1 Hz) it is better to use tapered lines. In particular, very satisfactory results were obtained using the exponential line.

It should be noted that all designs were carried out using ideal amplifiers. In the next Chapter we will focus our attention on the effects of using non-ideal amplifiers. For this purpose we will limit our consideration to realizations using $\overline{\text{URC}}$'s.

CHAPTER 4

ACTIVE SYNTHESIS OF SECOND ORDER FILTERS USING GROUNDED $\overline{\text{URC}}$'s

4.1 INTRODUCTION

In this chapter, further studies are carried out for the filter introduced in the previous chapter. These studies are restricted to filters realized using $\overline{\text{URC}}$'s although similar investigations could be carried out for the case of tapered lines.

Calculations to determine the effect of finite gain-band-width product (GB) on the design value of Q are first performed and the circuit compared, in this respect to other distributed designs. Further comparisons were carried out with respect to the variation of Q and ω_o due to changes in amplifier gains. Test results are presented for experimental prototypes.

A simple compensation scheme is introduced to extend the useful frequency of operation, limited by the finite GB.

Finally, designs for the notch and all-pass filters are presented

4.2 THE s → p TRANSFORMATION

The work in this chapter is carried out using the relation

$$p = \cosh \sqrt{\lambda s} \tag{4.1}$$

and the open circuit voltage transfer function of the $\overline{\text{URC}}$ is therefore written as

$$T(p) = \frac{1}{p} \tag{4.2}$$

The variable p is related to the variable u as follows:

Letting

$$u = \tanh^2\sqrt{s\lambda/4} \tag{4.3}$$

we can write

$$\frac{(p - f_z)(p - \bar{f}_z)}{(p - f_p)(p - \bar{f}_p)} = \frac{(1 + f_z)(1 + \bar{f}_z)}{(1 + f_p)(1 + \bar{f}_p)} \left[\frac{(u - \alpha)(u - \bar{\alpha})}{(u - \gamma)(u - \bar{\gamma})}\right] \tag{4.4}$$

where

$$\alpha = \frac{f_z + 1}{f_z - 1} \qquad \gamma = \frac{f_p + 1}{f_p - 1} \tag{4.5}$$

Conversely,

$$\frac{(u - \alpha)(u - \bar{\alpha})}{(u - \gamma)(u - \bar{\gamma})} = \frac{(1 - \alpha)(1 - \bar{\alpha})}{(1 - \gamma)(1 - \bar{\gamma})} \frac{(p - f_z)(p - \bar{f}_z)}{(p - f_p)(p - \bar{f}_p)} \tag{4.6}$$

where

$$f_z = \frac{1 + \alpha}{1 - \alpha} \qquad f_p = \frac{1 + \gamma}{1 - \gamma} \tag{4.7}$$

This is a bilinear transformation and the results in section 1.5.2 for the $s \to u$ mapping are applicable here by replacing λ in (1.18)-(1.21) by $\lambda/4$. The p-plane image of figure 1.4.a is shown in figure 4.1.

4.3 ANALYSIS

The open circuit voltage transfer function of the circuit in figure 3.1 where N1 and N2 are identical $\overline{\text{URC}}$'s, can be written as

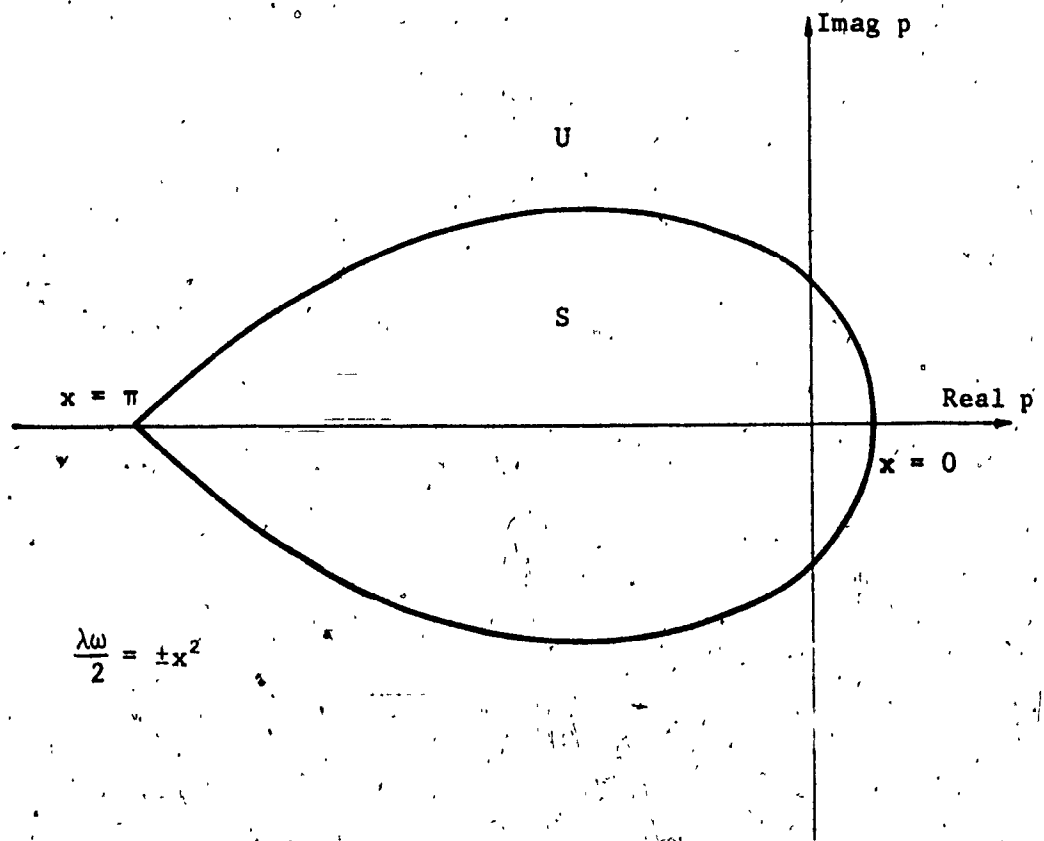

Figure 4.1: The s → p Transformation, p-plane

$$T(p) = \frac{K_5K_3p^2 + (K_5 + K_8K_5K_1 + K_1K_3)p + K_1}{p^2 - 2K_2p - K_4} \qquad (4.8)$$

where we have set $K_7 = 1$ and $K_6 = K_2$

As in Chapter 3, we can rewrite (4.8) as

$$T(p) = H \frac{(p - f_z)(p - \overline{f}_z)}{(p - f_p)(p - \overline{f}_p)} \qquad (4.9)$$

where f_p and f_z are related to the s-plane poles and zeros, to be realized, by equation (4.1).

The expressions obtained in Appendix E for the sensitivities of Q and ω_o can be applied to equation (4.9) when λ_1 is different than λ_2 . It is easy to show that

$$\frac{\delta D}{\delta \lambda_1} = \frac{s \sinh \sqrt{\lambda_1 s}}{2\sqrt{\lambda_1 s}} [\cosh \sqrt{\lambda_2 s} - K_2]$$

$$\frac{\delta D}{\delta \lambda_1} = \frac{s \sinh \sqrt{\lambda_2 s}}{2\sqrt{\lambda_2 s}} [\cosh \sqrt{\lambda_1 s} - K_2]$$

$$\frac{\delta D}{\delta s} = \Sigma_{i=1}^{2} \left(\frac{\lambda_i}{2\sqrt{\lambda_i s}} \sinh \sqrt{\lambda_i s} \cosh \sqrt{\lambda_i s} - \frac{K_2 \lambda_i}{2\sqrt{\lambda_i s}} \sinh \sqrt{\lambda_i s}\right)$$

Now letting $\lambda_1 = \lambda_2 = \lambda$, the sensitivities become,

$$S_{\lambda_1}^{Q} = S_{\lambda_2}^{Q} = 0 \quad , \quad \lambda_1 = \lambda_2 = \lambda$$

$$S_{\lambda_1}^{\omega_o} = S_{\lambda_2}^{\omega_o} = -\frac{1}{2}$$

It is further noted that, since $\lambda_1 = \lambda_2 = \lambda$, frequency scaling can be carried out by varying the lengths of the two lines.

4.4 Examples

A computer program was developed for the design of biquadratic filters using $\overline{\text{URC}}$'s. This program uses the same optimization and design criteria as given in Chapter 3. The program was extended to include such options as the calculation of the effect of the finite GB of the amplifiers, the possibility of altering the objective function and a wider range of filter characteristics. A flow chart is shown in Appendix G.

Of the many filters designed the following four are chosen for further studies in this chapter :

$$1 - \quad T(s) = \frac{1}{s^2 + 0.1s + 1}$$

$$2 - \quad T(s) = \frac{s}{s^2 + 0.125s + 1}$$

$$3 - \quad T(s) = \frac{s}{s^2 + 0.033s + 1}$$

$$4 - \quad T(s) = \frac{s^2}{s^2 + 0.1s + 1}$$

It should be noted that for these designs, the constants W_1, W_2, b_i's and c_i's of equation (3.9) were set equal to one and W_3 set equal to 0.25.

The average time taken by the program on the CDC 6400 computer was 40 seconds. Results for the above four examples are shown in figure 4.2.a - 4.2.d and table 4.1.

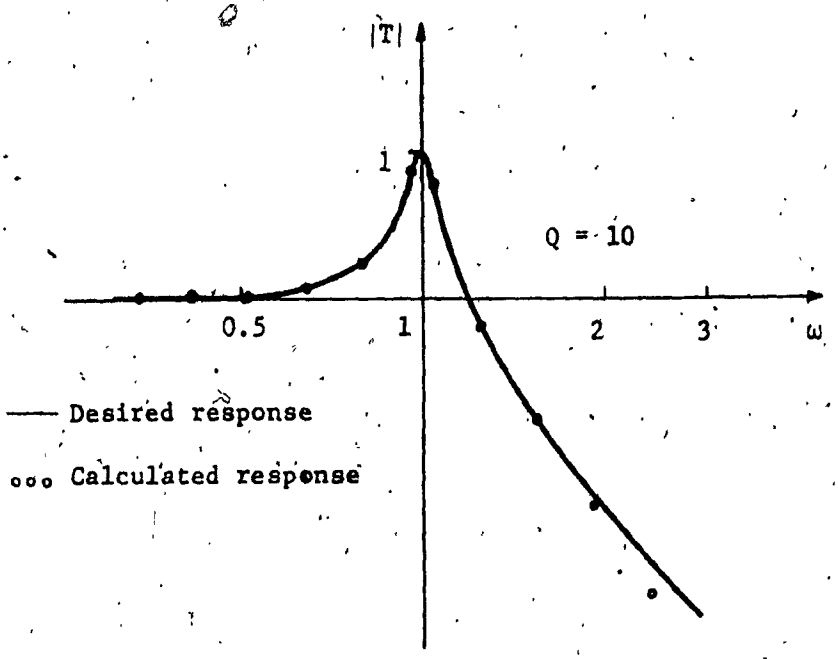

Figure 4.2.a: Frequency Response of Low Pass Filter

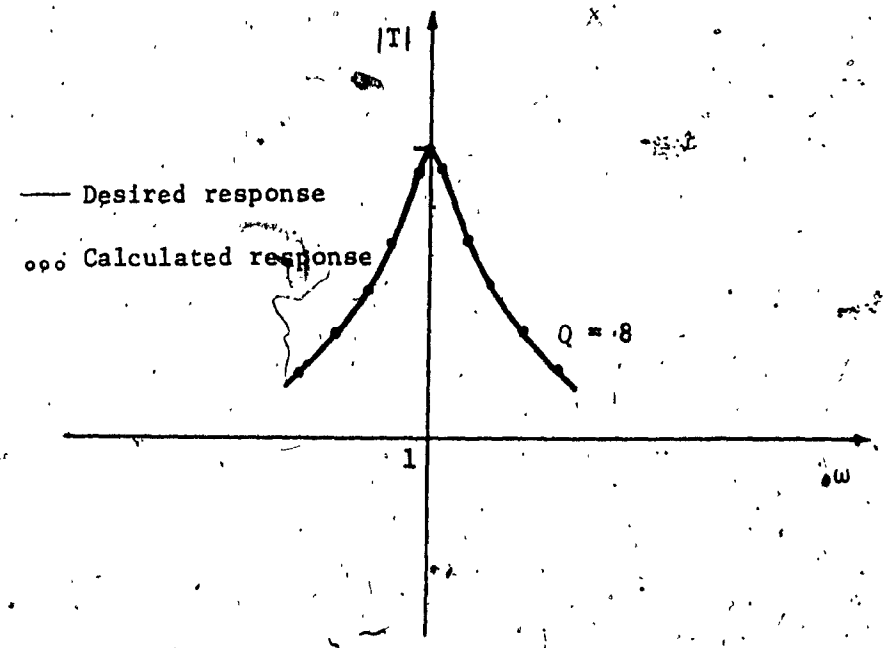

Figure 4.2.b: Frequency Response of Band Pass Filter

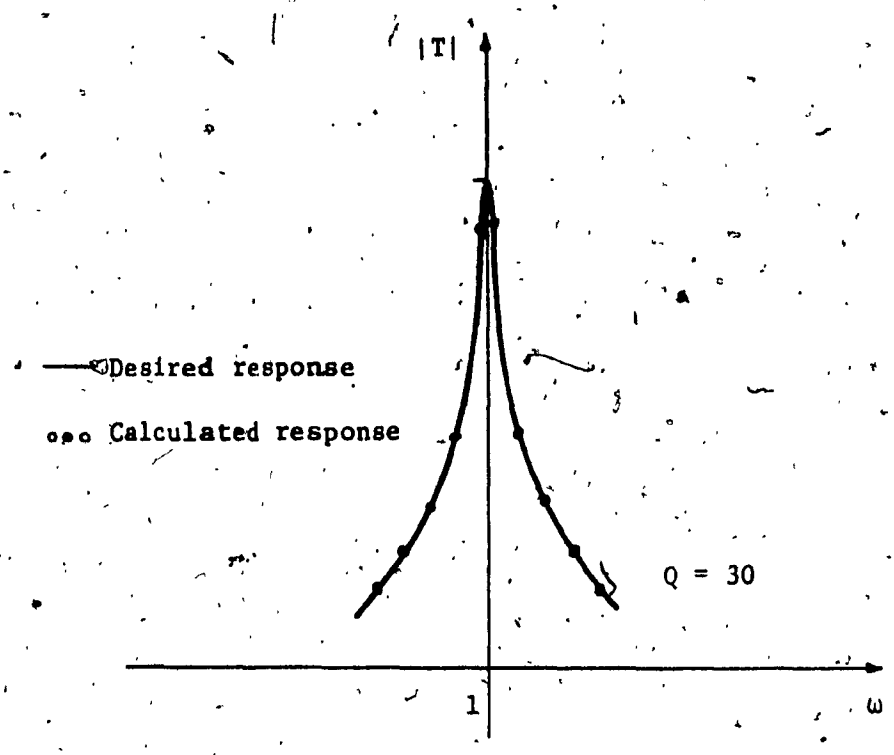

Figure 4.2.c: Frequency Response of Band Pass Filter

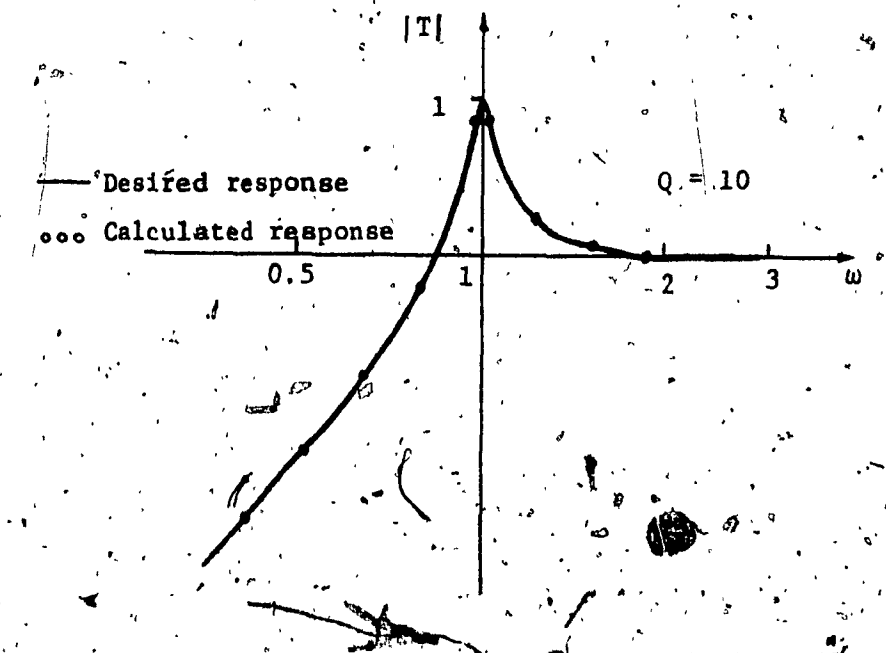

Figure 4.2.d: Frequency Response of High Pass Filter

TABLE 4.1

RESULTS FOR DESIGN OF LP , BP AND HP USING $\overline{URC}$'s

Transfer function	Example 1 Q = 10	Example 2 Q = 8	Example 3 Q = 30	Example 4 Q = 10
K_1	1.0	1.0	1.0	1.0
K_2	0.509	0.418	0.422	0.561
K_3	0	-1.0	-1.0	-1.0
K_4	-2.522	-2.733	-3.204	-2.335
K_5	0	0	0	0
K_6	0	0	0	0
λ	3.18	3.34	3.65	2.99
$S^{Q}_{K_1}$	-4.34	-2.664	-9.04	-5.072
$S^{Q}_{K_4}$	5.75	4.562	16.36	5.56
S^{Q}_{λ}	0	0	0	0
$S^{\omega_o}_{K_2}$	0.247	0.1795	0.1659	0.3012
S_{K_4}	-0.4435	-0.4087	-0.3936	-0.472
$S^{\omega_o}_{\lambda}$	-1.0	-1.0	-1.0	-1.0

4.5 EFFECT OF FINITE AMPLIFIER GAIN-BAND-WIDTH PRODUCT

The amplifier imperfections tend to impose some limitations on the response of the circuit. In this section we are concerned with the effects of the finite band width of the amplifiers on the design values of Q and ω_o. We, therefore, use the one-pole-roll-off model of the amplifier shown in figure (4.3).

Analysis of the circuit of figure (4.3) yields

$$e_o \left[\frac{1}{\mu_o} + \frac{1}{1 + R_f/R_1} \right] = \frac{\Sigma_i G_i e_i}{G} - \frac{e_1 R_f/R_1}{1 + R_f/R_1} \qquad (4.10)$$

$$i = 1,2, \ldots ,n$$

where

$$G_i = \frac{1}{R_i} \qquad (4.11)$$

$$G = \Sigma_i \frac{1}{R_i} \qquad (4.12)$$

Replacing μ_o by the one-pole-roll-off model

$$\mu = \frac{\mu_o}{\frac{s}{\omega_p} + 1} \qquad (4.13)$$

we obtain

$$\frac{e_o}{e_i} \approx \frac{GB}{r_i s + GB/K_i} \quad ; \quad i = 2,3,\ldots \qquad (4.14)$$

and

$$\frac{e}{e_1} \approx \frac{K_1 GB}{(1 - K_1)s + GB} \qquad (4.15)$$

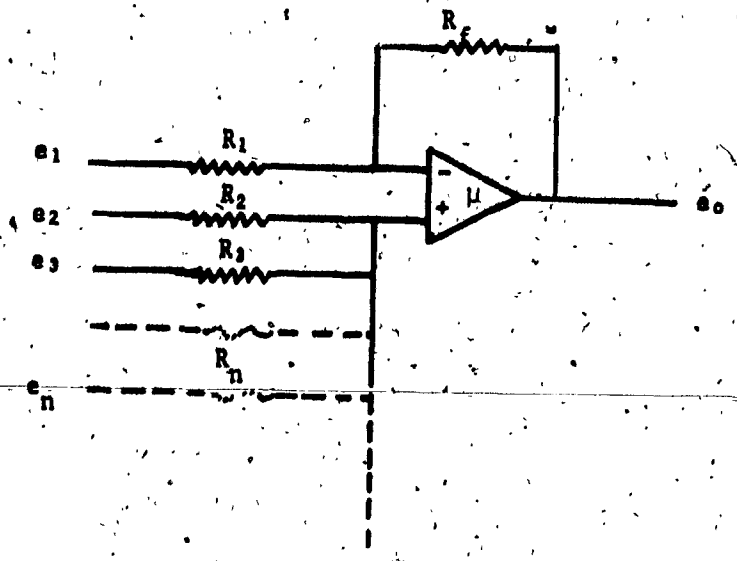

Figure 4.3: Amplifier Circuit

where

$$K_1 = \frac{G_1}{G}(1 + R_f/R_1) = \frac{1}{r_1}(1 + R_f/R_1) \qquad (4.16)$$

and

$$K_1 = -R_f/R_1 \qquad (4.17)$$

Note that the gains now have phase lag associated with them.

Replacing each of the ideal gains used in deriving equation (4.8) by expressions (4.14) or (4.15) will cause Q and ω_o to deviate from the design values. In order to obtain an indication of the degree of the deviation, calculations were carried out for several examples. Results are presented in figure 4.4 for a band pass filter having Q of 8, where it is assumed that the amplifiers have a nominal GB = 10^6 Hz curve A shows the percentage deviation in Q due to finite GB as a function of centre frequency ω_o. Curves B and C indicate the effect of ± 20% variations in GB. It was found that the effect of finite GB on centre frequency ω_o is small, ω_o varying less than 0.3% from the design value for all values of ω_o less than 10^4 rad/sec.

4.6 COMPARISON WITH OTHER $\overline{\text{URC}}$ ACTIVE FILTERS

The new circuit was compared with Kerwin's circuit [60] and Huelsman's circuit [61] both of which make use of $\overline{\text{URC}}$'s. The comparison was based on the sensitivities of Q and ω_o, and on the effect of the finite GB on these two quantities. The comparison was carried out for GB's ranging from 0.8×10^6 to 1.2×10^6 Hz.

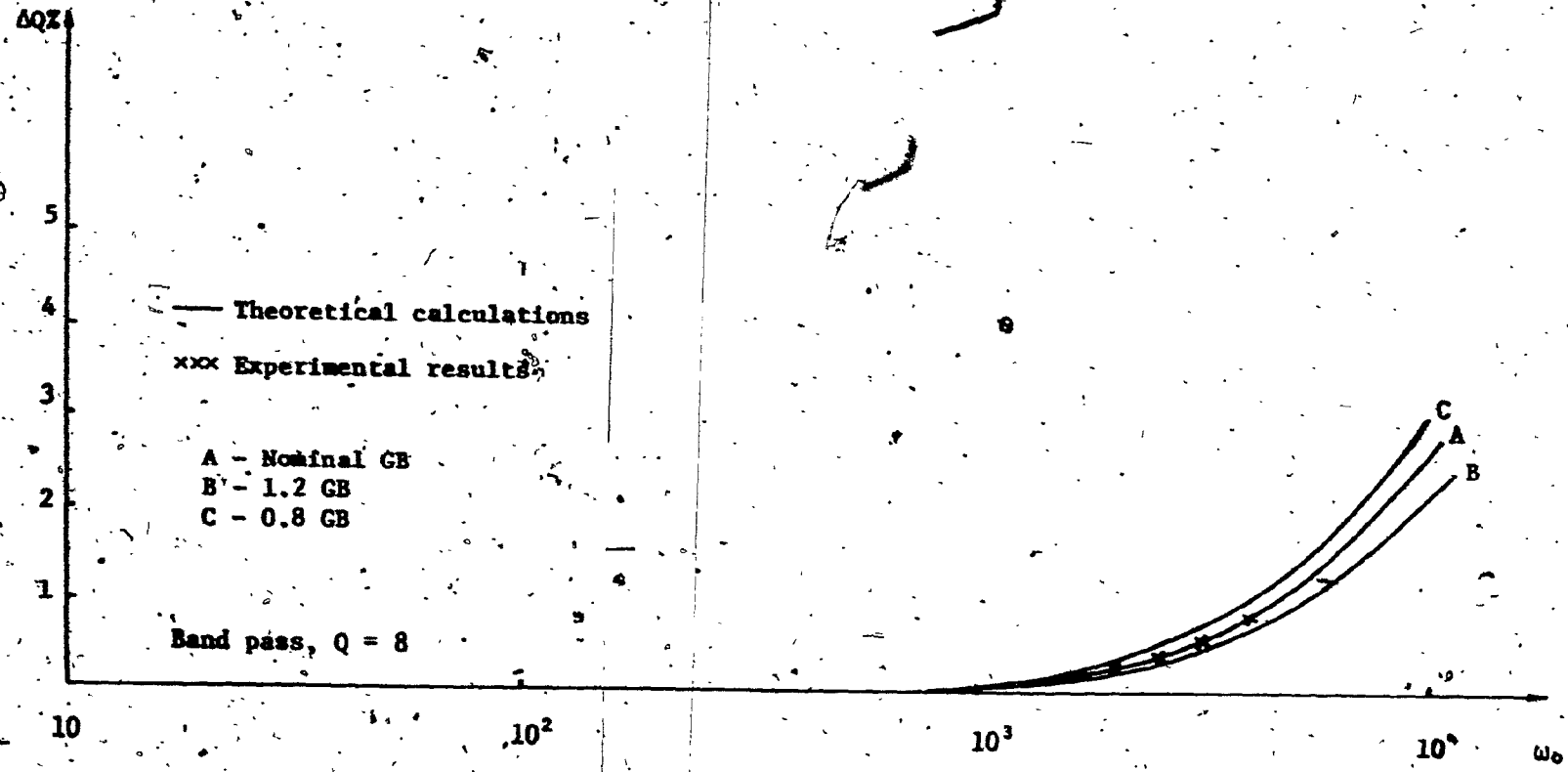

Figure 4.4: Q-variation due to Finite GB

Results of the comparison are shown in figures 4.5 - 4.7 and tables 4.2 - 4.3. Figures 4.5 - 4.7 show the effect of finite GB on Q of all circuits. It is noted that comparison with Kerwin's circuit was not possible for high values of Q since his circuit becomes unstable for $Q > 11.7$. Tables 4.2 - 4.3 show the effect on Q and ω_o of varying the amplifier gains.

From these results it can be seen that the sensitivities for the new circuit are much lower than those for Kerwin's circuit. The useful frequency of operation for Kerwin's circuit is limited by the finite GB to more than one decade lower than for the proposed circuit. The sensitivities for Huelsman's circuit are close to the sensitivities for the new circuit; however the useful frequency range is about 0.7 decade less than that of the new circuit.

4.7 EXPERIMENTAL RESULTS

In order to verify the theoretical predictions, several prototypes were built. Experimental results for example 2 are presented here. The values of the circuit elements used are shown in table 4.1 and the finite gains were realized using fairchild μA741 operational amplifiers of nominal GB of 10^6 Hz. The distributed elements were constructed using teledeltos paper and conducting foils and verified experimentally to be $\overline{URC}$'s. Different values of ω_o were obtained by altering the lengths of the $\overline{URC}$'s and hence their RC-products. A typical frequency response of this filter is shown in figure 4.8 for $f_o = \frac{\omega_o}{2\pi} = 247$ Hz.

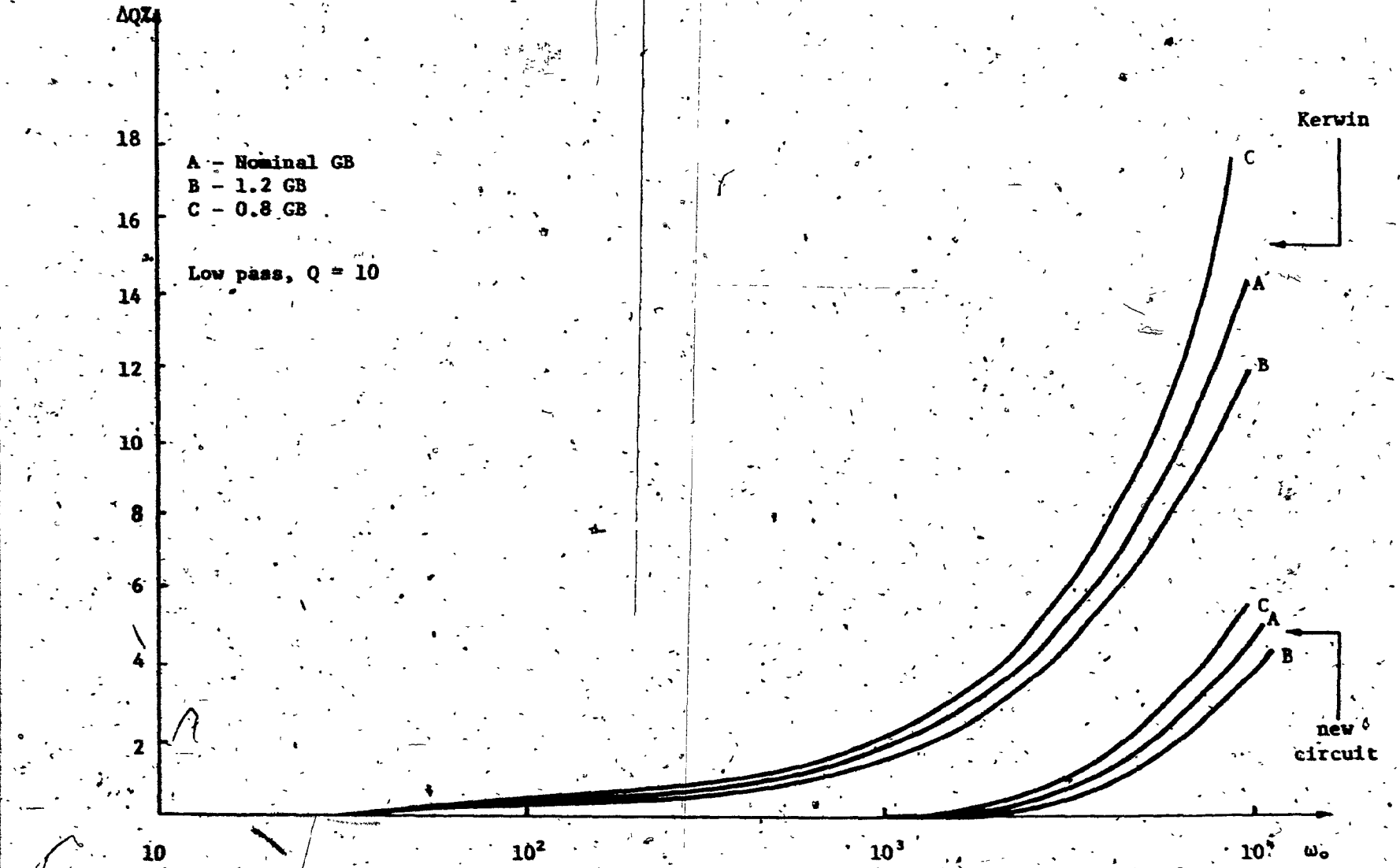

Figure 4.5: Q-variation due to Finite GB, Comparison with Kerwin

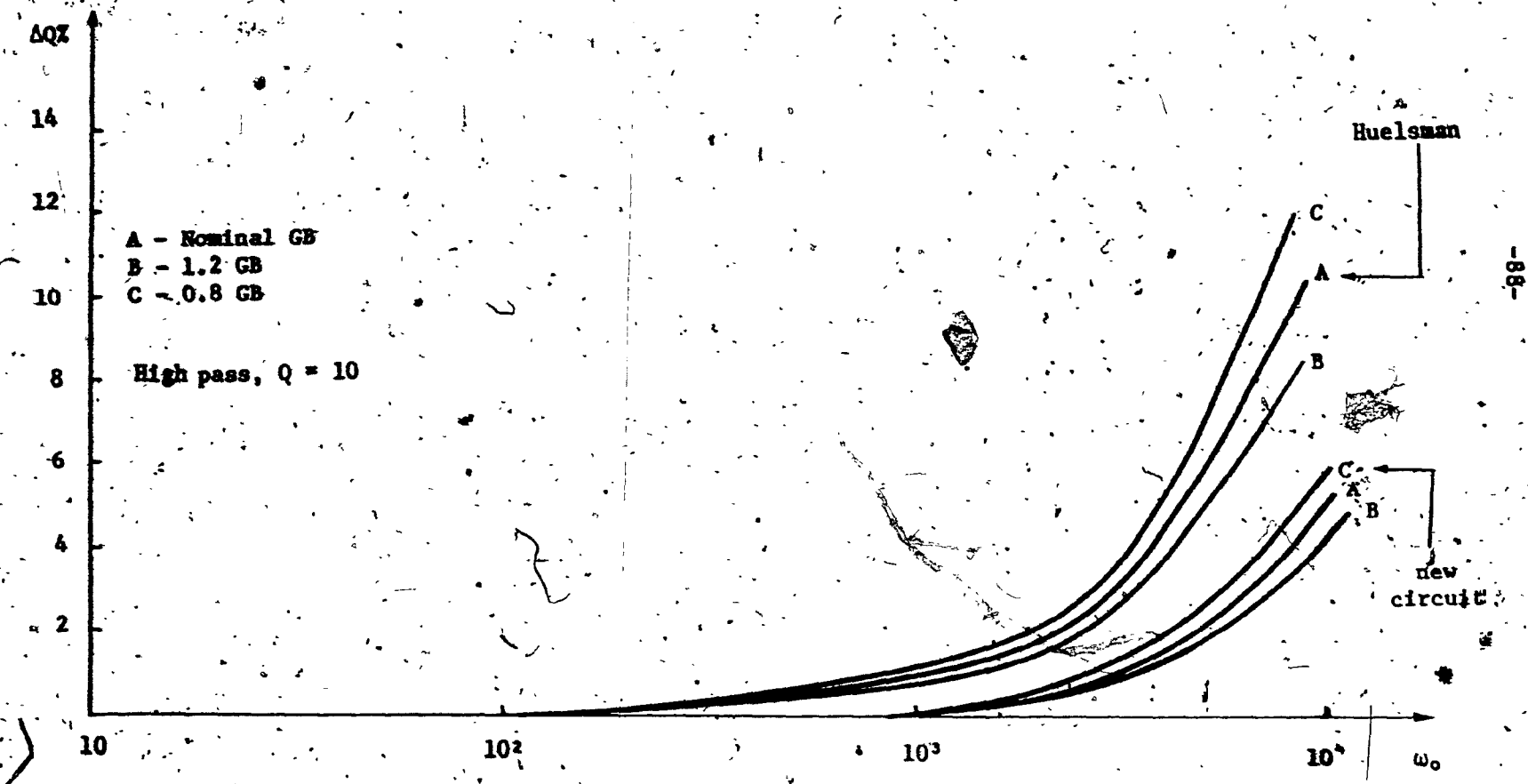

Figure 4.6: Q-variation due to Finite GB, Comparison with Huelsman, High Pass Filter

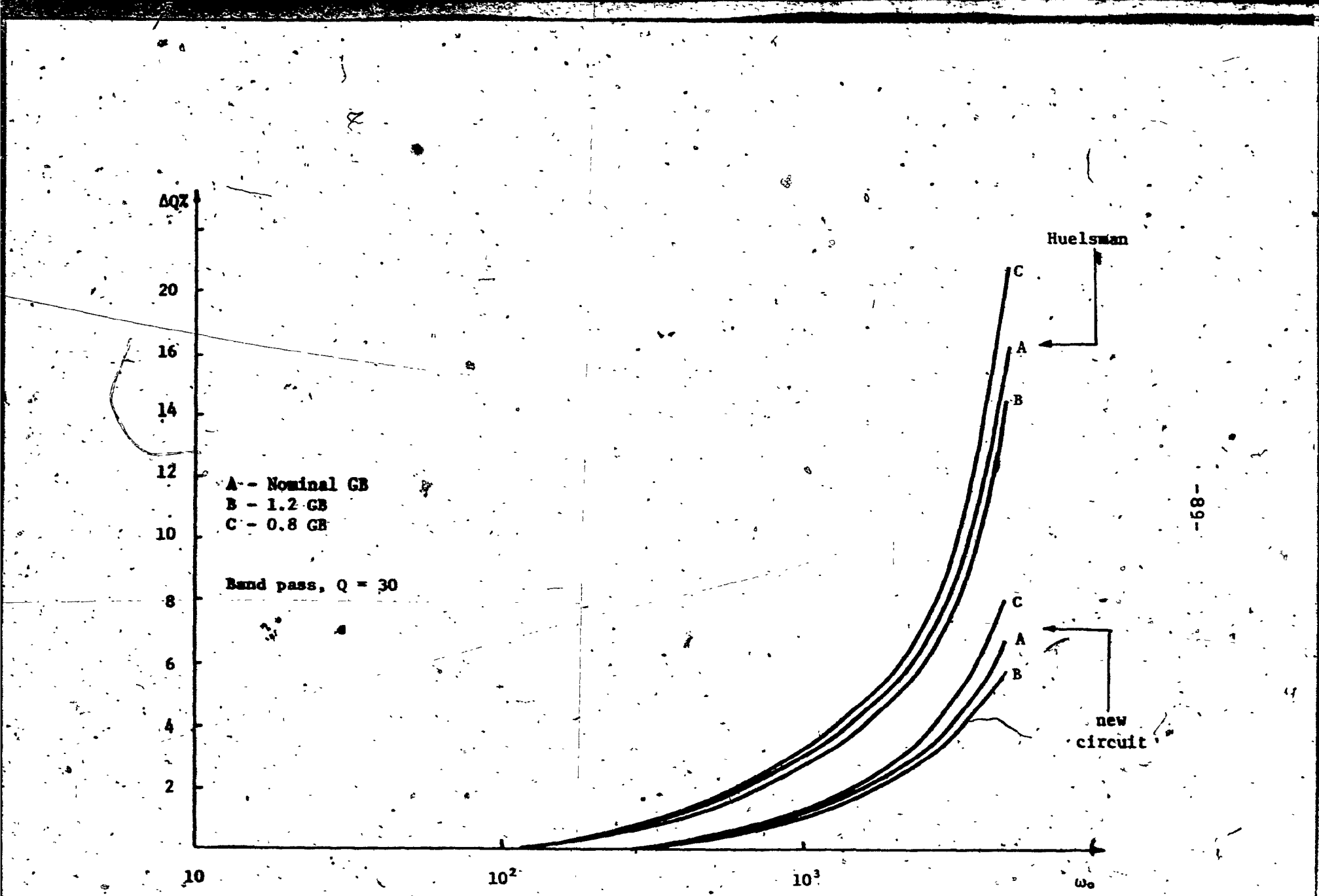

Figure 4.7: Q-variation due to Finite GB, Comparison with Huelsman, Band Pass Filter

TABLE 4.2

COMPARISON WITH HUELSMAN'S CIRCUIT
FOR A BP FILTER OF Q = 30

Δ K % (most effective)	The new circuit		Huelsman's circuit	
	Δ Q %	Δ ω_o %	Δ Q %	Δ ω_o %
-1.0	-14.55	-0.37	-16.2	-0.32
-0.5	-8.25	-0.17	-8.75	-0.16
+0.5	5.94	0.18	8.58	0.13
+1.0	15.82	0.37	21.1	0.29

TABLE 4.3

COMPARISON WITH KERWIN'S CIRCUIT
FOR LP FILTER OF Q = 10

Δ K % (most effective)	The new circuit		Kerwin's circuit	
	Δ Q %	Δ ω_o %	Δ Q %	Δ ω_o %
-1.0	-5.95	0.57	-38.93	-3.23
-0.5	-3.35	0.34	-21.2	-1.3
+0.5	1.6	0.07	68.4	2.4
+1.0	4.6	0.29	481.8	4.5

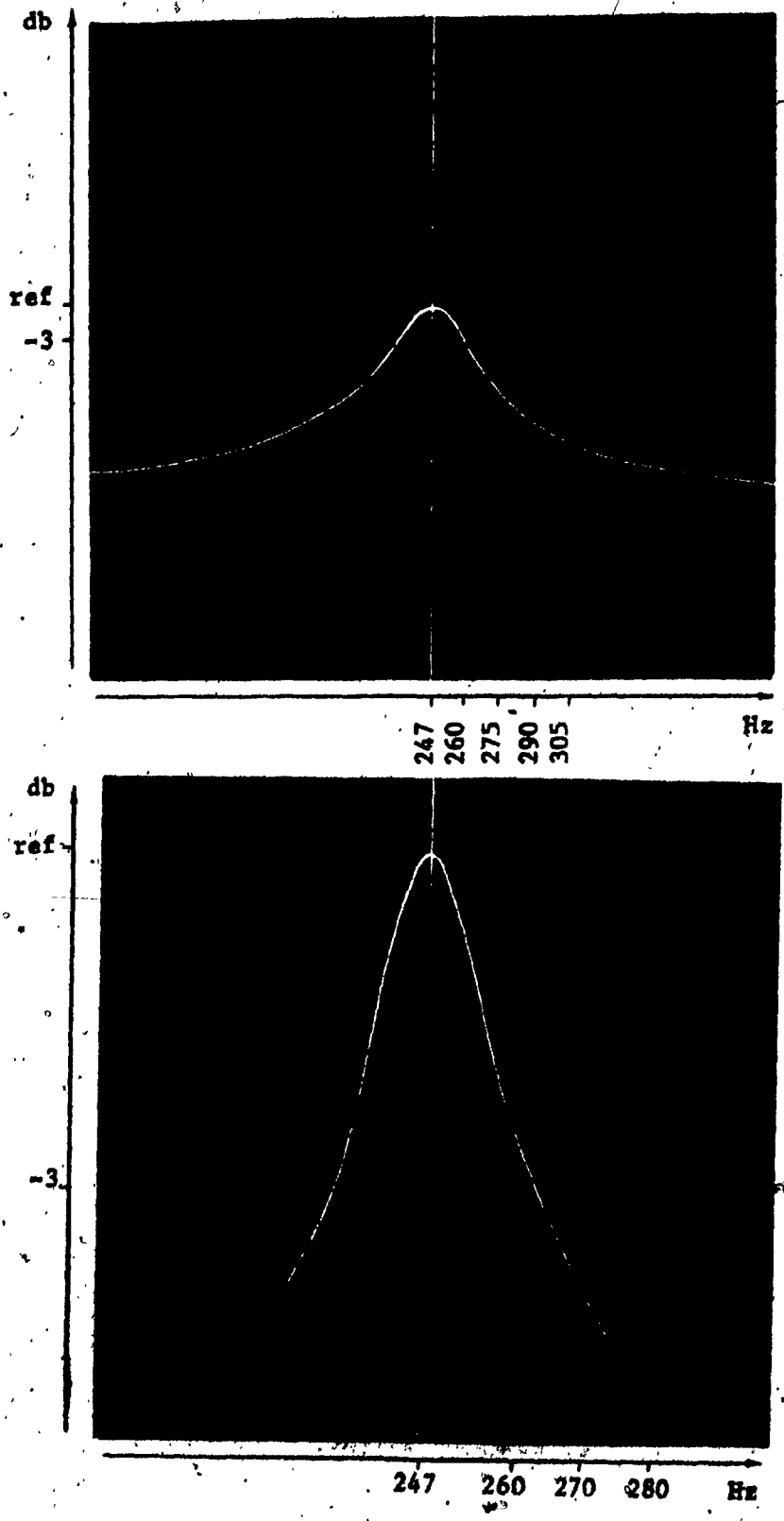

Figure 4.8: Band-Pass Response

It was found that the frequency response error was too small to be measured. It was also found that the effect of the finite GB on the design value of ω_o is negligible, whereas the effect on Q was in agreement with theoretical predications, as shown in figure 4.4. A ± 20% variation in the GB was achieved through a ± 14% variation in the supply voltage. The effect of this variation on the value of Q was found to match theoretical calculations.

4.8 COMPENSATION

It has been mentioned in section 4.5 that the phase lags introduced by the amplifiers result in a Q-enhancement, thus limiting the useful frequency range of the circuit. It is possible to counteract this effect by introducing a phase lead into one or both of the distributed networks.

It is easy to show that the circuit of figure 4.9 has the transfer function

$$T(s) = \frac{\cosh \theta_1}{\cosh \theta_2 \cosh \theta_3 + k \sinh \theta_2 \sinh \theta_3} \qquad (4.18)$$

where

$$k = \frac{R_{o2} C_{o3}}{R_{o3} C_{o2}}, \quad \theta_i = \sqrt{R_{oi} C_{oi} \ell_i^2 s} \qquad (4.19)$$

R_{o2}, R_{o3}, C_{o2} and C_{o3} are the resistances and capacitances per unit length of the lines.

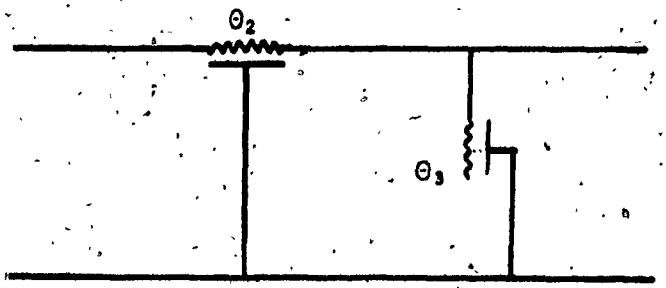

Figure 4.9: Compensation Scheme

letting k = 1, (4.18) becomes

$$T(s) = \frac{\cosh \theta_3}{\cosh \theta} = \frac{p_3}{p} \qquad (4.20)$$

where

$$\theta = \theta_2 + \theta_3$$

The use of this circuit instead of line 2 in the circuit of figure 3.1 results in the network shown in figure 4.10 which has the transfer function

$$T(p) = \frac{K_5K_3p_1p_2/p_3 + K_5p_1 + K_1K_3p_2/p_3 + K_4}{p_1p_2/p_3 - K_2p_2/p_3 - K_6p_1 - K_4} \qquad (4.21)$$

The choice of λ_3 is made such that the $Q - \omega_o$ relation remains flat for the largest possible frequency range. Several filters were compensated using this scheme and the resulting response i.e. the low variation in Q and ω_o from design values indicated the effectiveness of the technique. The Q and ω_o sensitivities were checked after compensation and were found to remain practically unaffected. A typical result of this compensation is shown in figure 4.11 for a low-pass filter of Q = 10.

4.9 DESIGN OF NOTCH FILTER

In this section we show that the same circuit is capable of realizing a notch filter having the voltage transfer function

$$T(s) = \frac{s^2 + \varepsilon s - \omega_n^2}{s^2 + \frac{\omega_o}{Q} s + \omega_o^2} \quad ; \varepsilon = Q \qquad (4.22)$$

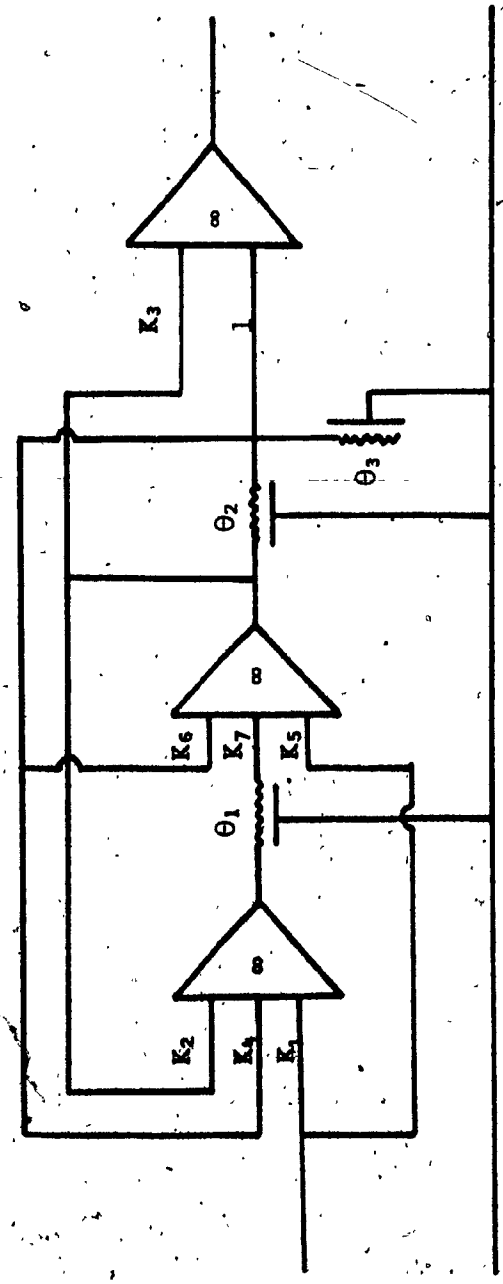

Figure 4.10: Compensated Circuit

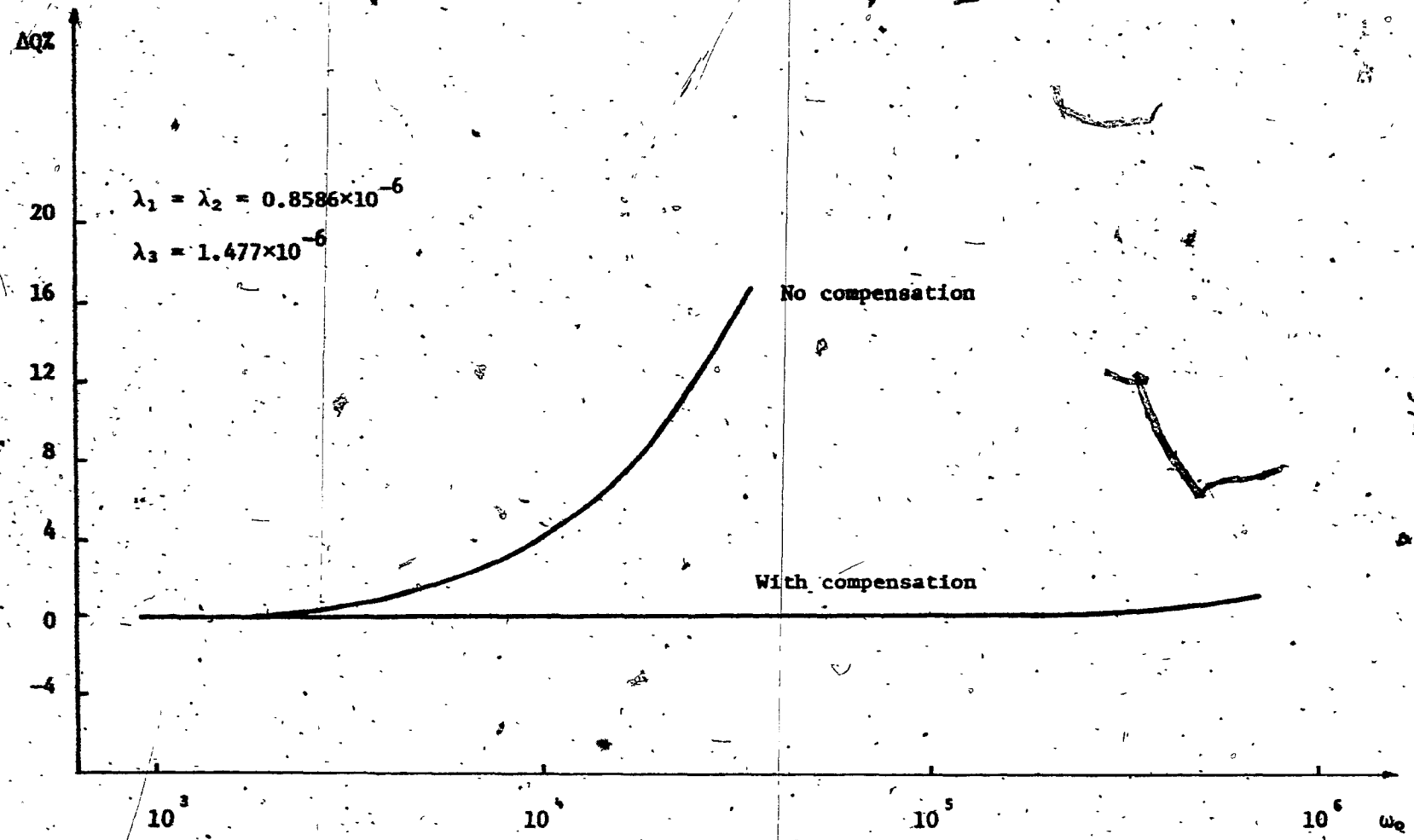

Figure 4.11: Compensated Q - ω_o Characteristics

In addition to Q and ω_o, the notch filter is characterised by ω_n. The factor ε is ideally zero, however, in practice it may be non-zero due to variation in the circuit parameters. A measure of the quality of the notch filter will be taken as

$$\frac{\omega_n}{\varepsilon} \tag{4.23}$$

where ε results from a worst case deviation of the circuit parameters.

Therefore, in the design of the notch filter, the objective function (3.9) is modified to include:

1) The sensitivity of ω_n to different amplifier gains

2) The value ε,

3) The sum of magnitudes of amplifier gains.

It can be easily shown (Appendix H) that

$$S_{y_i}^{\omega_n} = -\frac{y_i}{\omega_n} \text{Imag} \left(\frac{dN/dx_f}{dN/ds} \right)_{s = j\omega_n} \tag{4.24}$$

and

$$\Delta\varepsilon_{y_i} = -\Delta y_i \text{ Real} \left(\frac{dN/dy_i}{dN/ds} \right)_{s = j\omega_n} \tag{4.25}$$

where y_i is a circuit parameter and N is the numerator of the transfer function (4.8) and $\Delta\varepsilon_{y_i}$ is the variation in ε resulting from the largest variation Δy_i in y_i.

The objective function (3.9) then becomes

$$J = W_1 (Q - Qd)^2 + W_2 (\omega_o - \omega_d)^2 + W_3/(\lambda max - \lambda) + \Sigma_i b_i |S_{y_i}^{Q}| + \Sigma_i c_i |S_{y_i}^{\omega_o}| + W_4 \Sigma_i |K_i| + W_5 \Sigma_i |\Delta\varepsilon_{y_i}| \tag{4.26}$$

Several designs were carried out using (4.26). As an example results are presented here for a notch filter having a Q-value of 50 while ω_n is taken to be

1- $\omega_n = 0.8\ \omega_o$

2- $\omega_n = \omega_o$

3- $\omega_n = 1.2\ \omega_o$

The design values are shown in table 4.4. The quantity ε is calculated to be = 0.00118, for a tolerence of ± 0.1% in the amplifier gains. Thus for a notch frequency of 1K rad/sec

$$\frac{\omega_n}{\varepsilon} = 8.475 \times 10^5$$

which is quite high.

4.10 DESIGN OF ALL-PASS FILTER

In this section, the design of an All-pass function of the form

$$T(s) = \frac{s^2 - \omega_z/Q_z\, s + \omega_o^2}{s^2 + \omega_o/Q\, s + \omega_o^2} \qquad (4.27)$$

where $\omega_z = \omega_o$ and $Q_z = Q$, is considered.

In this case the optimization procedure has to result in values of Q_z and ω_z that are as near as possible to ω_o and Q. Therefore, the objective function used in this case is

$$J = W_1(Q - Q_d)^2 + W_2(\omega_o - \omega_{o_d})^2 + W_3(\lambda max - \lambda)$$
$$+ \Sigma_i b_i |S^Q_{y_i}| + \Sigma_i c_i |S^{\omega_o}_{y_i}| + W_4 \Sigma_i |K_i|$$
$$+ W_5(Q_z - Q)^2 + W_6(\omega_{o_z} - \omega_o)^2 \qquad (4.28)$$

TABLE 4.4

NOTCH FILTER DESIGN

	$\omega_n = .8\ \omega_o$	$\omega_n = \omega_o$	$\omega_n = 1.2\ \omega_o$
K_1	-1.13398	-1.297	-1.514
K_2	0.541	0.561	0.548
K_3	.05243	-0.472	-0.418
K_4	-2.789	-2.705	-2.757
K_5	1.0	1.0	1.0
K_6	0.541	0.561	0.548
K_8	1.377	1.467	1.589
λ	3.2753	3.199	3.246
$S^Q_{K_2}$	21.25	22.59	21.76
$S^Q_{K_4}$	26.55	26.47	26.52
S^Q_λ	0.0	0.0	0.0
$S^{\omega_o}_{K_2}$	-0.252	-0.272	-0.259
$S^{\omega_o}_{K_4}$	0.440	0.451	0.444
$S^{\omega_o}_\lambda$	-1.0	-1.0	-1.0

TABLE 4.4 CONTINUED

$S^{\omega_n}_{K_1}$	0.7245	0.688	0.665
$S^{\omega_n}_{K_3}$	-0.4619	-0.489	-0.508
$S^{\omega_n}_{K_5}$	-0.7245	-0.688	-0.665
$S^{\omega_n}_{K_6}$	0.547	0.5495	0.5628
$S^{\omega_n}_{K_8}$	0.547	0.5495	0.5628
$S^{\omega_n}_{\lambda}$	-1.0	-1.0	-1.0
$\Delta^{\epsilon}_{K_1}$	0.111	0.0661	0.0235
$\Delta^{\epsilon}_{K_3}$	-0.266	-0.231	-0.175
$\Delta^{\epsilon}_{K_5}$	-0.111	0.0661	-0.0235
$\Delta^{\epsilon}_{K_6}$	-0.32	-0.4568	-0.62
$\Delta^{\epsilon}_{K_8}$	-0.32	-0.4568	-0.62
$\Delta^{\epsilon}_{\lambda}$	0.0	0.0	0.0

The design was carried out for several all-pass filters by minimizing the approximation error and the sensitivities of ω_o, Q, ω_z and Q_z to the different parameters. Results for an all-pass section of $Q = 10$ are shown in table 4.5 and figure 4.12.

4.11 CONCLUSION

A new distributed RC-active configuration for realizing second order voltage transfer functions has been described. The configuration uses three finite gain amplifiers and two grounded commensurate $\overline{URC}$'s. The design is based on an optimization program which simultaneously yields a very close fit to the desired response and low sensitivity of Q and ω_o with respect to the various elements, while guaranteeing stable operation. Further, the Q-sensitivity to changes in the RC product of the $\overline{URC}$'s is identically zero. The method was used to design low-pass, band-pass, high-pass, notch and all-pass transfer functions having Q's up to 100 and centre frequency ω_o, of up to 10K rad/sec. The sensitivity of Q to changes in amplifier gains was found to be of the order of Q/2, while that of ω_o never exceeded 0.5. It was found that a gain-band-width product of 1MHz limited the design value of ω_o to about 350 Hz for a mixiumum of ±5% change in Q and an effective operating range of 3500 Hz. When second order filters were built and tested, experimental results were found to agree with theoretical predictions. The design was also found to compare favourably with circuits proposed by Kerwin and Hualsman.

The introduction of a compensation scheme extended the useful frequency range considerably, and the length of the $\overline{\text{URC}}$ required for compensation was comparable to the length of the main $\overline{\text{URC}}$'s.

TABLE 4.5

ALL-PASS DESIGN , Q = 10

Parameter	Value
λ	2.5998
K_2	0.65880
K_4	-1.99
K_1	-1.177
K_3	-.509
K_5	1.0
K_8	1.04
K_6	0.6588
$S_{K_2}^{Q}$	6.418
$S_{K_4}^{Q}$	5.597
S_{λ}^{Q}	0.0
$S_{K_2}^{\omega_o}$	-.4478
$S_{K_4}^{\omega_o}$	0.549
$S_{\lambda}^{\omega_o}$	-1.0
$S_{K_6}^{Q}$	8.167

TABLE 4.5 CONTINUED .

$\frac{Q_z}{S_{K_1}}$	4.08
$\frac{Q_z}{S_{K_3}}$	-7.61
$\frac{Q_z}{S_{K_5}}$	-4.08
$\frac{Q_z}{S_{K_\lambda}}$	0.0
$\frac{\omega_z}{S_{K_6}}$	0.5486
$\frac{\omega_z}{S_{K_1}}$	0.726
$\frac{\omega_z}{S_{K_3}}$	-0.452
$\frac{\omega_z}{S_{K_5}}$	-0.726
$\frac{\omega_z}{S_{K_6}}$	0.549
$\frac{\omega_z}{S_{K_\lambda}}$	-1.0

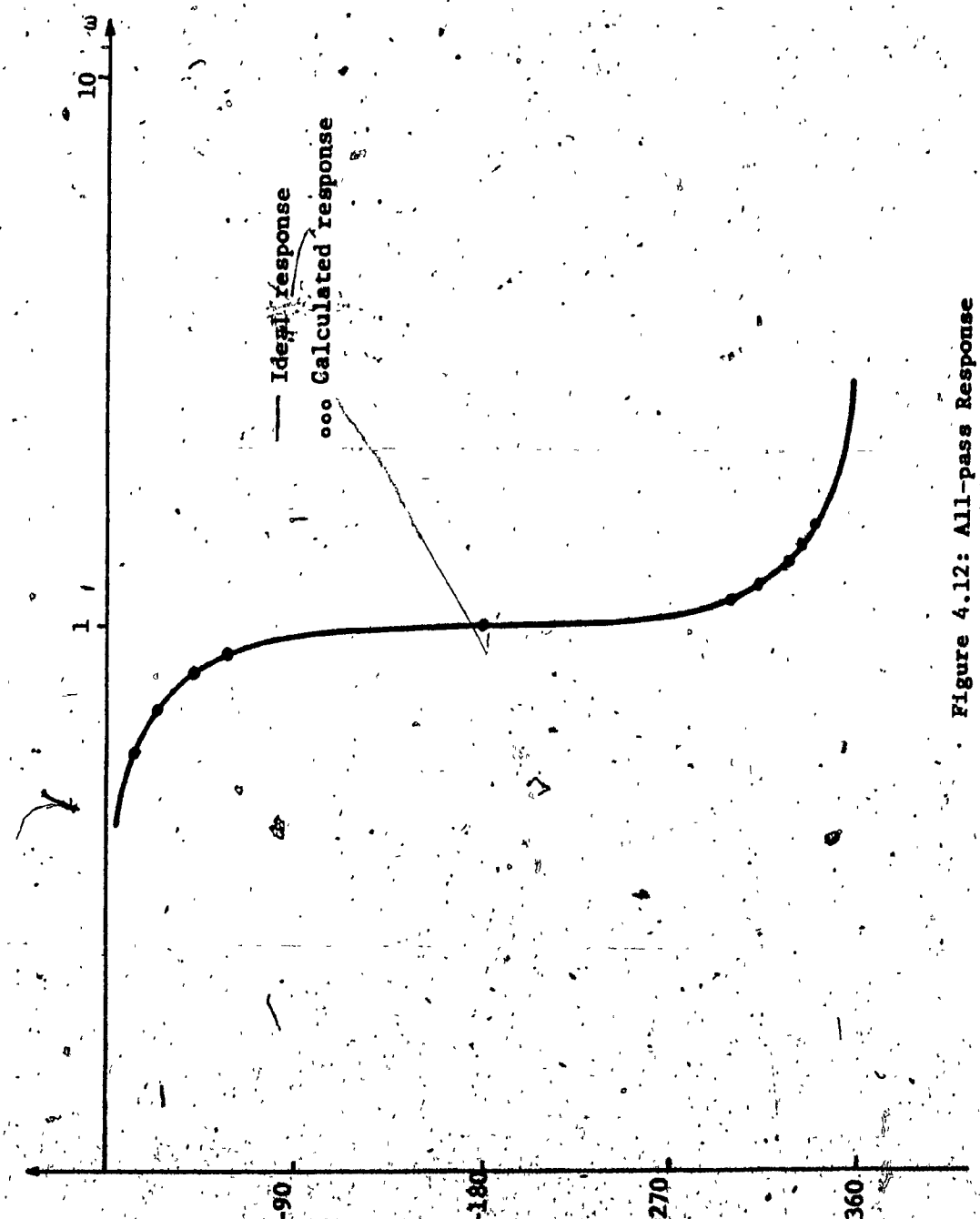

Figure 4.12: All-pass Response

CHAPTER 5

CONCLUSIONS AND SUGGESTIONS FOR FURTHER WORK

In Chapter 1, the problem of synthesizing transfer functions using distributed RC lines was considered and the approach to be used in the thesis defined.

In the remaining chapters, optimization techniques were used to design distributed passive and active circuits to meet various criteria. For the passive synthesis of all-pole voltage transfer functions an approximation procedure was presented and used to show that these functions could be approximated by cascades of $\overline{URC}$'s. The design problem was then formulated as an optimization problem where the performance criterion was a best approximation combined with a minimal area required by the network. It was shown that the problem possesses a unique optimal solution and the effectiveness of the optimization procedure demonstrated through several examples. A comparison with lumped realizations showed that the distributed design often requires less overall area. A grounded $\overline{URC}$ active network capable of realizing any transfer function was then presented. A design procedure was derived to achieve simultaneously very good approximation of the given specification together with minimum sensitivity of the response to parameter variations. The procedure was used to design low-pass, band-pass, high-pass , notch and all-pass filters. The results demonstrated the practicality of the design since:

1- The values of the amplifier gains were in the neighbourhood of unity.

2- The RC product was within the practical limits dictated by the technology.

3- The sensitivity of Q to the RC product was identically zero.

4- The sensitivity of Q to amplifier gains was of the order of Q/2

5- The sensitivities of ω_o to various parameters was always less than a half.

As the finite band width of the amplifiers limits the useful frequency of operation of the filter, a simple compensation scheme was introduced with which the frequency of operation could be considerably extended.

The effect of other parasitic impeffections of the operation amplifiers such as the input and output impedances were found to be neglible in the experimental prototypes tested.

The proposed network has also been shown to compare favourably with other circuits using distributed elements, insofar as the effect of GB product and the variation of amplifier gains is concerned.

For low frequency design it was demonstrated that the use of tapered $\overline{RC}$ lines is to be preferred, as these have much lower sensitivities than designs using $\overline{URC}$'s. It was possible to carry out designs using $\overline{ERC}$'s where the desired response had a centre frequency of 1 Hz. Such filters should be useful in such areas as biomedical engineering and stress analysis [58] - [59] .

Additional factors which could be considered in the design are the dynamic range of the filters and the effect of noise on the performance.

Although the effect of amplifier imperfections was studied, it would be of interest to incorporate these into the optimal design procedure.

A study of the cost of production, in comparison with other designs, should also be carried out.

Finally it is of academic interest to obtain an analytic evaluation for the errors of approximation using distributed parameter networks.

REFERENCES

[1] L.P.Huelsman , Ed. Active Filters: Lumped, Distributed, Integrated Digital and Parametric, New York, McGraw Hill, 1970.

[2] P.M. Chirlian, Integrated and Active Network Analysis and Synthesis, Prentice Hall, 1967.

[3] M.S. Ghausi and J.J. Kelly, Introduction to Distributed Parameter Networks with Application to Integrated Circuits, Holt, Rinehart and Winston, 1968.

[4] A.J. Khambata, Introduction to Integrated Semiconductor Circuits, John Wiley and Sons, 1963.

[5] S.N. Levine, Principles of Solid State Microelectronics, Holt Rinehart and Winston, 1963

[6] R.N. Newcomb, Active Integrated Circuit Synthesis, Englewood Cliffs, N.J., Prentice-Hall, 1968

[7] S.K. Mitra, Analysis and Synthesis of Linear Active Networks, New York: John Wiley, 1969.

[8] K.W. Heizer,"Distributed RC Networks with Rational Transfer Functions" IRE Trans., Vol. CT-9, p.p. 356-362, December 1962.

[9] S.Y. Hwang and W.C. Duesterhoeft Jr., "Distributed RC Networks with Rational y-Parameters Having Prescribed Poles", IEEE Trans., Vol. CT-16, No. 4, p.p. 423-428, November 1969.

[10] E.D. Walsh and C.M. Close, "On the Synthesis of Any RC-Realizable Rational Transfer Function Using a Non-uniform RC Distributed Circuit", IEEE Trans., Vol. CT-17, p.p. 217-223, May 1970.

[11] D.G. Barker, "Synthesis of Active Filters Employing Thin Film Distributed Parameter Networks", IEEE Int. Conv. Record, Vol. 13, Part 7, pp. 119-126, 1965.

[12] Y. Fu and J.S. Fu, "Synthesis of Active Distributed RC Networks", IEEE Trans., Vol. CT-13, September 1966, pp. 259-264.

[13] Y. Fu and J.S. Fu, "N-Port Rectangular-Shaped Distributed RC Networks", IEEE Trans., Vol. CT-13, pp. 222-226, 1966.

[14] R.A. Rohrer, S.A. Resh and R.A. Hoyt, "Distributed Network Synthesis for a Class of Integrated Circuits", IEEE Int. Conv. Rec., 1965, 13, Part 7, pp. 100-112.

[15] R.W. Wyndrum Jr., "The Exact Synthesis of Distributed RC Networks", New York University Technical Report 400-76, May 1963.

[16] R.W. Wyndrum Jr., "The Exact Realization of Distributed RC Driving Point Functions", Wescon Record, 1964, 8, Part 2, Paper 18.1.

[17] R.W. Wyndrum Jr., "The Realization of Monmorphic Thin Film Distributed RC-Networks", IEEE Int. Conv. Rec., 1965, 13, Part 10, pp. 90-95.

[18] R.P. O'Shea, "Synthesis Using Distributed RC Networks", IEEE Conv. Record, Vol. 13, Part 7, pp. 18-29, 1965.

[19] J.O. Scanlan and J.D. Rhodes, "Realizability and Synthesis of a Restricted Class of Distributed RC Networks", IEEE Trans. Vol., CT-12, pp. 277-285, December 1965.

[20] S.C. Lee, "Synthesis of Absolutely Stable Active Distributed RCG Networks", Proc. of the 11th Midwest Symposium on Circuit Theory, pp. 99-113, 1968.

[21] J.D.Rodhes , "Transfer Function Realizability of Grounded URC Networks", IEEE Trans., Vol. CT-14, pp. 129-139, June 1967.

[22] H.J. Riblet, "General Synthesis of Quarter-Wave Impedance Transformers", IRE Trans. On Microwave Theory and Techniques, p.p. 36-43, January 1957.

[23] M.S. Ghausi and V.C. Bello, "Design of Linear Phase Active Distributed RC Networks", IEEE Trans. Vol. CT-16, pp. 526-530, November 1969.

[24] W.J. Kerwin, "Synthesis of Active RC Networks Containing Lumped and Distributed Elements", Proc. First Asilomar Conference on Circuits and Systems", pp. 288-298, November 1967.

[25] M.N.S. Swamy and J. Walsh, "A Simple Design Procedure for Active Low Pass Filters Using Exponential Lines", Proc. 13th Midwest Symposium on Circuit Theory, Minneapolis, Minn., pp. x6.1-x6.10, May 1970.

[26] J. Walsh, "Basic Lines and Some of Their Applications as Distributed RC Circuit Elements", Ph.D. Thesis, The University of Calgary, Calgary, Alberta, April 1971.

[27] H. Mahdi, "Synthesis of Low Pass Linear Phase Active Circuits Using Distributed RC Networks", IEEE International Symposium On Circuit Theory, Symposium Digest pp. 110, December 1969.

[28] M.S. Abougabal, B.B. Bhattacharyya and M.N.S. Swamy, "A Low Sensitivity Active Distributed Realization of Rational Transfer Functions", IEEE Trans., Vol. CAS-21, pp. 391-395, May 1974.

[29] S.K. Mitra, Ed., Active Inductorless Filters, IEEE Press, 1971

[30] W.J. Kerwin, L.P. Huelsman and R.W. Newcomb, "State Variable Synthesis for Insensitive Integrated Circuit Transfer Functions", IEEE Journal of Solid State Circuits, Vol. SC-2, pp. 87-92, September 1967.

[31] R. Tarmi and M.S. Ghausi, "Very High Q Insensitive Active RC Networks", IEEE Trans., Vol. CT-17, pp. 358-366, August 1970.

[32] L.C. Thomas, "The Biquad: Part II - A Multipurpose Active Filtering System", IEEE Trans., Vol. CT-18, pp. 358-361, May 1971.

[33] T.A. Hamilton and A.S. Sedra, "Some New Configurations for Active Filters", IEEE Trans., Vol. CT-19, pp. 25-33, January 1972.

[34] P.O. Brackett, "A New Single Op-Amp. Active RC Network", Proc. 16th Midwest Symposium on Circuit Theory, April 1973.

[35] G.S. Moschytz and W. Thelen, "Design of Hybrid Integrated Filter Building Blocks", IEEE Journal of Solid State Circuits, Vol. SC-5 pp. 99 - 107, June 1970.

[36] G.S. Moschytz, "Gain-Sensitivity Product - A Figure of Merit for Hybrid Integrated Filters Using Single Operational Amplifiers", IEEE Journal of Solid State Circuits, Vol. SC-6, pp. 103-110, June, 1971.

[37] J.J. Stein, J.H. Mulligan and S.S. Shamis, "Realization of Transfer Functions Using Uniform RC Distributed Networks with Common-Ground Connections", Proc. of the Symposium of Generalized Networks, Polytechnique Institute of Brooklyn, pp. 149-172, April 1966.

[38] W. Happ and G. Riddle, "Limitations of Film-Type Circuits Consisting of Resistive and Capacitive Layers", IRE International Convention Record, Vol. 9, Part 6, pp. 141-165, 1961.

[39] J. Dupeak, Western Electric, "Manufacture of Thin Film Filters", Workshop on Active Networks, Organized by IEEE Circuits and Systems Society, November 1973.

[40] M. Fogiel, Microelectronics, N.Y. : Research and Education Association, 1969.

[41] Private Communication with Dr. B. Lombos, Concordia University, Montreal, Canada.

[42] B.B. Bhattacharyya, M.S. Abougabal and M.N.S. Swamy, "On an Integrable Active RC Filter", Proc. IEEE ISCT, pp. 256-259, April 1973.

[43] J.C. Giguere, M.N.S. Swamy and B.B. Bhattacharyya, "Driving Point Function Synthesis Using Non-uniform Lines", Proc. IEE. Vol. 116, No. 1, pp. 65-70, January 1969.

[44] J.C. Giguere, M.N.S. Swamy and B.B. Bhattacharyya, "Distributed RC Network Synthesis of Transfer Functions Using Symmetric Structures", IEEE Trans., Vol. CT-17, pp. 448-451, August 1970.

[45] J.C. Giguere, M.N.S. Swamy and B.B. Bhattacharyya, "Driving Point Function Synthesis Using Uniform Transmission Lines", Proc. IEEE (Corres.), 1968, 56, pp. 868-869.

[46] M.N.S. Swamy, J.C. Giguere and B.B. Bhattacharyya, "Synthesis using Symetric Distributed RC-Structures", The Radio and Electronic Engineer, Vol. 40, No. 1, pp. 38-44, July 1970.

[47] Van Valkenburg, Introduction to Modern Network Synthesis, John Wiley and Sons, 1960.

[48] J.C. Giguere, "The Synthesis of Network Functions Using Non-uniform Transmission Lines"., Ph.D. Thesis, Nova Scotia Technical College, 1968.

[49] M. El-Diwany and J. Giguere, "Area Minimization of Distributed RC Networks", Proc. of IEEE International Symposium on Circuit Theory, pp. 338-340, 1973.

[50] J.C. Giguere, M. Vidyasagar and M.N.S. Swamy, "Input Output Stability of two Broad Classes of Lumped-Distributed Networks", Journal of the Franklin Institute, Vo. 294, No. 3, pp. 203-213, September, 1972.

[51] A.V. Fiacco and C.P. McCormic, "The Sequential Unconstrained Minimization Technique for Nonlinear Programming, A Primal-Dual Method", Management Science, vol. 10, No. 2, pp. 360-366, Jan. 1964.

[52] A.V. Fiacco and G.P. McCormick, Nonlinear Programming, Sequential Unconstrained Minimization Techniques, John Wiley, New York, 1968

[53] _____, "Computational Algorithm for the Sequential Unconstrained Minimization Technique for Nonlinear Programming", Management Science, vol. 10, No. 4, pp. 601-617, July 1964.

[54] G.P. McCormick and A.V. Fiacco, "Experimental SUMT", Research Analysis Corp., McLean, Firginia, TP-151, March 1969.

[55] Information from the Microelectronics laboratory, Concordia University, Montreal, Canada.

[56] J.C. Giguere, "The Approximation of a Nonuniform Transmission Line by a Cascade of Uniform Lines", Electronics letters, pp. 511-512, September 1971.

[57] J. Kelly and M. Ghausi, "On the Effective Dominant Pole of the Distributed RC Networks", J. of Franklin Institute, Vol. 279, No. 6, pp. 417-428, June 1965.

[58] M. Clynes and J. Milsum, Biomedical Engineering Systems, N.Y., McGraw Hill, 1970.

[59] A.M. Khalil and P. Fazio "Moire-Fringe Measurement", Experimental Mechanics, Vol. 13, No. 6, pp. 253-254, June 1973.

[60] C.V. Shaffer and W.J. Kerwin, "Multiloop Distributed RC Active Networks for Low Parameter Sensitivity with Low Amplifier Gain", Proc. Second Asilomar Conference, pp. 197-201, 1968.

[61] S.P. Johnson and L.P. Huelsman, "High Pass and Band Pass Filters with Distributed Lumped Active Networks", Proc. IEEE, Vol. 59, pp. 328-331, February 1971.

[62] D.A. Pierre, Optimization Theory with Applications, John Wiley and Sons, 1969.

APPENDIX (A)

THE SEQUENTIAL UNCONSTRAINED MINIMIZATION TECHNIQUE (SUMT)

This technique consists of transforming a constrained minimization problem into an equivalent unconstrained one.

The problem is to determine a vector $\underline{Y}^* = [y_1^*, y_2^*, \ldots, y_n^*]$ such that

$f(\underline{Y})$ is minimum

$g_i(\underline{Y}) > 0 \quad , \quad i = 1, \ldots, n$

One of the four different versions of the SUMT uses a penalty function of the form

$$P(\underline{Y}, \rho) = f(\underline{Y}) + \rho \sum_{i=1}^{n} 1/g_i(\underline{Y})$$

The algorithm used for solving the problem consists of picking a proper value for ρ, minimizing P and then reducing ρ and minimizing p again. A theorem given by Fiacco and McCormick states that if the sequence of positive bounded numbers ρ_k is monotonically decreasing then the sequence of minimized function $P^*(\underline{Y}_k, \rho_k)$ will converge to the infimum of $f(\underline{Y})$. This is true if the functions involved satisfy the following conditions:

c1 : $\Phi^\circ = \{Y : g_i(\underline{Y}) > 0, \ i = 1, 2, \ldots, n\}$ is nonempty

c2 : The functions $f, g_1, g_2, \ldots, g_n$ are twice continuously differentiable.

c3 : For every finite κ, $\{\underline{Y} : f(\underline{Y}) \leq \kappa, \ \underline{Y} \in \Phi\}$ is a bounded set where Φ is the closure of Φ°.

c4 : $f(\underline{Y})$ is convex.

c5 : $g_1, g_2, \ldots, g_n$ are concave.

c6 : $P(\underline{Y},\rho)$ is, for each $\rho > 0$, strictly convex for $\underline{Y} \in \Phi$.

This is a very concise summary, the reader is referred to [51], [54] for more details.

APPENDIX B

PROOF OF THEOREM 2.1

In the continued fraction expansion of (2.6), let us consider the impedance remaining after the extraction of some lines. Let the poles and zeros of this impedance be p_i''s and z_i''s while those of the original function are p_i's and z_i's. A simple drawing of the impedance function during the realization process shows the monotinicity of the relations between p_i', z_i', p_i and z_i. Therefore it is enough to show that, at any stage of the realization, the ratio between the first two resistances has a convex relationship with p_i' and z_i'.

Consider the impedance

$$Z(v) = \frac{v^{m+1}+a_m v^m + a_{m-1} v^{m-1} + \ldots + a_o}{v^m + b_{m-1} v^{m-1} + \ldots\ldots\ldots + b_o} \qquad \text{(B-1)}$$

A continued fraction expansion yields

$$r_{21} = \frac{R_2}{R_1} = \frac{1-b_{m-1}-b_{m-2}+a_{m-1}}{b_{m-1}+b_{m-2}-a_{m-1}} \qquad \text{(B-2)}$$

From the properties of polynomials we have

$$b_{m-1} = -\Sigma p_i \,, \quad b_{m-2} = \sum_{i\neq j} \sum p_i p_j \,, \quad a_{m-1} = \sum_{i\neq j} \sum z_i z_j \,. \qquad \text{(B-3)}$$

Let

$$b'_{m-1} + b'_{m-2} \triangleq \mu_1$$

and

$$a_{m-1} \triangleq \mu_2 \qquad \text{(B-4)}$$

then we obtain

$$r_{21} = \frac{1 - \mu_1 + \mu_2}{\mu_1 - \mu_2} \tag{B-5}$$

$$r_{12} = \frac{\mu_1 - \mu_2}{1 - \mu_1 + \mu_2} \tag{B-6}$$

It follows that

$$\frac{\delta^2 r_{21}}{\delta p_i^2} = \frac{-(\mu_1-\mu_2)^2\mu_1'' + 2(\mu_1-\mu_2)\,(\mu_1')^2}{(\mu_1 - \mu_2)^4} \tag{B-7a}$$

$$\frac{\delta^2 r_{21}}{\delta z_i^2} = \frac{(\mu_1-\mu_2)^2\mu_2'' + 2(\mu_1-\mu_2)\,(\mu_2')^2}{(\mu_1 - \mu_2)^4} \tag{B-7b}$$

$$\frac{\delta^2 r_{12}}{\delta p_i^2} = \frac{(1-\mu_1+\mu_2)^2\mu_1'' + 2(1-\mu_1+\mu_2)(\mu_1')^2}{(1 - \mu_1 + \mu_2)^4} \tag{B-7c}$$

$$\frac{\delta^2 r_{12}}{\delta z_i^2} = \frac{(1-\mu_1+\mu_2)^2\mu_2'' + 2(1-\mu_1+\mu_2)(\mu_2')^2}{(1 - \mu_1 + \mu_2)^4} \tag{B-7d}$$

From (4), (5) and (7), we have

$$p_{-i} = -2 - p_i,\ z_{-i} = -2 - z_i \tag{B-8}$$

where p_{-i} and p_i, (z_{-i} and z_i) are symmetric roots around the point $v = -1$.

Hence

$$\mu_1' = \frac{\delta \mu_1}{\delta p_i} = -2 - 2p_i \qquad \text{(B-9a)}$$

$$\mu_1'' = \frac{\delta^2 \mu_1}{\delta p_i^2} = -2 \qquad \text{(B-9b)}$$

$$\mu_2' = \frac{\delta \mu_2}{\delta z_i} = -2 - 2z_i \qquad \text{(B-9c)}$$

$$\mu_2'' = \frac{\delta^2 \mu_2}{\delta z_i^2} = -2 \qquad \text{(B-9d)}$$

Substituting from (B-9) into (B-7) and noting that $1 > \mu_1 - \mu_2 > 0$ and $1 > 1 - \mu_1 + \mu_2 > 0$ it can be seen that all the second derivatives are positive. This shows that the ratio between any two line resistances has a strictly convex relationship with the poles of z(v).

Using the slack variable ψ as an upper bound for the ratios we have $\psi - r_{ij} > 0$, $i,j = 1,2,\ldots,\ell$ (B-10) where the minimization of ψ is in fact a minimization of the maximum resistance ratio.

Now we are in position to investigate the conditions of problem A:

1. The nonemptiness of $\Phi^\circ = \{\underline{Y}: g_i(\underline{Y}) > 0, i = 1, \ldots, n\}$ is guarnateed by (2.9) and the fact that $y_1 = 0$.
2. It is clear that ψ, g_ℓ's and g_i's are continuous in Φ°.

3. The boundedness of $\underline{Y}$ is guaranteed by the fact that all roots in the v-plane are between zero and -2.

4. ψ is convex in ϕ.

5. When r_{ij} is convex in ϕ, g_ℓ's are concave, g_i's are also concave in ϕ.

6. When ψ and $\frac{1}{g_i}$ are both convex and $\frac{1}{g_\ell}$ is strictly convex, it can be seen that $\forall \rho > 0$, P is strictly convex in ϕ.

It is clear now that problem A satisfies the conditions in Appendix A.

APPENDIX C

THE RELATION BETWEEN λ AND THE POLES OF THE DRIVING POINT FUNCTION $z_{11}(v)$

From equation (2.15) we can write for the case of negative real poles, $s_i = \sigma_i$.

$$u_i = u(-s_i) = -\tan^2 \sqrt{\lambda\sigma_i} \tag{C-1}$$

Using (2.2) and (C-1)

$$u_i = \frac{p^2(s_i) - 1}{p^2(s_i)} = \frac{p_i^2 - 1}{p_i^2} \tag{C-2}$$

Hence we can write the factor $(u-u_i)$ as

$$u - u_i = \frac{p^2 - 1}{p^2} - \frac{p_i^2 - 1}{p_i^2}$$

$$= \frac{1}{p^2 p_i^2}(p^2 - p_i^2) \tag{C-3}$$

From (C-1), (C-3) and (2.2) we have

$$u - u_i = \frac{1}{p^2 p_i^2}(p^2 - \cos^2 \sqrt{\lambda\sigma_i}) \tag{C-4}$$

From (C-4), (2.5) and (2.6) it is seen that the v-plane poles are related to λ by the relation.

$$v_i = p_i - 1 = \cos \sqrt{\lambda\sigma_i} \tag{C-5}$$

And if we note that $-2 \leq v_i \leq 0$ we can see that the function $\lambda \rightarrow v_i$ is single valued and monotonic

APPENDIX D

FLOWCHART FOR THE DESIGN PROCEDURE IN CHAPTER 2

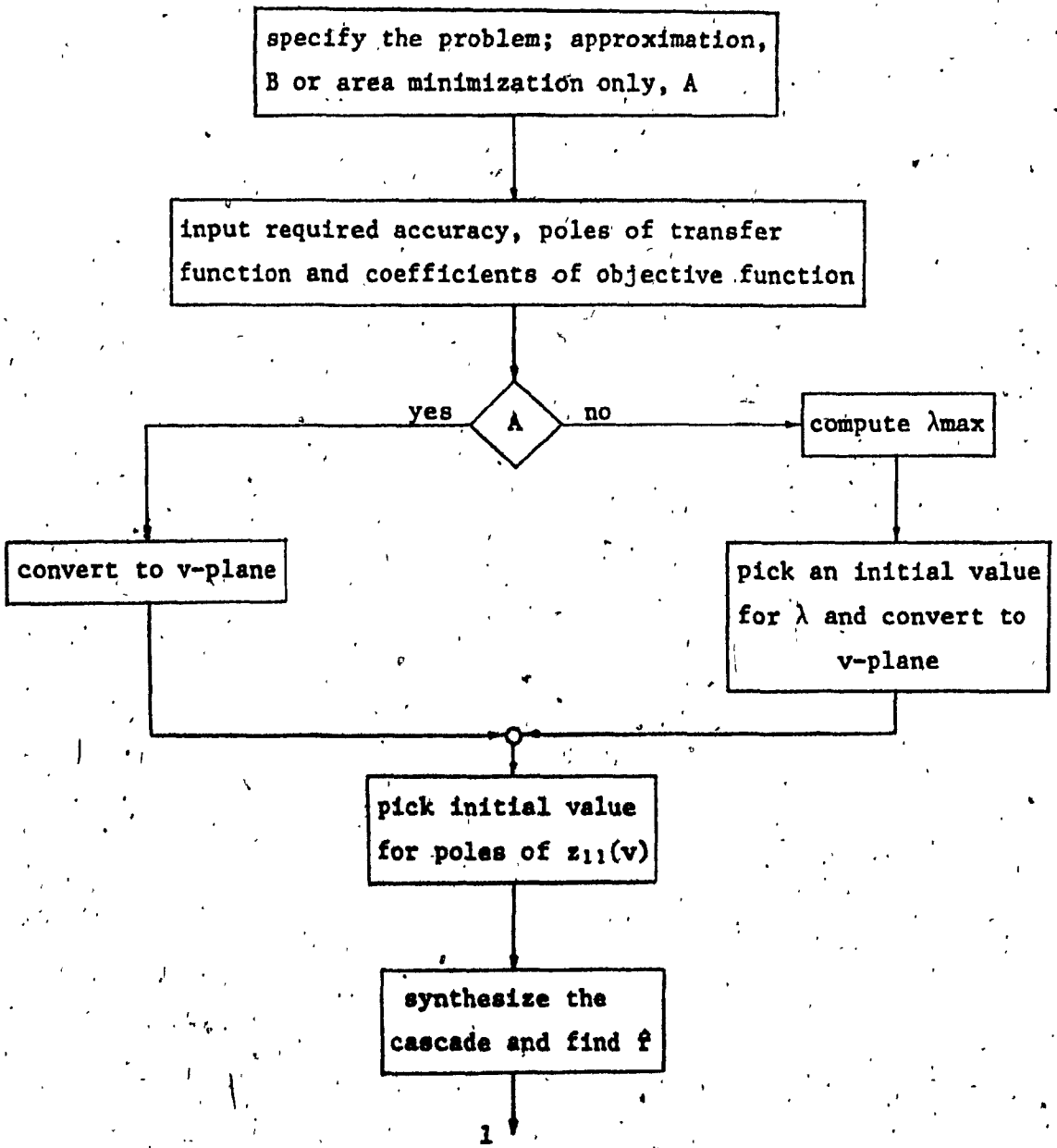

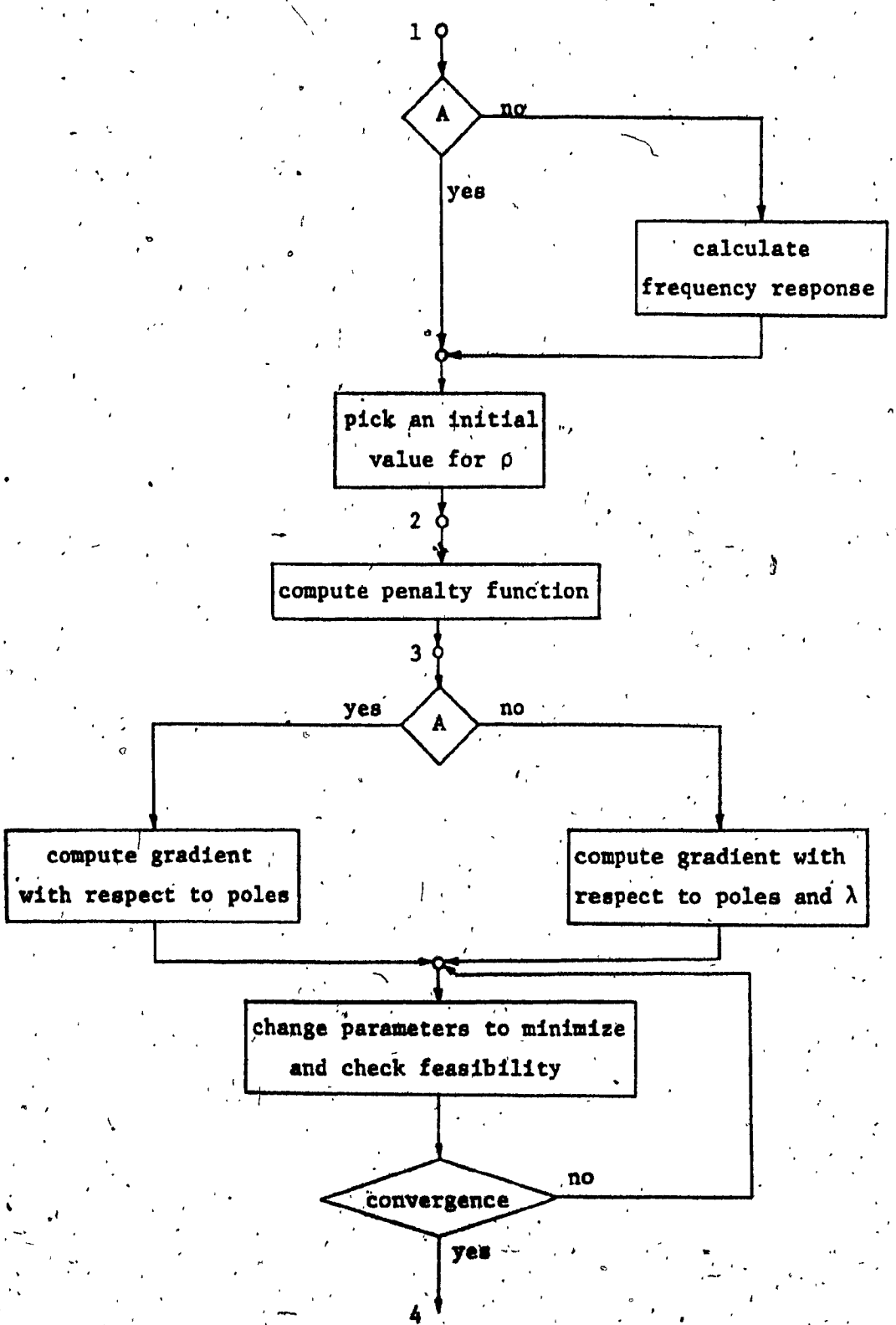
1
A
no
yes
calculate
frequency response
pick an initial
value for ρ
2
compute penalty function
3
yes
A
no
compute gradient
with respect to poles
compute gradient with
respect to poles and λ
change parameters to minimize
and check feasibility
convergence
no
yes
4

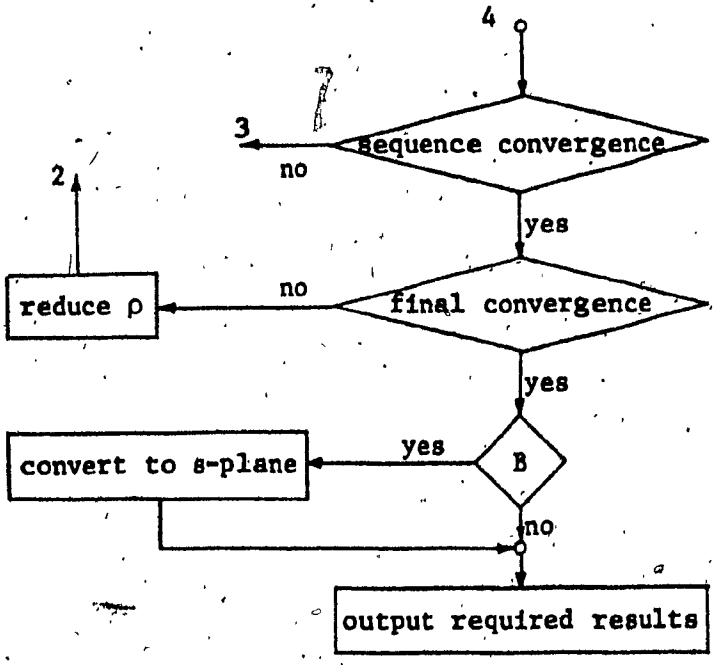
4
3
sequence convergence
no
yes
2
reduce ρ
no
final convergence
yes
convert to s-plane
yes
B
no
output required results

APPENDIX E

SENSITIVITIES OF Q AND ω_o

As we are dealing with transcendental functions, the expressions Q and ω_o are not readily obtainable, and hence the sensitivity expressions for Q and ω_o are obtained as follows: Let D(s,x) denote the denominator of T(s) where x is any circuit parameter. Assuming that both s and x vary such that the value of D(s,x) remains constant, we have

$$dD = 0 = \frac{\delta D}{\delta x}\, dx + \frac{\delta D}{\delta s}\, ds \qquad \text{(E-1)}$$

or

$$\frac{ds}{dx} = - \frac{\delta D/\delta x}{\delta D/\delta s} \qquad \text{(E-2)}$$

Let

$$s_o = \sigma_o + j\beta_o$$

For high values of Q we may assume that $\beta_o = \omega_o$.

Hence,

$$Q = \omega_o / 2\sigma_o \qquad \text{(E-3)}$$

$$ds_o = d\sigma_o + j\, d\omega_o \qquad \text{(E-4)}$$

From (E-3) we get

$$\frac{dQ}{Q} = \frac{d\omega_o}{\omega_o} - \frac{d\sigma_o}{\sigma_o}$$

$$= \frac{1}{\omega_o} \text{Imag } ds_o - \frac{1}{\sigma_o} \text{Real } ds_o \qquad \text{(E-5)}$$

Hence ,

$$S_x^Q = S_x^{\omega_o} - S_x^{\sigma_o}$$

$$= \frac{x}{\omega_o} \text{ Imag } \frac{ds_o}{dx} - \frac{x}{\sigma_o} \text{ Real } \frac{ds_o}{dx}$$

Using (E-2) the above may be re-written as

$$S_x^Q = \left[- \frac{x}{\omega_o} \text{ Imag } \frac{\delta D/\delta x}{\delta D/\delta s} + \frac{x}{\sigma_o} \text{ Real } \frac{\delta D/\delta x}{\delta D/\delta s} \right]_{s = s_o} \quad (E-6)$$

It is also obvious that,

$$S_{x_o}^{\omega} = \left[\frac{-x}{\omega_o} \text{ Imag } \frac{\delta D/\delta x}{\delta D/\delta s} \right]_{s = s_o} \quad (E-7)$$

APPENDIX F

FLOWCHART FOR THE DESIGN PROCEDURE IN CHAPTER 3

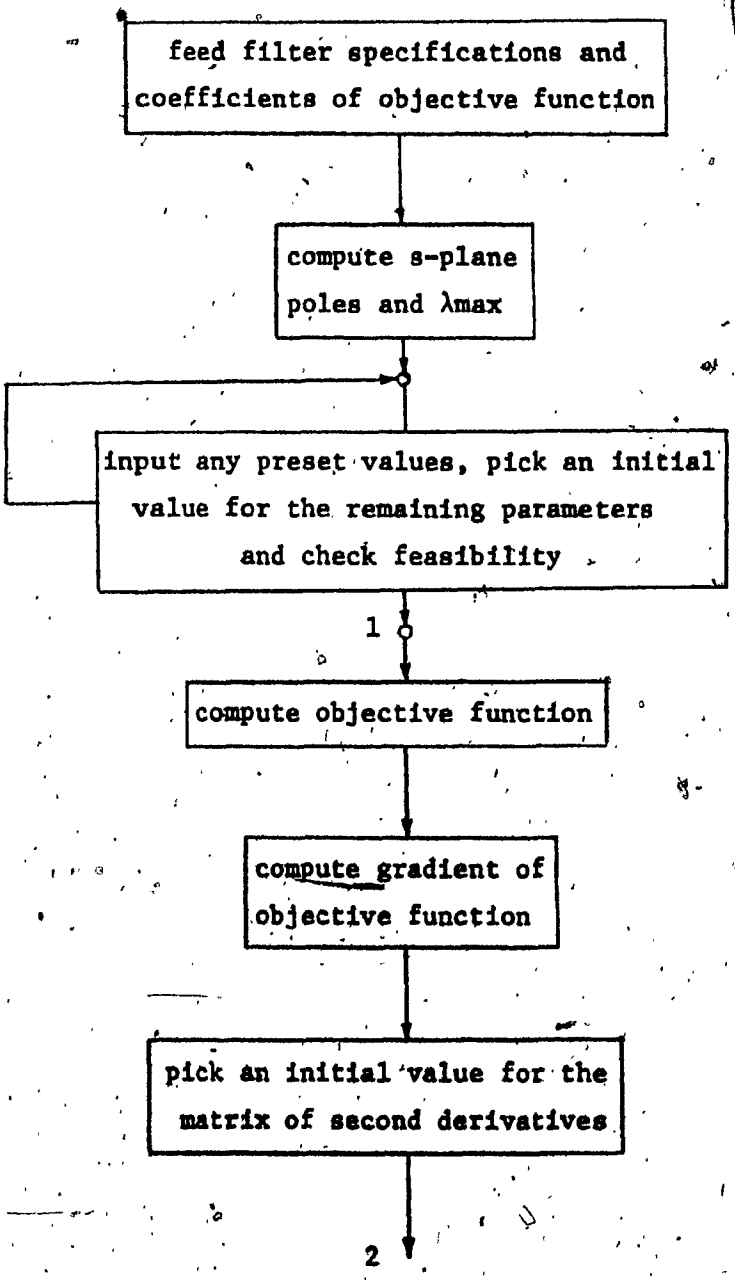

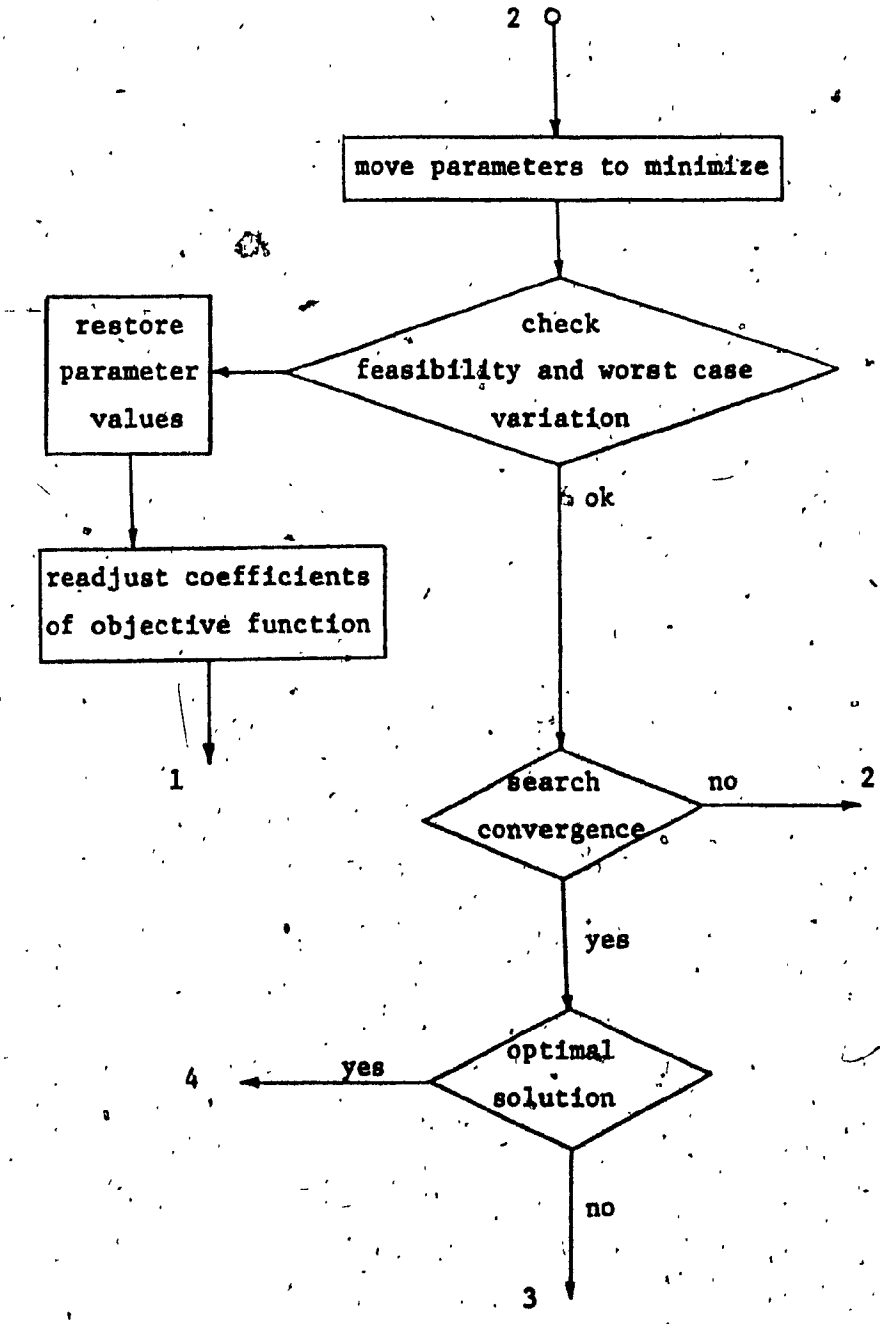
2
move parameters to minimize
check feasibility and worst case variation
restore parameter values
ok
readjust coefficients of objective function
1
search convergence
no
2
yes
optimal solution
yes
4
no
3

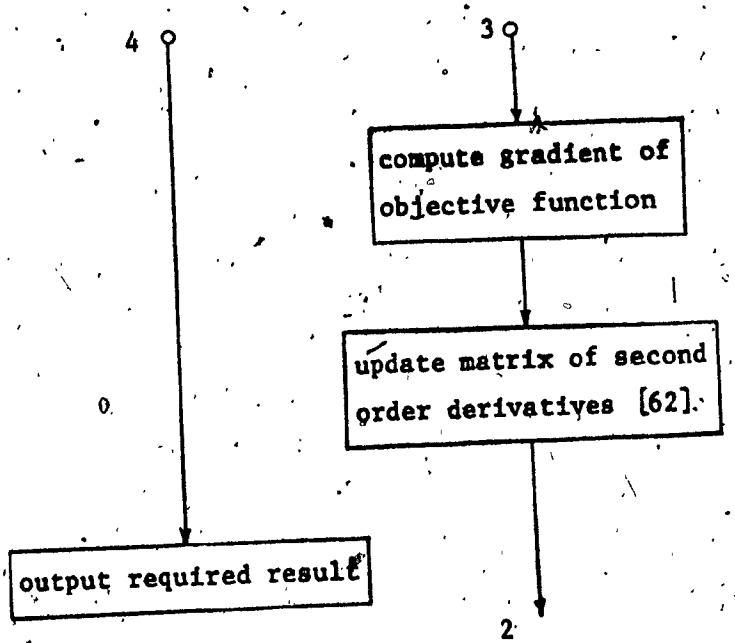
4
3
compute gradient of objective function
update matrix of second order derivatives [62].
output required result
2

APPENDIX G

FLOWCHART FOR THE DESIGN PROCEDURE IN CHAPTER 4

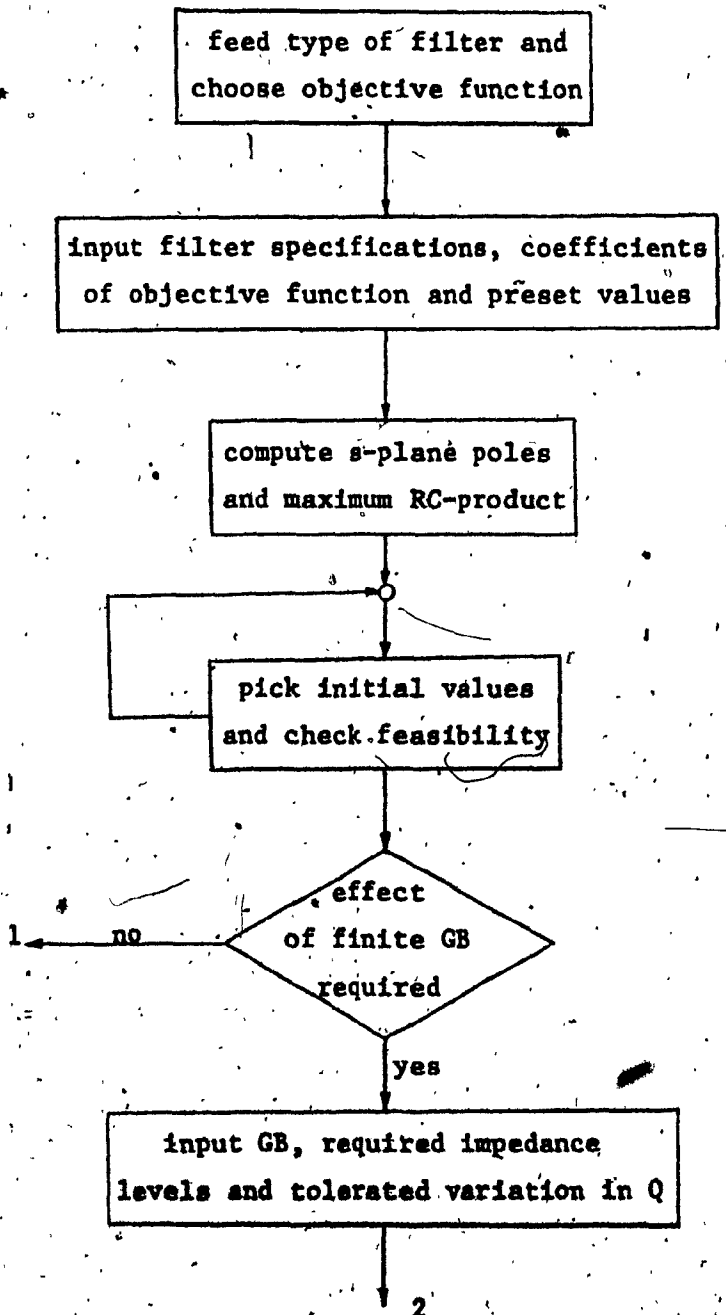

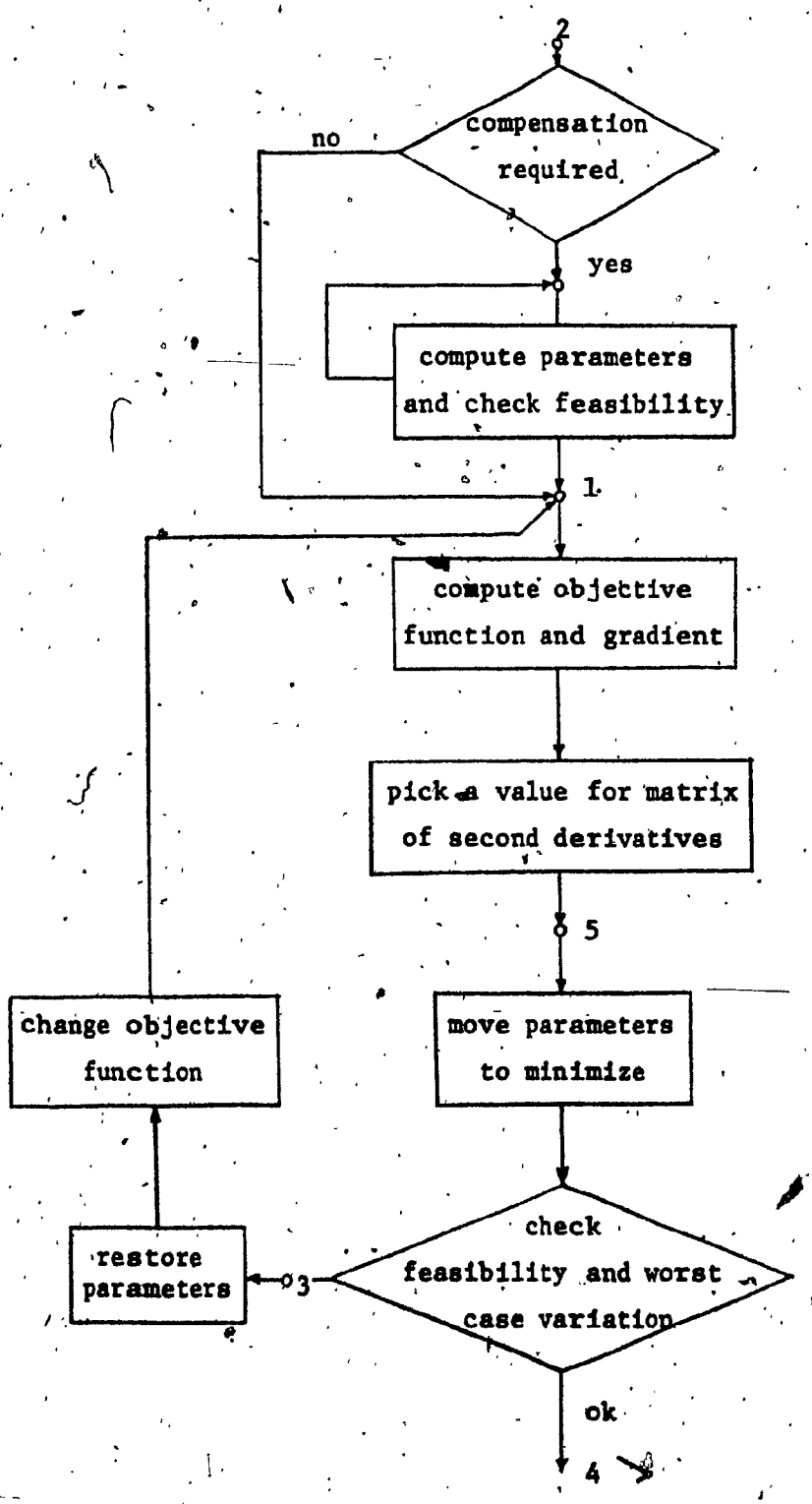
2
compensation required
no
yes
compute parameters and check feasibility
1
compute objective function and gradient
pick a value for matrix of second derivatives
5
move parameters to minimize
check feasibility and worst case variation
3
restore parameters
change objective function
ok
4

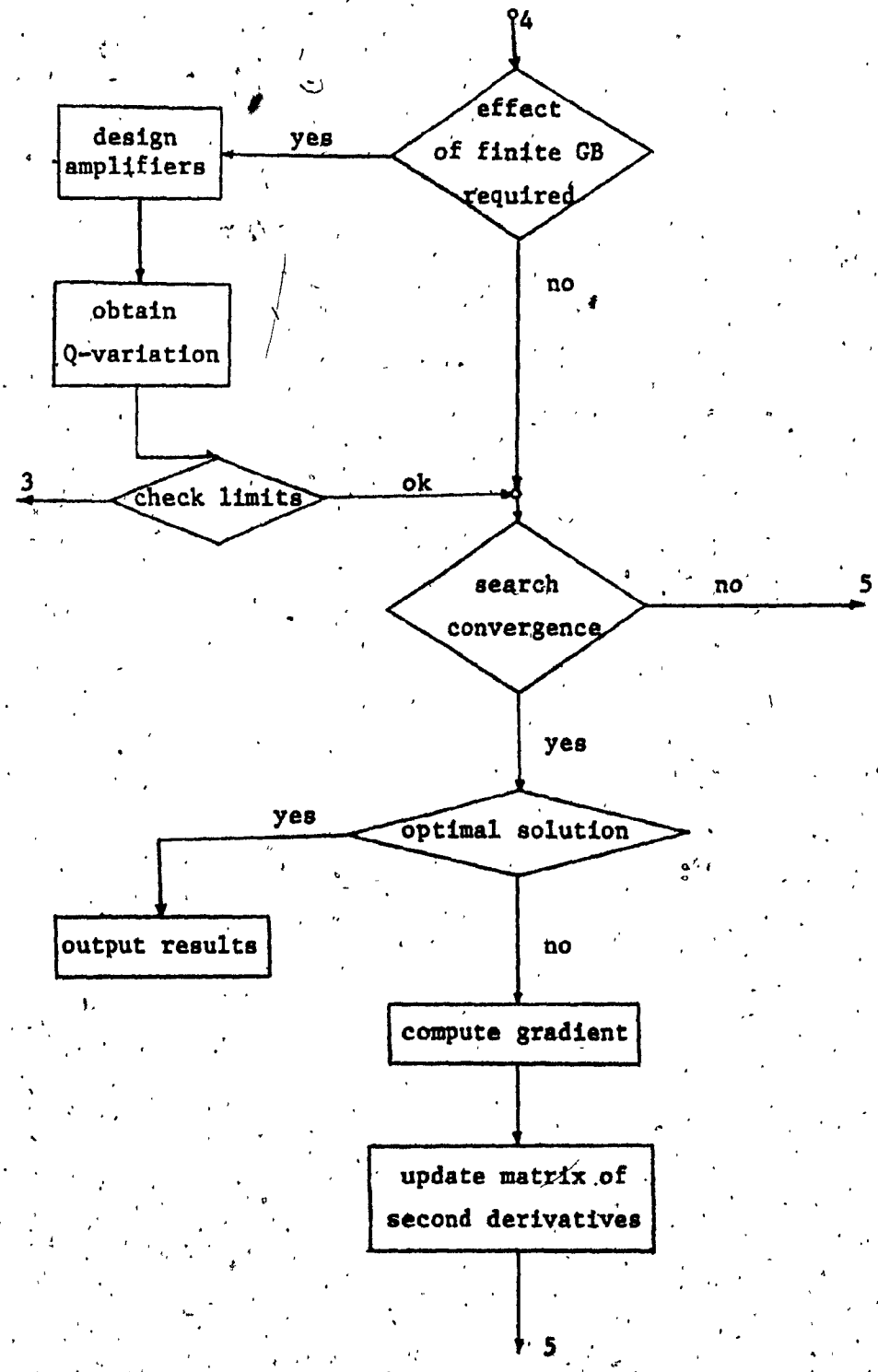
4
effect of finite GB required
yes
design amplifiers
obtain Q-variation
no
3
check limits
ok
search convergence
no
5
yes
yes
optimal solution
output results
no
compute gradient
update matrix of second derivatives
5

APPENDIX H

SENSITIVITY OF THE NOTCH FREQUENCY

Let $N(s,x)$ denote the numerator of $T(p)$ where x is any circuit parameter . Assuming that both s and x vary such that the value of N remains constant , we have

$$dN = 0 = \frac{\delta N}{\delta s}\, ds + \frac{\delta N}{\delta x}\, dx$$

therefore , at the notch frequency s_n

$$\frac{ds_n}{dx} = - \frac{\delta N/\delta x}{\delta N/\delta s} \Bigg|_{s_n}$$

letting

$$s_n = \sigma_n + j\omega_n$$

we have

$$\frac{\delta \omega_n}{\delta x} = - \text{Imag} \frac{\delta N/\delta x}{\delta N/\delta s} \Bigg|_{s_n}$$

$$\frac{\delta \sigma_n}{\delta x} = - \text{Real} \frac{\delta N/\delta x}{\delta N/\delta s} \Bigg|_{s_n}$$

for a notch frequency $s_n = j\omega_n$ we will set $\sigma = \epsilon$

therefore ,

$$S_x^{\omega_n} = \frac{x}{\omega_n} \frac{\delta \omega_n}{\delta x} = - \frac{x}{\omega_n} \text{Imag} \frac{\delta N/\delta x}{\delta N/\delta s} \Bigg|_{s_n} \qquad \text{(H-1)}$$

and,

$$\Delta\varepsilon_{x_i} = - \Delta x_i \text{ Real } \frac{\delta N/\delta x}{\delta N/\delta s}\Big|_{s_n} \qquad \text{(H-2)}$$